Age-related reorganization of working memory in the human brain

By

Timothy Bradley Meier

A dissertation submitted in partial fulfillment of the requirements for the degree of

Doctor of Philosophy

(Neuroscience)

at the

UNIVERSITY OF WISCONSIN-MADISON

2012

Date of final oral examination: 06/22/12

The dissertation is approved by the following members of the Final Oral Committee:

Vivek Prabhakaran, Assistant Professor, Radiology
Elizabeth Meyerand, Professor, Medical Physics
Rasmus Birn, Assistant Professor, Psychiatry
Sterling Johnson, Associate Professor, Medicine
Vaishali Bakshi, Assistant Professor, Psychiatry
Jerry Yin, Professor, Genetics

Table of Contents

Acknowledgements

My advisor: First, I would like to thank Dr. Vivek Prabhakaran, for allowing me to join his lab despite having no experience in neuroimaging. This work was only possible because of his expert guidance and advice. It has been my absolute pleasure to work with him.

My committee: Many thanks to my thesis committee members: Drs. Beth Meyerand, Rasmus Birn, Sterling Johnson, Vaishali Bakshi, and Jerry Yin. There were extremely helpful, and incredibly supportive, both of which I appreciate very much.

Coworkers and collaborator: There are numerous collaborators that have made all of the work present here possible. First, I thank the entire Prabhakaran Lab, especially Dr. Veena Nair, whom had the responsibility of initially training me upon joining the lab, and the several undergraduate students that have helped me complete some of my more tedious tasks.

I want to acknowledge various co-authors for introducing me to new techniques and other valuable contributions, including Alok Deshpande, Joe Wildenberg, Svyatoslav Vergun, and Jie Song, Lin Naing, Lisa Thomas, Argye Hillis, Jingyu Liu, Jiayu Chen, and Vince Calhoun.

I would like to thank the various faculty members that I have worked with during the collection of our so-called MiniConnectome data, including Dr. M. Beth Meyerand, Dr. Bharat Biswal, and Dr. Rasmus Birn. I truly enjoyed learning from and working with you.

Finally, a special thanks to Drs. Joe Wildenberg and Rasmus Birn for their willingness to share their impressive understanding of neuroimaging methods with me on countless occasions.

Neuroscience Training Program: I thank the Neuroscience Training Program for their support, especially during my lab transition.

Family and friends: I want to thank my friends, with special shout-outs to Mike Dash, Léo Walton, and Joe Wildenberg, for making the past five years pretty darn fun. I'd like to thank Chelsey Smith for her support and encouragement. Finally, I express my deepest gratitude to my parents, Michael and Marjorie Meier, and my brother, Jason Meier, for their love and support.

Age-related reorganization of working memory in the human brain

Timothy Bradley Meier

Under the supervision of Dr. Vivek Prabhakaran at the
University of Wisconsin-Madison

Chapter 1

Introduction and overview

Over the last several decades the brain basis of normal age-related changes in cognition has received extensive interest in order to differentiate these changes from those that often accompany many age-related diseases. In addition, there is increasing interest in developing methods of utilizing the brain's natural plasticity in order to attenuate age-related decrements in different cognitive domains that are known to occur even in healthy aging.

One cognitive process that is highly involved in most higher-order cognitive abilities is working memory, which is the maintenance and manipulation of information over short periods of time (Baddeley and Hitch, 1974). Despite the vast amounts of literature regarding the effect of aging on working memory, the exact nature of its age-related reorganization remains to be resolved. This dissertation addresses the age-related reorganization of spatial and verbal working memory using three different, but complementary, methods. First, I employ functional MRI to investigate the age-related reorganization of working memory systems involved in the integration, or binding, of spatial and verbal information in working memory. Second, I employ an increasingly popular method to infer functional brain connectivity, resting-state fMRI, to further investigate brain regions associated with working memory. Finally, I use lesion data to validate a characterization of age-related functional imaging findings commonly observed in working memory studies.

Specific Aims

I. To investigate age-related changes in brain activation during the integration of separable working memory domains.

a. To characterize brain activity associated with the integration of spatial and verbal information during the working memory processes of encoding, maintenance, and retrieval.

b. To test the hypothesis that there are age-related behavioral and brain activity differences in the integration of spatial and verbal information during encoding, maintenance, and retrieval working memory processes.

II. To investigate age-related changes in resting state functional connectivity in brain networks associated with working memory.

a. To test the hypothesis that there are age-related differences in resting state functional connectivity in sensorimotor, cingulo-opercular, fronto-parietal, and default networks.

III. To validate functional neuroimaging findings regarding normal age-related changes in brain activation during working memory task performance using unilateral stroke patients.

a. To test the hypothesis that older adults require both hemispheres to perform a verbal working memory task normally associated with the left hemisphere in younger adults using data from acute unilateral stroke patients.

Background

Working memory

Normal aging leads to anatomical and physiological changes that are reflected in age-related deficits in many cognitive processes, including working memory (Hedden and Gabrieli, 2004; Raz, 2000). Working memory is broadly defined as the system involved in the maintenance, monitoring, and manipulation of short-term goal-related information, and is involved in most higher-order functions including language, reading, reasoning, conscious awareness, and problem solving (Baddeley and Hitch, 1974; Fuster, 2008). Although the prefrontal cortex (PFC) is primarily associated with it, working memory cannot be ascribed to any one individual brain area. Rather, it is a phenomenon that is widely distributed throughout the brain. In addition to the canonical frontal and parietal areas associated with working memory (Cabeza and Nyberg, 2000; D'Esposito et al., 1998; Wager and Smith, 2003), other areas that have been linked to working memory include the anterior cingulate cortex (Bunge et al., 2001; Kondo et al., 2004), medial PFC (Duncan and Owen, 2000), parts of the cerebellum (Marvel and Desmond, 2010; Timmann and Daum, 2007), the medial temporal lobe (Bedwell et al., 2005; Park et al., 2003; Ranganath et al., 2004), the basal ganglia (McNab and Klingberg, 2008; Postle and D'Esposito, 1999), and the thalamus (Floresco et al., 1999). Brain areas involved in working memory can loosely be separated into three different categories: posterior regions such as the parietal and temporal cortices that are thought to maintain sensory information for working memory; motor and premotor areas that are thought to code for the prospective goal-related action, or rehearsal; and the PFC which

is thought to focus attention on, or act as the bridge between, the perceptions and actions of working memory (Curtis and D'Esposito, 2003, 2006; Fuster, 2008; Wager and Smith, 2003). Neuroimaging evidence and psychological models of working memory also suggest a separation of working memory into two parallel systems, a phonological loop for verbal working memory and a visuo-spatial sketchpad for visual and spatial working memory, and a central executive responsible for the manipulation of information in working memory (Baddeley, 2000, 2003; Baddeley and Hitch, 1974). Recently, an additional component, known as the episodic buffer, has been proposed to be the interface of long-term memory and working memory, as well as the storage system of integrated, multi-modal information (Baddeley, 2000).

Age-related changes in working memory

The process of normal aging leads to changes in brain macro-structure that may partially underlie changes in working memory. For example, grey matter volume has been shown to decrease linearly with age (Ge et al., 2002; Gonoi et al., 2009; Raz et al., 2005; Riello et al., 2005) with areas involved in working memory, such as frontal and parietal regions, showing particular sensitivity to age (Bergfield et al., 2010; Good et al., 2001; Raz, 2000; Smith et al., 2007). Additionally, white matter integrity and volume in regions responsible for working memory performance are also sensitive to advanced aging (Charlton et al., 2010; Davis et al., 2009; Head et al., 2004; Pfefferbaum et al., 2005; Raz, 2000; Raz et al., 2005; Wen and Sachdev, 2004). Behaviorally, normal aging leads to a decrease in the total number of items that can be held successfully in

working memory, as well as reduced response times in working memory tasks (Park et al., 2002; Salthouse, 1994; Verhaeghen et al., 1993). Age-related deficits are especially evident in working memory tasks that require manipulation of information in working memory, versus only maintenance.

There have been numerous neuroimaging studies over the past two decades that have documented age-related changes in brain activity during performance of working memory tasks. Generally speaking, two patterns of age-related changes in brain activation have been consistently observed. The first pattern is a reduction of asymmetry of brain activity with age, particularly in the PFC (Cabeza, 2001; Cabeza et al., 1997; Reuter-Lorenz et al., 2000). For example, the performance of a verbal working memory task is highly left lateralized in younger adults, whereas older adults display bilateral brain activity. This pattern is known as the hemispheric asymmetry reduction in older adults, or HAROLD, model (Cabeza, 2002). The second pattern of age-related changes in brain activity is a shift from more posterior brain activity in young adults to more anterior brain activity in older adults, known as the posterior-anterior shift in aging, or PASA, model (Cabeza et al., 2004; Davis et al., 2008; Grady et al., 1994; Madden et al., 2002; Nyberg et al., 2003; Rypma and D'Esposito, 2000).

Several cognitive neuroscience theories have emerged that attempt to account for the functional imaging patterns and behavioral changes that are observed with advancing age (Park and Reuter-Lorenz, 2009a; Reuter-Lorenz and Cappell, 2008; Rypma and D'Esposito, 2000; Stern, 2009). However, these models differ in regards to the nature of the activation changes, for example, if they represent compensatory

recruitment of additional brain regions or the dedifferentiation of specific neural specializations, and no true consensus has emerged. In this thesis, I present work utilizing three different, but complementary, methods in an attempt to further characterize the natural of age-related reorganization of working memory.

The neurocognitive theories of age-related changes in working memory are based primarily on task-related neuroimaging studies. Therefore, the first aim of this research is to identify age-related changes in an event-related working memory fMRI task. **Chapter Two** describes a study that characterizes the brain activity associated with working memory of integrated verbal and spatial information in younger adults, relating directly to *Aim Ia*. This study investigates the neural basis of working memory 'binding' at each phase of a classic working memory task, and provides evidence that an area in the ventral-medial visual cortex, specifically the left lingual gyrus, is responsible for the encoding of integrated verbal and spatial objects in working memory. In addition, I show that this region is less functionally connected to task-negative regions during the integration of verbal and spatial information in working memory compared to a task requiring the simultaneous working memory of verbal and spatial information presented in a separate fashion. These results highlight the importance of the relationship between task-positive activations and task-induced deactivations in working memory binding.

In **Chapter Three**, which is dedicated to *Aim Ib*, I present a study investigating the age-related differences in performance and brain activity of the working memory binding task characterized in Chapter Two. At the behavioral level, although older adults

performed worse compared to younger adults in a working memory task requiring the integration of verbal and spatial working memory, the deficit seemed to be a consequence of a general working memory deficit and not a deficit in binding. However, in terms of brain activation and connectivity, older adults did not display the greater dissociation between task-positive regions and task negative-regions in the bound task compared to the unbound task that younger adults did. I conclude that the binding of letters and locations in working memory is not as efficient in older adults as it is in younger adults, possibly due to the inability to suppress brain regions not directly involved in working memory.

Task-based analyses present many confounding factors that could potentially contribute to the lack of consensus among the different models of age-related changes in working memory. For example, it can often be difficult to control for attention, motivation, and the use of different strategies by individuals during task performance. The use of a relatively new method called resting- state fMRI (rs-fMRI), which has become increasingly popular in investigating brain networks in healthy and patient populations, has the potential to avoid such confounding factors. It has been proposed that the full set of functional networks usually defined by task-based neuroimaging studies are continually present as temporally correlated low frequency fluctuations even when not explicitly being utilized (Biswal et al., 1995; Smith et al., 2009). Therefore, rs-fMRI is a method that can be used to investigate the intrinsic age-related reorganization of brain regions responsible for working memory.

In **Chapter Four** I describe a study using a novel multivariate, multimodal method to investigate the relationship between common resting state networks (derived from rs-fMRI) and a variety of behavioral indices. Although this chapter is focused on young adults, one of the key observations was that this method identified areas in the left inferior frontal gyrus whose connectivity to a bilateral resting state network differentially covaried with performance in the bound working memory task from *Aim Ia*. In addition, this study demonstrates a powerful method to simultaneously investigate resting state fMRI and multiple behavioral measures, laying the foundation for future work with this method to address complex questions of age-related brain-behavior relationships.

Chapter Five describes a study investigating the age-related reorganization of resting state functional connectivity in four networks that are essential for working memory, addressing *Aim II*. In this study, a support vector machine is applied to resting state data from younger and older adults. Machine learning classifiers, such as support vector machines, are multivariate tools that can be used to classify subjects into specific categories based on input variables, called features. Using a support vector machine, I was able to successfully classify participants as being older or young based solely on their resting state connectivity profile. In addition, the support vector machine allowed for the identification of specific features that were the distinguishing characteristics of age-related changes in resting state functional connectivity.

While functional imaging data provides information on what areas of the brain are activated during different cognitive tasks, and on the intrinsic connectivity of brain

networks at rest, it cannot provide information on what areas of the brain are absolutely essential for any particular task. Therefore, it is important to validate results obtained from functional imaging studies, and one common method to do so is with lesion studies (Muller and Knight, 2006; Rorden and Karnath, 2004). Lesion patients have been used extensively to test the necessity of the affected area for many cognitive tasks, including working memory. The lesion-deficit model allows for determination of the necessity of the lesion area for any task in which lesions preferentially disrupt (Price et al., 2006). Lesion studies can also help clarify the nature of age-related reorganizations that are observed in brain regions associated with working memory. The study presented in **Chapter Six** is dedicated to *Aim III*. In this study, a model characterizing age-related differences in brain activity patterns during cognitive tasks is tested in acute stroke patients. Using this lesion population, along with a unique control population, I demonstrate the necessity of bi-hemispheric activity in older adults during verbal working memory tasks, a phenomenon that is routinely observed in neuroimaging studies of aging.

References

Baddeley, A., 2000. The episodic buffer: a new component of working memory? Trends Cogn Sci 4, 417-423.

Baddeley, A., 2003. Working memory: looking back and looking forward. Nat Rev Neurosci 4, 829-839.

Baddeley, A., Hitch, G., 1974. Working memory. In: Bower, G.H. (Ed.), The psychology of learning and motivation: Advances in research and theory. Academic Press, New York, pp. 47-89.

Bedwell, J.S., Horner, M.D., Yamanaka, K., Li, X., Myrick, H., Nahas, Z., George, M.S., 2005. Functional neuroanatomy of subcomponent cognitive processes involved in verbal working memory. Int J Neurosci 115, 1017-1032.

Bergfield, K.L., Hanson, K.D., Chen, K., Teipel, S.J., Hampel, H., Rapoport, S.I., Moeller, J.R., Alexander, G.E., 2010. Age-related networks of regional covariance in MRI gray matter: reproducible multivariate patterns in healthy aging. Neuroimage 49, 1750-1759.

Biswal, B., Yetkin, F.Z., Haughton, V.M., Hyde, J.S., 1995. Functional connectivity in the motor cortex of resting human brain using echo-planar MRI. Magn Reson Med 34, 537-541.

Bunge, S.A., Ochsner, K.N., Desmond, J.E., Glover, G.H., Gabrieli, J.D., 2001. Prefrontal regions involved in keeping information in and out of mind. Brain 124, 2074-2086.

Cabeza, R., 2001. Cognitive neuroscience of aging: contributions of functional neuroimaging. Scand J Psychol 42, 277-286.

Cabeza, R., 2002. Hemispheric asymmetry reduction in older adults: the HAROLD model. Psychol Aging 17, 85-100.

Cabeza, R., Daselaar, S.M., Dolcos, F., Prince, S.E., Budde, M., Nyberg, L., 2004. Task-independent and task-specific age effects on brain activity during working memory, visual attention and episodic retrieval. Cereb Cortex 14, 364-375.

Cabeza, R., Grady, C.L., Nyberg, L., McIntosh, A.R., Tulving, E., Kapur, S., Jennings, J.M., Houle, S., Craik, F.I., 1997. Age-related differences in neural activity during memory encoding and retrieval: a positron emission tomography study. J Neurosci 17, 391-400.

Cabeza, R., Nyberg, L., 2000. Imaging cognition II: An empirical review of 275 PET and fMRI studies. J Cogn Neurosci 12, 1-47.

Charlton, R.A., Barrick, T.R., Lawes, I.N., Markus, H.S., Morris, R.G., 2010. White matter pathways associated with working memory in normal aging. Cortex 46, 474-489.

Curtis, C.E., D'Esposito, M., 2003. Persistent activity in the prefrontal cortex during working memory. Trends Cogn Sci 7, 415-423.

Curtis, C.E., D'Esposito, M., 2006. Functional Neuroimaging of Working Memory. In: Cabeza, A., Kingstone, A. (Eds.), Handbook of Functional Neuroimaging of Cognition. MIT Press, Cambridge, MA.

D'Esposito, M., Aguirre, G.K., Zarahn, E., Ballard, D., Shin, R.K., Lease, J., 1998. Functional MRI studies of spatial and nonspatial working memory. Brain Res Cogn Brain Res 7, 1-13.

Davis, S.W., Dennis, N.A., Buchler, N.G., White, L.E., Madden, D.J., Cabeza, R., 2009. Assessing the effects of age on long white matter tracts using diffusion tensor tractography. Neuroimage 46, 530-541.

Davis, S.W., Dennis, N.A., Daselaar, S.M., Fleck, M.S., Cabeza, R., 2008. Que PASA? The posterior-anterior shift in aging. Cereb Cortex 18, 1201-1209.

Duncan, J., Owen, A.M., 2000. Common regions of the human frontal lobe recruited by diverse cognitive demands. Trends Neurosci 23, 475-483.

Floresco, S.B., Braaksma, D.N., Phillips, A.G., 1999. Thalamic-cortical-striatal circuitry subserves working memory during delayed responding on a radial arm maze. J Neurosci 19, 11061-11071.

Fuster, J.M., 2008. The Prefrontal Cortex, Fourth Edition ed. Academic Press, London.

Ge, Y., Grossman, R.I., Babb, J.S., Rabin, M.L., Mannon, L.J., Kolson, D.L., 2002. Age-related total gray matter and white matter changes in normal adult brain. Part I: volumetric MR imaging analysis. AJNR Am J Neuroradiol 23, 1327-1333.

Gonoi, W., Abe, O., Yamasue, H., Yamada, H., Masutani, Y., Takao, H., Kasai, K., Aoki, S., Ohtomo, K., 2009. Age-related changes in regional brain volume evaluated by atlas-based method. Neuroradiology.

Good, C.D., Johnsrude, I.S., Ashburner, J., Henson, R.N., Friston, K.J., Frackowiak, R.S., 2001. A voxel-based morphometric study of ageing in 465 normal adult human brains. Neuroimage 14, 21-36.

Grady, C.L., Maisog, J.M., Horwitz, B., Ungerleider, L.G., Mentis, M.J., Salerno, J.A., Pietrini, P., Wagner, E., Haxby, J.V., 1994. Age-related changes in cortical blood flow activation during visual processing of faces and location. J Neurosci 14, 1450-1462.

Head, D., Buckner, R.L., Shimony, J.S., Williams, L.E., Akbudak, E., Conturo, T.E., McAvoy, M., Morris, J.C., Snyder, A.Z., 2004. Differential vulnerability of anterior white matter in nondemented aging with minimal acceleration in dementia of the Alzheimer type: evidence from diffusion tensor imaging. Cereb Cortex 14, 410-423.

Hedden, T., Gabrieli, J.D., 2004. Insights into the ageing mind: a view from cognitive neuroscience. Nat Rev Neurosci 5, 87-96.

Kondo, H., Morishita, M., Osaka, N., Osaka, M., Fukuyama, H., Shibasaki, H., 2004. Functional roles of the cingulo-frontal network in performance on working memory. Neuroimage 21, 2-14.

Madden, D.J., Langley, L.K., Denny, L.L., Turkington, T.G., Provenzale, J.M., Hawk, T.C., Coleman, R.E., 2002. Adult age differences in visual word identification: functional neuroanatomy by positron emission tomography. Brain Cogn 49, 297-321.

Marvel, C.L., Desmond, J.E., 2010. Functional Topography of the Cerebellum in Verbal Working Memory. Neuropsychol Rev.

McNab, F., Klingberg, T., 2008. Prefrontal cortex and basal ganglia control access to working memory. Nat Neurosci 11, 103-107.

Muller, N.G., Knight, R.T., 2006. The functional neuroanatomy of working memory: contributions of human brain lesion studies. Neuroscience 139, 51-58.

Nyberg, L., Maitland, S.B., Ronnlund, M., Backman, L., Dixon, R.A., Wahlin, A., Nilsson, L.G., 2003. Selective adult age differences in an age-invariant multifactor model of declarative memory. Psychol Aging 18, 149-160.

Park, D.C., Lautenschlager, G., Hedden, T., Davidson, N.S., Smith, A.D., Smith, P.K., 2002. Models of visuospatial and verbal memory across the adult life span. Psychol Aging 17, 299-320.

Park, D.C., Reuter-Lorenz, P., 2009. The adaptive brain: aging and neurocognitive scaffolding. Annu Rev Psychol 60, 173-196.

Park, D.C., Welsh, R.C., Marshuetz, C., Gutchess, A.H., Mikels, J., Polk, T.A., Noll, D.C., Taylor, S.F., 2003. Working memory for complex scenes: age differences in frontal and hippocampal activations. J Cogn Neurosci 15, 1122-1134.

Pfefferbaum, A., Adalsteinsson, E., Sullivan, E.V., 2005. Frontal circuitry degradation marks healthy adult aging: Evidence from diffusion tensor imaging. Neuroimage 26, 891-899.

Postle, B.R., D'Esposito, M., 1999. Dissociation of human caudate nucleus activity in spatial and nonspatial working memory: an event-related fMRI study. Brain Res Cogn Brain Res 8, 107-115.

Price, C.J., Noppeney, U., Friston, K., 2006. Functional Neuroimaging of Neuropsychologically Impaired. In: Cabeza, R., Kingstone, A. (Eds.), Handbook of Functional Neuroimaging of Cognition. MIT Press, Cambridge, MA, pp. 455-478.

Ranganath, C., DeGutis, J., D'Esposito, M., 2004. Category-specific modulation of inferior temporal activity during working memory encoding and maintenance. Brain Res Cogn Brain Res 20, 37-45.

Raz, N., 2000. Aging of the brain and its impact on cognitive performance: Integration of structural and functional findings. In: Craik, F.I.S., T. A. (Ed.), Handbook of Aging and Cognition. Erlbaum, Mahwah, NJ.

Raz, N., Lindenberger, U., Rodrigue, K.M., Kennedy, K.M., Head, D., Williamson, A., Dahle, C., Gerstorf, D., Acker, J.D., 2005. Regional brain changes in aging healthy adults: general trends, individual differences and modifiers. Cereb Cortex 15, 1676-1689.

Reuter-Lorenz, P., Cappell, K.A., 2008. Neurocognitive Aging and the Compensation Hypothesis. Curr Dir in Psych Sci 17, 177-182.

Reuter-Lorenz, P.A., Jonides, J., Smith, E.E., Hartley, A., Miller, A., Marshuetz, C., Koeppe, R.A., 2000. Age differences in the frontal lateralization of verbal and spatial working memory revealed by PET. J Cogn Neurosci 12, 174-187.

Riello, R., Sabattoli, F., Beltramello, A., Bonetti, M., Bono, G., Falini, A., Magnani, G., Minonzio, G., Piovan, E., Alaimo, G., Ettori, M., Galluzzi, S., Locatelli, E., Noiszewska, M., Testa, C., Frisoni, G.B., 2005. Brain volumes in healthy adults aged 40 years and over: a voxel-based morphometry study. Aging Clin Exp Res 17, 329-336.

Rorden, C., Karnath, H.O., 2004. Using human brain lesions to infer function: a relic from a past era in the fMRI age? Nat Rev Neurosci 5, 813-819.

Rypma, B., D'Esposito, M., 2000. Isolating the neural mechanisms of age-related changes in human working memory. Nat Neurosci 3, 509-515.

Salthouse, T.A., 1994. Aging associations: influence of speed on adult age differences in associative learning. J Exp Psychol Learn Mem Cogn 20, 1486-1503.

Smith, C.D., Chebrolu, H., Wekstein, D.R., Schmitt, F.A., Markesbery, W.R., 2007. Age and gender effects on human brain anatomy: a voxel-based morphometric study in healthy elderly. Neurobiol Aging 28, 1075-1087.

Smith, S.M., Fox, P.T., Miller, K.L., Glahn, D.C., Fox, P.M., Mackay, C.E., Filippini, N., Watkins, K.E., Toro, R., Laird, A.R., Beckmann, C.F., 2009. Correspondence of the brain's functional architecture during activation and rest. Proc Natl Acad Sci U S A 106, 13040-13045.

Stern, Y., 2009. Cognitive reserve. Neuropsychologia 47, 2015-2028.
Timmann, D., Daum, I., 2007. Cerebellar contributions to cognitive functions: a progress report after two decades of research. Cerebellum 6, 159-162.

Verhaeghen, P., Marcoen, A., Goossens, L., 1993. Facts and fiction about memory aging: a quantitative integration of research findings. J Gerontol 48, P157-171.

Wager, T.D., Smith, E.E., 2003. Neuroimaging studies of working memory: a meta-analysis. Cogn Affect Behav Neurosci 3, 255-274.

Wen, W., Sachdev, P., 2004. The topography of white matter hyperintensities on brain MRI in healthy 60- to 64-year-old individuals. Neuroimage 22, 144-154.

Chapter 2

The integration of verbal and spatial information in working memory

Timothy B. Meier, Rasmus M. Birn, Mary E. Meyerand, Vivek Prabhakaran

In preparation

Abstract

In this study we use event-related fMRI tasks to investigate the neural correlates of letter and location binding at each phase of working memory. Participants performed four versions of an item-recognition task: a spatial version, a verbal version, and two combined verbal and spatial versions. For the bound version, each letter was paired with a particular location, allowing verbal-spatial binding. In the unbound combined task, letters and locations were presented separately. Participants performed more accurately in the bound task than in the unbound task, confirming that binding is behaviorally more efficient than not binding. Univariate analysis of brain activity demonstrated that, during the encoding phase, the left lingual gyrus was the only area to have greater bound task than unbound task activity, and activity in this region positively correlated with performance on the bound task. A secondary analysis identified the right superior parietal lobule as having greater bound task activity than the average of verbal and spatial task activity. Functional connectivity analyses demonstrated that these putative binding regions were significantly less connected to task-negative regions in the bound task than in the unbound task. Finally, our data suggests that the binding of verbal and spatial information is spatially driven, as performance and activity in the bound task was more similar to the spatial task alone than the verbal task alone, consistent with a hypothesis of binding in working memory set forth by Treisman (Treisman, 2006).

Introduction

The ability to bind, or integrate, information has been proposed as a mechanism to increase the total amount of features that can be held in working memory (Luck and Vogel, 1997). Based on this view, the limit of working memory capacity is defined by the number of bound items that can be successfully remembered after a short delay, and not by the total number of individual features. Several decades of research have been dedicated to understanding the nature of feature binding at the visual perceptual level (Treisman, 1996; Treisman and Gelade, 1980). However, the neural and behavioral basis of binding in working memory is still unclear.

Different types of information are thought to be processed by different systems in working memory, conceptualized as the phonological loop and visuo-spatial sketchpad in Baddeley's influential multi-component model of working memory (Baddeley, 2000). Accordingly, neuroimaging research has established that, generally speaking, verbal working memory is highly lateralized to the left hemisphere while spatial working memory is more associated with the right hemisphere (D'Esposito et al., 1998; Jonides et al., 1993; Kapur et al., 1994; Owen et al., 1998; Paulesu et al., 1993; Smith et al., 1996). How verbal and spatial information are bound in working memory, and what areas are responsible for this binding, remain unresolved. One possibility, as proposed by Baddeley in an addition to the multi-component model, is the so-called episodic buffer that is responsible for integration of verbal and visuo-spatial information in working memory, as well as linking working memory to long-term memory (Baddeley,

2000). In this context, the episodic buffer can also be thought to be responsible for the maintenance of bound items in working memory. Previous studies have attempted to identify brain regions that might be responsible for functions attributed to the episodic buffer, and have implicated the prefrontal cortex (Mitchell et al., 2000a; Munk et al., 2002; Prabhakaran et al., 2000), the superior parietal lobule (Campo et al., 2008; Friedman-Hill et al., 1995; Shafritz et al., 2002; Todd and Marois, 2004; Xu, 2007), and medial temporal lobe regions (Finke et al., 2008; Hannula and Ranganath, 2008; Luck et al., 2010; Mitchell et al., 2000a; Olson et al., 2006; Piekema et al., 2006; Piekema et al., 2009) as possible areas responsible for the working memory of bound information. Conversely, it has also been proposed that no integrated item is stored in working memory at all, but instead the verbal and spatial information can be maintained in parallel in their respective systems (Wheeler and Treisman, 2002).

Here, we use event-related fMRI to investigate the integration, or binding, of spatial and verbal information in working memory. The goals of this research were to identify what brain regions, if any, were responsible for the encoding, maintenance, and retrieval of bound information in working memory. To do so, variations of a standard item-recognition task were developed to compare behavior and brain activity of verbal-spatial binding to control scenarios in which the same amount of information was presented in a separate fashion. In addition, we also investigated differences in functional connectivity of binding-related regions at each phase of working memory task during verbal-spatial binding compared to a control task in which no binding was possible.

Methods

Subjects

Twenty-one young adults (13 male, 8 female; 24.6 ± 0.69 years old) were enrolled for this study after providing informed consent. All subjects were confirmed to be right hand dominant based on the Edinburgh Handedness Inventory and had normal or corrected to normal vision. Additionally, participants reported no use of prescription medications and no history of mental illness. All aspects of this study were approved by the University of Wisconsin-Madison Health Sciences Institutional Review Board.

Task design

Each participant performed four variations of an item-recognition task in the scanner consisting of spatial, verbal, or both spatial and verbal stimuli, based on the tasks used in a previous study on working memory binding (Prabhakaran et al., 2000). All stimuli were presented in the center of a back-projected screen and participants responded using a MR-compatible button box, with their right index finger representing a ‘yes’ response and their middle finger representing a ‘no’ response. All four task variations included 32 trials that each consisted of an encoding phase of two seconds during which the to-be-remembered stimuli were presented, a six second maintenance phase during which the subjects were instructed to maintain the stimuli in working memory, and a two second retrieval phase during which participants responded whether or not a single probe item was included in the test set observed in the encoding phase. A jittered length inter-trial interval (ITI) followed each trial. Task order was randomized

across subjects. Each task type included an equal number of positive probes requiring a ‘yes’ response and negative probes requiring a ‘no’ response.

For the *verbal* version, three upper-case letters were presented at the center of the screen during the encoding phase. Following the maintenance phase, a single lower-case letter was presented in the center of the screen. Participants had to indicate whether or not the single lower-case letter presented in the retrieval phase was one of the three upper-case letters presented for that trial. All consonants except for ‘Y’ and ‘L’ were used as stimuli. Changing the case of the letters ensured that participants encoded the letter verbally. For the *spatial* version, three locations indicated by parentheses around an imaginary clock-face were presented during the encoding phase. Participants had to indicate whether or not a single location presented during the retrieval phase was included in that trial’s encoding phase.

Participants also performed two task variations that involved both spatial and verbal stimuli. The instructions for both of these tasks were the same, but the tasks differed in the way the stimuli were presented at the encoding phase. In the *unbound* version, three upper-case letters were presented in the center of the screen and three locations indicated by parentheses were presented around an imaginary clock-face during the encoding phase. At the retrieval phase, a single lower-case letter was presented at a single location and participants had to decide whether or not both the letter and location were included in the encoding set. If either the letter or location were not, then the correct response would have been ‘no’ (**Figure 2.1**).

In the *bound* version, three upper-case letters enclosed in parentheses were presented around an imaginary clock-face during the encoding phase. During the retrieval phase, a single lower-case letter enclosed in parentheses was presented at a single location. Subjects had to decide whether or not both the letter and location were included in the encoding phase. If either the letter or location were not, then the correct response would have been 'no'. There were two types of positive trials for the bound task. In *congruent* trials, the lower-case letter presented during the retrieval phase was in the exact same location that it was in the encoding phase. For *incongruent* trials, the lower-case letter presented during the retrieval phase was not in the same location as it was in the encoding phase. However, it was in one of the other two locations that were in the encoding phase, and would therefore require a 'yes' response (**Figure 2.1**).

The total information presented for the bound and the unbound tasks was equivalent, but the bound task provides the opportunity for subjects to bind, or integrate, letters with specific locations. Comparison of performance on bound congruent and incongruent trials provides a way to determine whether participants were successfully binding the letters and locations. Participants practiced the task outside of the scanner until it was deemed that they understood the task rules. Prior to each specific scan, subjects were reminded of the rules for the task version they were about to complete.

fMRI acquisition and preprocessing

Scans were collected on a 3T MRI scanner (GE Healthcare, Waukesha, WI) using gradient-echo echo-planar imaging with the following parameters: TR = 2.6 s, TE

= 22 ms, field of view = 22.4 cm, flip angle = 60°, 40 sagittal slices, acquisition matrix = 64 x 64, 3.5 mm isotropic voxel size, 231 time-points. T1-weighted anatomical images were collected using a FSPGR BRAVO sequence (TR = 8.132 ms, TE = 3.18 ms) over a 256 x 256 matrix and 156 slices (flip angle = 12°, FOV = 25.6 cm, slice thickness = 1 mm). For each task variation a separate scan consisting of 185 volumes was collected, with approximately ten seconds of baseline signal acquired before and after each scan. All scans were collected during the same visit.

The first three volumes from each scan were removed to allow for magnet stabilization. Each functional scan was then despiked, registered to its first volume for motion correction, slice time corrected, spatially smoothed with a 4 mm FWHM Gaussian kernel, and converted to percent signal change. All preprocessing and analysis of imaging data was done in the AFNI program suite (Cox, 1996).

Behavioral analysis

Percent accuracy and response time for bound task versus unbound, spatial, and verbal tasks, as well as congruent bound trials versus incongruent bound trials, were compared using paired t-tests. Only trials in which participants attempted were included in the analyses.

fMRI analysis

A fixed-effect model was used at the subject level for each task variation. Functional data were modeled using the general linear model in which the encoding,

maintenance, and retrieval phases were modeled separately by convolving a 2 second, 6 second, and 2 second block stimulus, respectively, to each event with a canonical hemodynamic response function. Correct and incorrect trials were modeled separately, however, only correct trials were carried forward to the group analysis. In order to allow comparison across subjects, each subject's anatomical scan was aligned to their functional scan and then both the aligned anatomical and the statistical images were normalized to a standard template space and re-sampled to 3 x 3 x 3 mm.

Brain-wide analysis

Group data were analyzed using a random effects analysis. A 3 by 4 repeated measures analysis of variance was conducted on the functional data with verbal, spatial, bound, and unbound as the levels of factor *task* and encoding, maintenance, and retrieval as the levels of factor *phase*. There were six *a priori* contrasts of interest. The primary goal of this study was to identify the neural correlates of binding spatial and verbal information in working memory. In order to identify binding specific regions, brain activity at each phase for the bound task was compared to activity at each phase of the unbound task (B-U). A set of secondary comparisons was carried out to further probe the neural substrates of binding. For this set, the activity during the bound task was compared to the averaged verbal and spatial task activity at each phase (B-(V+S)/2). Finally, the activity in response to the bound task was also compared to the activity in response to the verbal and spatial tasks alone, at each phase. The approximate smoothness of our data was estimated via 3dFWHMx program in AFNI, and 3dClustSim

was used to estimate the appropriate cluster size and threshold to meet statistical significance at family-wise error rate of 0.05 following Bonferroni correction.

Task functional connectivity

A modified beta-series correlation method was used in order to assess functional connectivity of specific regions during each phase of task performance. Beta-series correlation is a multivariate method in which each trial or event is separately modeled as a covariate, or regressor, of interest in the general linear model (GLM) (Rissman et al., 2004). The resultant beta values for each covariate are grouped according to trial type and then concatenated in time. Seed-based correlation analyses can then be computed on the beta series. A modification of this method has been recently suggested (Mumford et al., 2012). For this method, which the authors refer to as the Least Squares Separate method (LSS), a separate GLM is run for each trial in which that trial is modeled as a regressor of interest and all other trials are modeled as regressors of no interest. The major benefit of the LSS method is that it reduces the collinearity between regressors, a common problem in event-related working memory designs.

Here we applied the LSS method and ran separate GLM for each phase of each trial in which all other phases and trials were modeled as regressors. The beta values were grouped according to phase and then concatenated over time. This resulted in three series of beta values (beta-series), one for each phase of the working memory task. This process was done for both the bound and unbound tasks. Following this, traditional seed-based connectivity analyses were performed on the beta-series. Seed-

regions were selected based on the whole-brain univariate analyses (see results). For each seed-region, the beta-series of every voxel within a 5mm radius sphere were averaged and the resultant series was correlated with the beta-series of every other voxel in the brain. The resultant correlation coefficients were Fisher-transformed and normalized to a z-score to allow for group level statistics. Paired t-tests were then computed to compare connectivity of each seed-region during the bound task to connectivity during the unbound task at the encoding, maintenance, and retrieval phases. As for the univariate data, 3dClustSim was used to estimate the appropriate cluster size and threshold to meet statistical significance at family-wise error rate of 0.05 following Bonferroni correction.

Results

Behavioral data

Performance on the bound and unbound tasks was compared to see if the opportunity to bind letters to specific locations had any behavioral benefits. Participants were significantly more accurate in the bound task than in the unbound task ($t(20)=2.4$, $p < .05$), but average response time did not differ between the tasks ($t = .23$; **Figure 2.2a**). Participants responded significantly faster in both the verbal task ($t(20)=10.5$, $p < .001$) and the spatial task ($t(20)=4.4$, $p < .001$) than in the bound task. However, while participants were significantly more accurate in the verbal task than in the bound task ($t(20)=2.2$, $p < .05$), accuracy in the spatial task was significantly lower than accuracy in the bound task ($t(20)=2.5$, $p < .05$).

In order to confirm participants were indeed binding the locations and letters together during the bound task, we compared performance for congruent and incongruent positive trials. Participants responded significantly faster in congruent bound trial types than incongruent trial types ($t(20) = 2.75$, $p < .05$). There was no significant difference in accuracy between congruent and incongruent trial types (t=0.90; **Figure 2.2b**). Although the task could theoretically be completed without binding, the faster response time in congruent trials suggests that participants were indeed binding the spatial and verbal information together.

Imaging data – bound task

In this study we were specifically interested in brain regions that are responsible for working memory binding of verbal and spatial information. To do so, we first identified all brain regions that were activated during working memory of integrated, or bound, verbal and spatial information measured at the encoding, maintenance, and retrieval phases. Performance of the bound working memory task evoked activation in a wide array of regions (**Figure 2.3**). At the encoding phase, activation was observed in posterior regions including bilateral occipital cortex, lingual and fusiform gyri, bilateral cerebellar regions, and bilateral superior and inferior parietal lobules (BA 7, 40). Sub-cortical encoding activity was observed bilaterally in the thalamus, pallidum, putamen, and brainstem. Frontal regions displaying encoding related activity included bilateral anterior insular cortex, precentral gyrus, middle and inferior frontal gyri (BA 6, 44), and medial frontal gyrus corresponding to the supplementary motor area. In addition, there

were several areas that displayed significant deactivation during the encoding phase of the bound task. These regions included bilateral superior and middle temporal gyri, posterior insula, postcentral gyri extending into the superior parietal lobule (BA 5, 7), angular gyri (BA 39), and superior medial frontal gyri (BA 8).

Activity during the maintenance phase of the bound task was less robust than the activity observed during the encoding and retrieval phases. Positive activation was observed bilaterally in the inferior and superior inferior lobule (BA 7, 40), in the middle frontal gyri extending into the precentral gyri (BA 6), the supplementary motor area, and in a left cluster covering the inferior and middle temporal gyrus extending into the middle occipital gyrus. Extensive maintenance related deactivation was observed in visual areas along with regions generally associated with the default mode network. These included bilateral fusiform and lingual gyri, cuneus, posterior cingulate cortex, cingulate cortex, anterior cingulate cortex, supramarginal gyri (BA 40), insula, inferior frontal gyri (BA 47), superior temporal gyri, postcentral gyri (BA 5), cerebellum, and right superior frontal gyrus (BA 8).

Robust activations were observed at the retrieval phase of the bound task. These included bilateral activity in the middle frontal gyri (BA 6) extending into the precentral gyri, inferior frontal gyri (BA 44/45), superior frontal gyri (BA 10), anterior insula, anterior cingulate, and the superior medial frontal gyrus corresponding to the supplementary motor area. In addition, activation likely related to the button response was observed in left lateralized precentral and postcentral gyri (BA 4, 3, 2). Bilateral posterior regions

included the inferior parietal lobule (BA 7, 40), lingual and fusiform gyri, middle occipital gyri, cuneus, middle temporal gyri, inferior temporal gyri, superior temporal gyri, and the cerebellum. Significant activity was observed sub-cortically in the bilateral thalamus, putamen, pallidum, and brainstem. Retrieval phase deactivation was observed in the bilateral cerebellum, superior medial frontal gyri (BA 8, 9), and in the left cingulate gyrus. Significant retrieval phase deactivation was observed bilaterally in the cerebellum and the superior medial frontal gyri (BA 10).

Encoding phase contrasts

In order to identify brain regions specifically involved in working memory binding, contrasts of bound versus unbound task at each working memory phase were carried out. Regions identified in these contrasts could help identify the neural substrates of letter-location binding, as the total number of items in each task type was equivalent. At the encoding phase, subjects displayed more activation in the unbound task than the bound task in five clusters (**Table 2.1; Figure 2.4**). The largest cluster included the angular gyrus (BA 39) and supramarginal gyrus (BA 40) of the right inferior parietal lobule, and portions of the right precuneus (BA 7). A second cluster with greater unbound task activity included primarily the right putamen and pallidum, and extended into the caudate and parts of the thalamus. There was also greater unbound task activity observed in a cluster in the left precuneus (BA 7), supramarginal gyrus (BA 40), and angular gyrus (BA 39). A fourth cluster was located in right precuneus (BA 7), and a final cluster was located in the right middle frontal gyrus (BA 9).

There was only one cluster that displayed greater bound than unbound related activity during the encoding phase. It consisted primarily of the left lingual gyrus (BA 18), approximately the ventral regions of visual areas 3 and 4, and extended into the cuneus (BA 17; **Figure 2.4**).

As an additional set of comparisons, the encoding-related activity during the bound task was compared to the averaged activity during the spatial and verbal tasks (**Table 2.2; Figure 2.4**). This contrast revealed a large cluster of posterior regions that displayed significantly greater bound task activity including bilateral middle occipital gyri, cuneus, lingual gyri, and fusiform gyrus. This extended into the right middle temporal gyrus (BA 39) and right posterior cingulate. A smaller cluster of greater bound related activity was also evident in the right precuneus and superior parietal lobule (BA 7).

Activation at the encoding phase was also compared to activation at the encoding phases of the verbal and spatial tasks alone (**Table 2.3 and 2.4; Figure 2.4**). Bound task activity was more different than the verbal task than the spatial task. Compared to the spatial task, participants displayed significantly more activity in the bound task in the left fusiform and bilateral inferior occipital gyri. Conversely, several regions displayed significant differences in activity between the bound and verbal task at the encoding phase. These included a large posterior cluster covering bilateral lingual gyri, middle occipital gyri, superior parietal lobules (BA 40), inferior parietal lobules (BA 7), cuneus, and fusiform gyri along with a right lateralized middle temporal gyrus and right posterior cingulate that displayed greater bound activity than verbal activity. Two

clusters in the left and right middle frontal gyri (BA 6) extending into the precentral gyri also displayed greater bound activity than verbal activity. Clusters in bilateral angular gyri (BA 39) and the right posterior insula extending into the middle temporal gyrus and superior temporal gyrus (BA 22) were significantly more deactivated in the bound task than in the verbal task. There was significantly more verbal activity than bound activity in the right cerebellum and right lateral inferior occipital gyrus (BA 18).

Maintenance phase contrasts

At the maintenance phase, the contrast of the bound task versus the unbound task revealed no regions that were significantly more active for the bound task. However, there were two clusters in which subjects had significantly more deactivation during maintenance of the bound task than during maintenance of the unbound task (**Table 2.1; Figure 2.4**). These clusters included the left and right lingual gyrus, and extended down into the cerebellum. A third cluster in the left cerebellum displayed significantly more activity during the maintenance period of the unbound task than the bound task.

For the B-(V+S)/2 contrast, a cluster in the right superior parietal lobule and precuneus (BA 7) displayed significantly more activity during the bound task compared to the averaged verbal and spatial tasks during the maintenance phase (**Table 2.2; Figure 2.4**).

As in the encoding phase, the maintenance phase of the bound task was more similar to the spatial task than the verbal task alone (**Table 2.3 and 2.4; Figure 2.4**). In

fact, there were no significant differences between the spatial task and bound task at the maintenance phase. Compared to the verbal task, participants displayed significantly more activity in the bilateral superior parietal lobule (BA 7), inferior parietal lobule (BA 40), and middle frontal gyrus (BA 6) extending into the precentral gyrus, and in the right inferior frontal gyrus (BA 9) and middle occipital gyrus extending into the fusiform gyrus (BA 37). Participants displayed significant more bound task-induced deactivation in the right cerebellum and right superior medial frontal gyrus (BA 6).

Retrieval phase contrasts

The contrast of bound task activity versus unbound task activity at the retrieval phase displayed no significant differences in activation. However, greater sub-threshold activity in the unbound task compared to the bound task was observed bilaterally in the fusiform gyri, the right middle frontal gyrus (BA 10), the left middle frontal gyrus (BA 8) and the left middle temporal gyrus.

However, greater bound activity was seen compared to the averaged spatial and verbal tasks at the retrieval phase (**Table 2.2; Figure 2.4**). This included clusters in the left and right fusiform gyri, lingual gyri, and extended into the parahippocampal gyri. Interestingly, the greater bound-related activity displayed in the left lingual gyrus corresponds to the same location as the left lingual gyrus activity observed in the contrasts at the encoding phase.

Again at the retrieval phase, the bound task had more differences than the verbal task alone than compared to the spatial task alone (**Table 2.3 and 2.4; Figure 2.4**).

Compared to the spatial task, participants had significantly more activity in the left middle and inferior frontal gyri (BA 45, 46) in the bound task. Compared to the verbal task, participants displayed significantly more retrieval phase activity in the bound task in several posterior regions, including a large cluster covering the bilateral fusiform gyri, lingual gyri, parahippocampal gyri, posterior cingulate, middle occipital gyri, and the right middle temporal gyrus. A second cluster encompassing the right superior parietal lobule/precuneus (BA 7) also had significantly more activity in the bound task than the verbal task.

Brain-behavior relationship

Two separate contrasts from the group analysis identified a region in the left visual cortex that displayed significantly greater brain activity during the encoding phase of the bound working memory task than in tasks with the same amount of verbal and spatial information presented in a separate fashion. Therefore, we wanted to determine whether brain activity in the left visual cortex during the bound working memory task was related to performance on that task. To do so, a mask of the intersection between the two contrasts that showed bound preferential activity during the encoding phase was created. The region of interest consisted of 156 voxels located primarily in the left lingual gyrus and extending into the cuneus (BA 17, 18; center of mass -10, -74, -7 MNI). Brain activation (beta values) within this region of interest at the encoding, maintenance, and retrieval phase was correlated with accuracy on the bound task. Accuracy was investigated because participants were significantly more accurate in the

bound task than the unbound task. Activity in the left lingual gyrus during the encoding phase of the bound task was moderately correlated with performance on that task ($r(19) = .44$, $p < .05$), such that subjects with more lingual gyrus activity performed more accurately in the task (**Figure 2.5**). Activity in the left lingual gyrus during the retrieval phase was positively correlated with accuracy in the bound task, but at a not quite trending towards significant level ($r(19) = .36$, $p = .11$). Activity in this region during the maintenance phase did not correlate with accuracy in the bound task ($r = .03$).

Task functional connectivity

The functional connectivity of multiple regions identified by the whole-brain analysis and brain behavior analyses was compared between the bound and unbound task at each phase using LSS, a modified beta-series correlation (Mumford et al., 2012; Rissman et al., 2004). Two seed-regions were selected, based on regions identified by the univariate contrasts reported above. Multiple univariate contrasts identified a region consisting primarily of the left lingual gyrus that displayed bound preferential activity. Therefore, the first seed region was based on the peak activation difference in the left lingual gyrus cluster from the bound versus unbound contrast at the encoding phase (-18, -72, -16 MNI coordinates). In addition, two contrasts of bound task activity versus the averaged spatial and verbal task activity indentified the right superior parietal lobule as a bound preferential region. Several studies have previously implicated the superior parietal lobule as a binding region (Campo et al., 2008; Friedman-Hill et al., 1995;

Shafritz et al., 2002). Accordingly, the second seed-region was placed at the peak voxel from this contrast at the maintenance phase (18, -69, 55 MNI coordinates).

The LSS analysis for the left lingual gyrus seed-region identified four clusters that were significantly less connected to the lingual gyrus during the encoding phase of the bound task compared to the encoding phase of the unbound task (**Table 2.5; Figure 2.6**). Two of these clusters were located in the left and right insula extending into the inferior parietal lobule, postcentral gyri, and superior temporal gyri. A third cluster was located near the midline, with peak connectivity to the right cingulate and medial frontal gyrus corresponding to the supplementary motor area (BA 6). The final cluster was located in the left cerebellum.

During the maintenance phase, the left lingual gyrus demonstrated significantly less connectivity to a region in the right fusiform gyrus that extended into the cerebellum during the bound task compared to the unbound task. There were no differences in lingual gyrus connectivity between the unbound and bound tasks at the retrieval phase.

For the right superior parietal lobule seed-region there were several clusters in regions that were significantly more connected during the unbound task than the bound task at the encoding phase (**Table 2.6; Figure 2.6**). The largest cluster was located in the left posterior insula and extended into the inferior parietal lobule (BA 40), and the transverse temporal area. A second cluster was located in the right posterior insula extending into the inferior parietal lobule (BA 40). A right lateralized cluster in the anterior insula extending into the inferior frontal gyrus (BA 47) and temporal pole, and a

left lateralized cluster in the anterior insula extending into the superior temporal gyrus also displayed more connectivity to the right superior parietal lobule in the unbound task than the bound task at the encoding phase. Finally, two midline clusters located in the medial frontal gyrus (BA 9, 10) also had more connectivity during the encoding phase in the unbound task than the bound task.

At the maintenance phase, the right SPL seed-region was significantly more connectivity to the medial frontal gyrus (BA 9, 10) and the posterior cingulate (BA 30/23) during the unbound task than the bound task. As in the lingual gyrus seed-region, there were no differences in connectivity during the retrieval phase.

Discussion

Behavioral analysis

In this study we used event-related fMRI to investigate the neural correlates of binding in working memory at the encoding, maintenance, and retrieval phases. The higher accuracy for working memory of bound spatial and verbal items compared to working memory of the same amount of items presented in a separate fashion is consistent with the role of binding as a mechanism of increasing working memory capacity (Luck and Vogel, 1997). Interestingly, while response time was faster in the verbal or spatial task alone than in the bound task, accuracy was better in the verbal task and worse in the spatial task compared to the bound task. Therefore, according to our data, the behavioral benefit of binding is limited by the performance on the more difficult item feature. The fact that accuracy in the spatial task was lower than in the

bound task could be explained by the fact that in many cases the bound task could be performed accurately without spatial information. For example, in trials in which the letter at the retrieval phase did not match any of the target letters. It should be noted that the binding task presented here could potentially have been performed accurately without actually creating bound representations of the items, but instead separately holding the verbal and spatial information of each item (Morey, 2009; Wheeler and Treisman, 2002). However, the fact that participants performed more accurately in the bound task than in the unbound task, and the fact they responded faster to congruent bound trials than incongruent bound trials, suggests that they were binding the letters and location together.

Univariate analyses- task-positive activations

The major finding of this paper is that the ventral-medial occipital lobe, specifically the left lingual gyrus, appears to be responsible for the encoding of verbal and spatial information in working memory. The primary comparison of interest in this work was the activity during the bound task compared to activity during the unbound task. The total number of verbal and spatial information presented is equivalent in these two tasks. However, in the bound task each letter can be paired with a location, while in the unbound task the letters and locations are presented separately. Comparison of these two regions at each phase of the working memory task resulted in only one region, the left lingual gyrus, which had more bound than unbound activity. In fact, during the encoding phase there were several regions that were more active in the

unbound task than the bound task. These regions, the posterior parietal cortex and basal ganglia, have been implicated in encoding in working memory and perhaps could reflect the fact that the effective working memory load is higher in the unbound task (Chang et al., 2007; Habeck et al., 2005; Narayanan et al., 2005).

We observed no regions that displayed greater bound versus unbound activity during working memory maintenance. This finding is consistent with the parallel stores hypothesis, which posits that there is no specific region responsible for the storage of bound items, but rather each type of information is stored in its own separate system (Wheeler and Treisman, 2002). However, other studies have implicated various regions as being responsible for bound-specific storage including the prefrontal cortex (Mitchell et al., 2000a; Munk et al., 2002; Prabhakaran et al., 2000), superior parietal cortex (Campo et al., 2008; Friedman-Hill et al., 1995; Shafritz et al., 2002; Todd and Marois, 2004; Xu, 2007), and medial temporal regions (Finke et al., 2008; Hannula and Ranganath, 2008; Luck et al., 2010; Mitchell et al., 2000a; Olson et al., 2006; Piekema et al., 2006; Piekema et al., 2009). In some of these previous studies, instead of a control condition in which both letters and locations are presented simultaneously in a separate fashion (as done here in the unbound task), binding related activity was contrasted to the average activity of verbal and spatial tasks performed separately. By using a similar comparison, we identified a region in the right superior parietal lobule that displayed significantly more bound-related activity than the average spatial and verbal activity in both the encoding and maintenance phase. This contrast also resulted in robust bound-preferential activity in the visual cortex during both the encoding and

retrieval phase. The results from these contrasts further highlight the importance of the visual cortex in the encoding, and possibly retrieval, of bound verbal and spatial items. Additionally, these contrasts suggest some role of the right superior parietal lobule in the working memory of bound information, consistent with several previous studies on binding (Campo et al., 2008; Friedman-Hill et al., 1995; Shafritz et al., 2002).

Univariate analyses –task-induced deactivations

More difficult tasks and higher task loads have previously been shown to elicit great task-induced deactivations in default mode regions (Mayer et al., 2010; McKiernan et al., 2006; McKiernan et al., 2003; Tomasi et al., 2006). Interestingly, we observed greater deactivation during the maintenance phase in the bound task than in the unbound task, although behaviorally the unbound task proved to be more difficult. Also, qualitatively, we observed more task-induced deactivations at each phase of working memory for the bound task compared to the ITI than for the unbound task. A relatively common set of brain regions, termed the default mode network, display deactivations across a variety of tasks (Buckner et al., 2008; Raichle et al., 2001). Task-induced deactivations are thought to represent the reallocation of processing from task-irrelevant brain regions to task specific regions (Fox et al., 2005). It has also been hypothesized that greater deactivations in sensory cortices are necessary to inhibit extrinsic stimuli during tasks requiring attention to internal, or stored, information (Azulay et al., 2009). Therefore, the process of binding letters and locations requires additional cognitive control, in terms of limiting processing in default mode areas. It is intriguing that nearly

the same region greater bound versus unbound activity in the encoding phase had greater bound versus unbound deactivation in the maintenance phase. One possibility, known as the filter hypothesis (Shulman et al., 2007; Shulman et al., 2003), is that the greater maintenance phase deactivation in the visual cortex during the bound task is due to the fact that this region is responding to specific information (bound letters and locations), whereas at during the ITI and the unbound maintenance phase it is responsive to less specific visual stimuli.

Brain-behavior analysis

In addition to observing greater bound-related activity in the left lingual gyrus during the encoding phase versus two different control conditions, we also demonstrate that the activity in this region during the bound task at encoding positively correlates with accuracy in that task. The lingual gyrus displays load-sensitive activity to the visual encoding of objects (Rombouts et al., 1999), and has been proposed as the locale of a homologue to the non-human primate ventral V4, which is involved in visual form processing and visual attention (Gallant et al., 2000). The activation we observed in the lingual gyrus is near the parahippocampal place area, or the lingual landmark area, which is responsible for the encoding and retrieval of visual stimuli of scenes and landscapes (Aguirre et al., 1998; Epstein and Kanwisher, 1998). In regards to being the possible neural substrate for the encoding of letter-location bound items, even early visual areas, including V1 and V2, have been implicated in integrative functions, including attention-driven multi-modal integration (Macaluso et al., 2000) and visual

feature integration (Koivisto and Silvanto, 2012). Finally, it is worth noting that a recent study in non-human primates found that theta-band synchronization, which in humans has been associated with verbal-spatial binding (Wu et al., 2007c), between V4 and the prefrontal cortex predicted performance on a short-term memory task (Liebe et al., 2012).

Connectivity analyses

Functional connectivity analyses can provide complementary information to standard univariate analyses of task activity. For example, the integration of verbal and spatial information in working memory may be a consequence of changes in how different regions interact with each other and not a consequence of changes in activity, *per se*. In our univariate analyses we identified two regions that displayed bound-preferential activity: the left lingual gyrus and the right superior parietal lobule. In subsequent analyses, we compared the functional connectivity of these regions at each working memory phase during the bound and unbound task. Interestingly, we observed that the only region that displayed significantly more activity in the bound task than in the unbound task, the left lingual gyrus, displayed significantly less connectivity in the bound task than in the unbound task to regions that displayed task-induced deactivations. Likewise, the right superior parietal lobule seed-region derived from the secondary comparison of bound task activity versus the averaged verbal and spatial task activity was also significantly less connected in the bound task than in the unbound task to regions displaying task-induced deactivations. Even though the superior parietal

lobule see-region did not differ in activity during the bound task versus the unbound task, its connectivity to other regions did. The fact that both the right superior parietal lobule and the left lingual gyrus seed-regions had significantly less connectivity to several deactivated regions during the bound task further illustrates the importance of the interaction between task-induced activations and deactivations in working memory binding. This echoes a recent study investigating the relationship of memory load and feature binding in working memory (Kochan et al., 2011). During the retrieval phase of a working memory task, they observed an interaction between task type (bound or single features) and load in regions of the default mode network, with higher loads resulting in greater task-induced deactivations. Again, as in the univariate analyses, we find that the binding of letters and locations in working memory requires greater disengagement of default mode region compared to separately holding letters and locations in working memory.

Bound working memory closely resembles spatial working memory

Comparisons of the bound task to the verbal and spatial tasks alone suggest that binding in working memory is spatially driven and limited, as both performance and activity in the spatial task were more similar to the bound task than performance and activity in the verbal task. According to the Feature Integration Theory (Treisman and Gelade, 1980), multiple features are bound together at the perceptual level by attention to the location of the bound construct, referred to as an object file. The role of spatial attention has also been extended to binding in working memory, as it is likely that same

neural mechanisms involved in feature binding are at least partially involved in binding in working memory (Treisman, 2006). The fact that both the imaging and behavior observed for the bound in this study most closely resembled that for the spatial task is consistent with several studies supporting this hypothesis (Campo et al., 2008; Friedman-Hill et al., 1995; Macaluso and Driver, 2005; Shafritz et al., 2002; Treisman and Gelade, 1980).

Limitations and discrepancies with previous studies

This study does have limitations. One limitation that is inherent in many event-related working memory designs is the possibility of high collinearity between the encoding, maintenance, and retrieval variables. Interval time between each trial was jittered, but the length of each task phase was held constant in an attempt to keep the duty cycle comparable for all trials and tasks. However, phases of each task were not compared to each other, but rather were compared to the same phase in different tasks, and similar designs have been used in several studies of working memory (e.g. Kochan et al., 2011; Narayanan et al., 2005). Also, we employed an updated beta-series correlation method for the functional connectivity analyses that reduces the correlation between regressors in the GLM (Mumford et al., 2012; Rissman et al., 2004). Still, given the current design, it is possible that separation of successive encoding, maintenance, and retrieval phases was imperfect, especially for the univariate analyses.

These limitations, along with other differences in methodology, may explain some of the discrepancies between our findings and previous studies on binding in working

memory. For example, some prior studies have identified the prefrontal cortex (Mitchell et al., 2000a; Munk et al., 2002; Prabhakaran et al., 2000) and the hippocampus (Hannula and Ranganath, 2008; Mitchell et al., 2000a; Piekema et al., 2006; Piekema et al., 2009) as being involved in working memory integration, although other studies have not (Campo et al., 2008). Differences in binding instructions, performance, and strategy between study groups could be one source of the observed differences in prefrontal and hippocampus involvement in binding. Further studies will need to address this issue.

Conclusion

In this study we demonstrate the role of visual cortex, primarily the left lingual gyrus, in the encoding of bound verbal and spatial items in working memory. The activity in this region during the encoding phase of the bound task significantly correlated with performance in that task, implicating this region in the initial formation of the bound construct. Furthermore, functional connectivity analyses showed that this region, which was the only region that was more active in the bound task than the unbound task, was significantly less connected to task-negative regions in the bound task than the unbound task. This illustrates the importance of the interplay between task positive and task negative regions in cognitive control. Comparison of bound task activity to a second control condition implicated the right superior parietal lobe a potential bound-relevant region, consistent with previous literature on binding. Finally, our data suggests that the binding of verbal and spatial information is spatially driven, as performance and activity in the bound task was more similar to the spatial task alone

than the verbal task alone. These results fit well with the hypothesis of binding in working memory set forth by Treisman (Treisman, 2006). Accordingly, based on the present data, we suggest that: 1) bound constructs, or object files, are created in the encoding phase, possibly automatically, with the lingual gyrus as a possible neural substrate, 2) these binding are driven, and limited, by spatial attention, with the superior parietal lobule being one candidate region, and 3) no bound constructs are stored, *per se*, during the maintenance phase, but focused attention is necessary to maintain the association between the linked features as evident by the greater connectivity of bound-preferential regions to deactivated regions in the bound task.

Table 2.1

Significant bound task versus unbound task activation

Encoding

Volume	Peak Voxel			Contrast	Hemisphere	Brodmann	Regions
	x	y	z				
7776	48	-45	37	U>	Right	39, 40, 7	Angular gyrus, supramarginal gyrus, precuneus, superior parietal lobule
5130	-18	-72	-16	B>	Left	18, 17	Lingual gyrus, cuneus
4050	18	2	9	U>	Right	--	Putamen, caudate, pallidum, thalamus
2295	-24	-73	24	U>	Left	39, 40, 7	Angular gyrus, supramarginal gyrus, precuneus, superior parietal lobule
2241	18	-77	48	U>	Right	7	Precuneus, superior parietal lobule
1458	44	29	34	U>	Right	9	Middle frontal gyrus

Maintenance

Volume	Peak Voxel			Contrast	Hemisphere	Brodmann	Regions
	x	y	z				
46784	-24	-68	-4	U>	Left	18, 19	Lingual gyrus, cerebellum
24752	14	-61	-15	U>	Right	18	Lingual gyrus, cerebellum
17952	-22	-64	-39	U>	Left	--	Cerebellum

Retrieval

--

Table 2.1: There were multiple clusters of significant differences between the bound task and the unbound task at the encoding and maintenance phases. Volumes are listed in mm^3 and coordinates of the peak voxel for each cluster are in MNI space.

Table 2.2

Significant bound task versus averaged spatial and verbal task activation

Encoding

Volume	Peak Voxel			Contrast	Hemisphere	Brodmann	Regions
	x	y	z				
50112	-28	-94	15	B>	Bilateral	17, 18, 19, 21, 31, 37	Cuneus, lingual gyrus, middle occipital gyrus, middle temporal gyrus, fusiform gyrus, posterior cingulate
2943	20	-80	37	B>	Right	7	Superior parietal lobule, precuneus

Maintenance

Volume	Peak Voxel			Contrast	Hemisphere	Brodmann	Regions
	x	y	z				
7344	18	-69	55	B>	Right	7	Superior parietal lobule, precuneus

Retrieval

Volume	Peak Voxel			Contrast	Hemisphere	Brodmann	Regions
	x	y	z				
4563	-24	-68	-11	B>	Left	18, 19, 37	Lingual gyrus, parahippocampal gyrus, fusiform gyrus
3186	26	-66	-11	B>	Right	18, 19, 37	Lingual gyrus, parahippocampus gyrus, fusiform gyrus

Table 2.2: Multiple clusters had significant differences between bound task activity and the average of spatial and verbal task activity. Volumes are listed in mm^3 and coordinates of the peak voxel for each cluster are in MNI space.

Table 2.3

Significant bound task versus spatial task activation

Encoding

Volume	Peak Voxel			Contrast	Hemisphere	Brodmann	Regions
	x	y	z				
1971	-36	-55	-17	B>	Left	37	Fusiform gyrus
1701	-24	-92	-17	B>	Left	17, 18	Inferior occipital gyrus
1377	24	-92	-12	B>	Right	17, 18	Inferior occipital gyrus

Maintenance

--

Retrieval

Volume	Peak Voxel			Contrast	Hemisphere	Brodmann	Regions
	x	y	z				
1566	-46	26	23	B>	Left	45, 46	Inferior frontal gyrus, middle frontal gyrus

Table 2.3: Only a few clusters had significant differences between bound task activity and spatial task activity. Volumes are listed in mm^3 and coordinates of the peak voxel for each cluster are in MNI space.

Table 2.4

Significant bound task versus verbal task activation

Encoding

Volume	Peak Voxel			Contrast	Hemisphere	Brodmann	Regions
	x	y	z				
97281	-22	-91	10	B>	Bilateral	17, 18, 19, 7, 40, 30, 37	Lingual gyrus, middle occipital gyrus, cuneus, superior parietal lobule, inferior parietal lobule, fusiform gyrus, right middle temporal gyrus, right posterior cingulate
4026	63	-35	-2	V>	Right	22, 21, 13	Middle temporal gyrus, superior temporal gyrus, posterior insula
3807	24	-7	54	B>	Right	6	Middle frontal gyrus, precentral gyrus
2781	36	-92	-12	V>	Right	18	Inferior occipital gyrus
2754	-22	-13	58	B>	Left	6	Middle frontal gyrus, precentral gyrus
2565	44	-62	36	V>	Right	39	Inferior parietal lobule (angular gyrus)
2160	-36	-63	29	V>	Left	39	Inferior parietal lobule (angular gyrus)
1458	30	-76	-52	V>	Right	Crus I	Cerebellum

Maintenance

Volume	Peak Voxel			Contrast	Hemisphere	Brodmann	Regions
	x	y	z				
34290	18	-71	55	B>	Bilateral	7, 40, 19	Superior parietal lobule/precuneus, inferior parietal lobule, middle temporal gyrus, middle occipital gyrus
4536	24	-7	58	B>	Right	6	Middle frontal gyrus, precentral gyrus
2403	55	7	29	B>	Right	9	Inferior frontal gyrus
1944	-22	-15	51	B>	Left	6	Middle frontal gyrus, precentral gyrus
1782	8	17	68	V>	Right	6	Superior medial frontal gyrus
1728	32	-83	-48	V>	Right	Crus II	Cerebellum
1701	38	-60	-8	B>	Right	37, 20, 19	Fusiform gyrus, middle occipital gyrus

Retrieval

Volume	Peak Voxel			Contrast	Hemisphere	Brodmann	Regions
	x	y	z				
46467	-12	-80	-19	B>	Bilateral	18, 19, 37, 30	Fusiform gyrus, lingual gyrus, parahippocampal gyrus, posterior cingulate, middle occipital gyrus, right middle temporal gyrus
2187	24	-76	42	B>	Right	7	Superior parietal lobule/precuneus

Table 2.4: There were numerous clusters that had significant differences between bound task activity and verbal task activity. Volumes are listed in mm^3 and coordinates of the peak voxel for each cluster are in MNI space.

Table 2.5

Left lingual gyrus connectivity- Bound vs. Unbound

Encoding

Volume	Peak Voxel			Contrast	Hemisphere	Brodmann	Regions
	x	y	z				
3726	-48	-32	20	U>	Left	13, 40, 42	Insula, superior temporal gyrus, inferior parietal lobule
2619	8	-8	41	U>	Mid/Right	6, 24	Cingulate, SMA
2052	51	-30	14	U>	Right	13, 40, 42	Insula, superior temporal gyrus, inferior parietal lobule
1701	-22	-48	-24	U>	Left	--	Cerebellum

Maintenance

Volume	Peak Voxel			Contrast	Hemisphere	Brodmann	Regions
	x	y	z				
1755	30	-40	-24	U>	Right	37	Fusiform, cerebellum

Retrieval

--

Table 2.5: There were differences in functional connectivity to the left lingual gyrus seed-region between the bound task and the unbound task at the encoding and maintenance phases. Volumes are listed in mm^3 and coordinates of the peak voxel for each cluster are in MNI space.

Table 2.6

Right superior parietal lobule connectivity- Bound vs. Unbound

Encoding

Volume	Peak Voxel			Contrast	Hemisphere	Brodmann	Regions
	x	y	z				
4482	-42	-26	18	U>	Left	13, 40, 41, 42	Posterior insula, transverse temporal area, inferior parietal lobule
2511	57	-26	25	U>	Right	13, 40	Posterior insula, inferior parietal lobule
2457	-40	1	-19	U>	Left	13, 22	Anterior insula, superior temporal gyrus
1890	38	13	-6	U>	Right	13, 38, 47	Anterior insula, inferior frontal gyrus, temporal pole
1701	6	44	24	U>	Mid/Right	9	Medial frontal gyrus
1539	-6	49	9	U>	Mid/Left	10	Medial frontal gyrus

Maintenance

Volume	Peak Voxel			Contrast	Hemisphere	Brodmann	Regions
	x	y	Z				
5751	2	44	31	U>	Midline	9, 10	Medial frontal gyrus
1863	-12	-56	6	U>	Mid/Left	30/23	Posterior cingulate

Retrieval

--

Table 2.6: There were differences in functional connectivity to the right superior parietal seed-region between the bound task and the unbound task at the encoding and maintenance phases. Volumes are listed in mm^3 and coordinates of the peak voxel for each cluster are in MNI space.

Figure 2.1

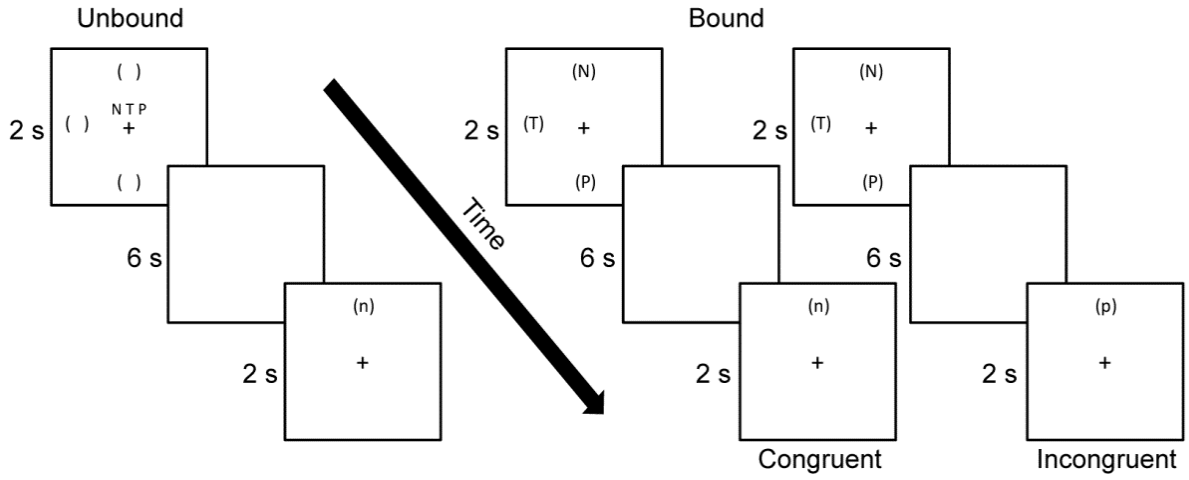
Unbound
Bound
( )
NTP
( ) +
( )
2 s
6 s
2 s
(n)
+
Time
(N)
(T) +
(P)
2 s
6 s
2 s
(n)
+
Congruent
(N)
(T) +
(P)
2 s
6 s
2 s
(p)
+
Incongruent

Figure 2.1: Displayed are examples of the bound and unbound task design. Each is an example of a trial that would require a ‘yes’ response by the participant.

Figure 2.2

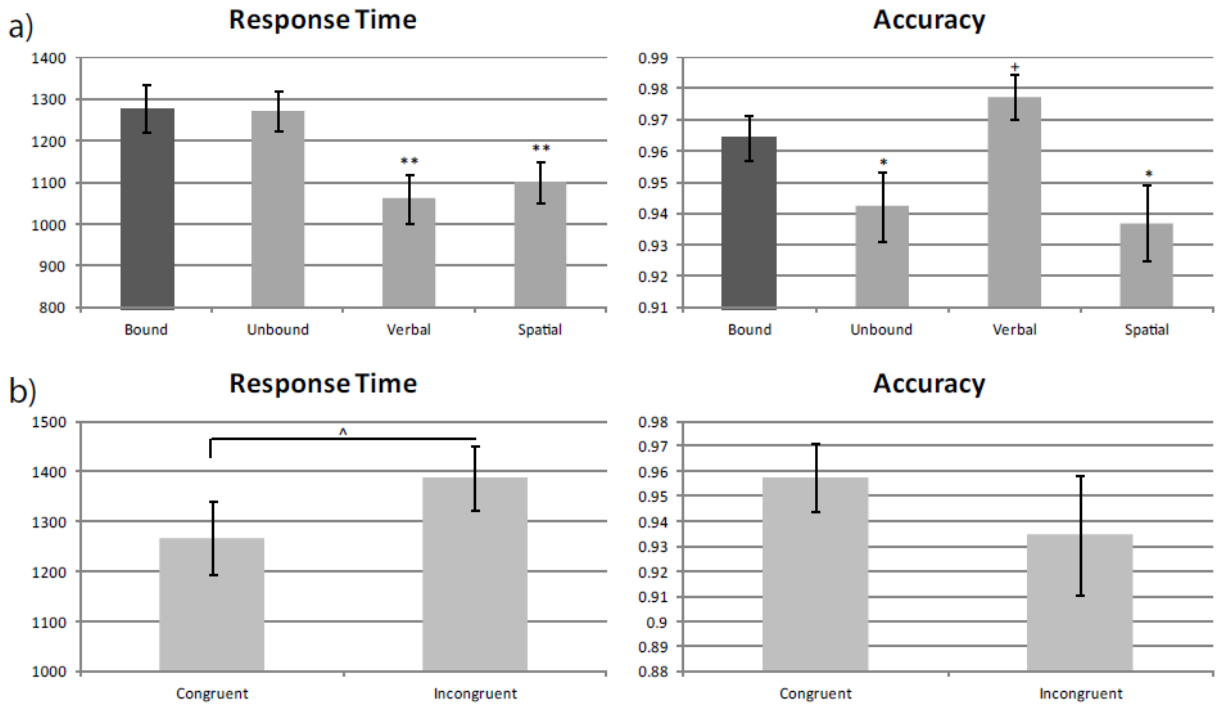
a)
Response Time
1400
1300
1200
1100
1000
900
800
**
**
Bound
Unbound
Verbal
Spatial
Accuracy
0.99
0.98
0.97
0.96
0.95
0.94
0.93
0.92
0.91
+
*
*
Bound
Unbound
Verbal
Spatial
b)
Response Time
1500
1400
1300
1200
1100
1000
^
Congruent
Incongruent
Accuracy
0.98
0.97
0.96
0.95
0.94
0.93
0.92
0.91
0.9
0.89
0.88
Congruent
Incongruent

Figure 2.2: Participants responded significantly faster in the spatial and verbal tasks compared to the bound task (*a*; ** p < .0005). While participants were significantly more accurate in the bound task compared the unbound and spatial tasks (*p < .05), they were significantly less accurate in the bound task compared to the verbal task (+P < .05). Participants responded significantly faster to congruent bound trials than incongruent bound trials, suggesting that they were binding the letters and locations together (*b*; ^p < .05).

Figure 2.3

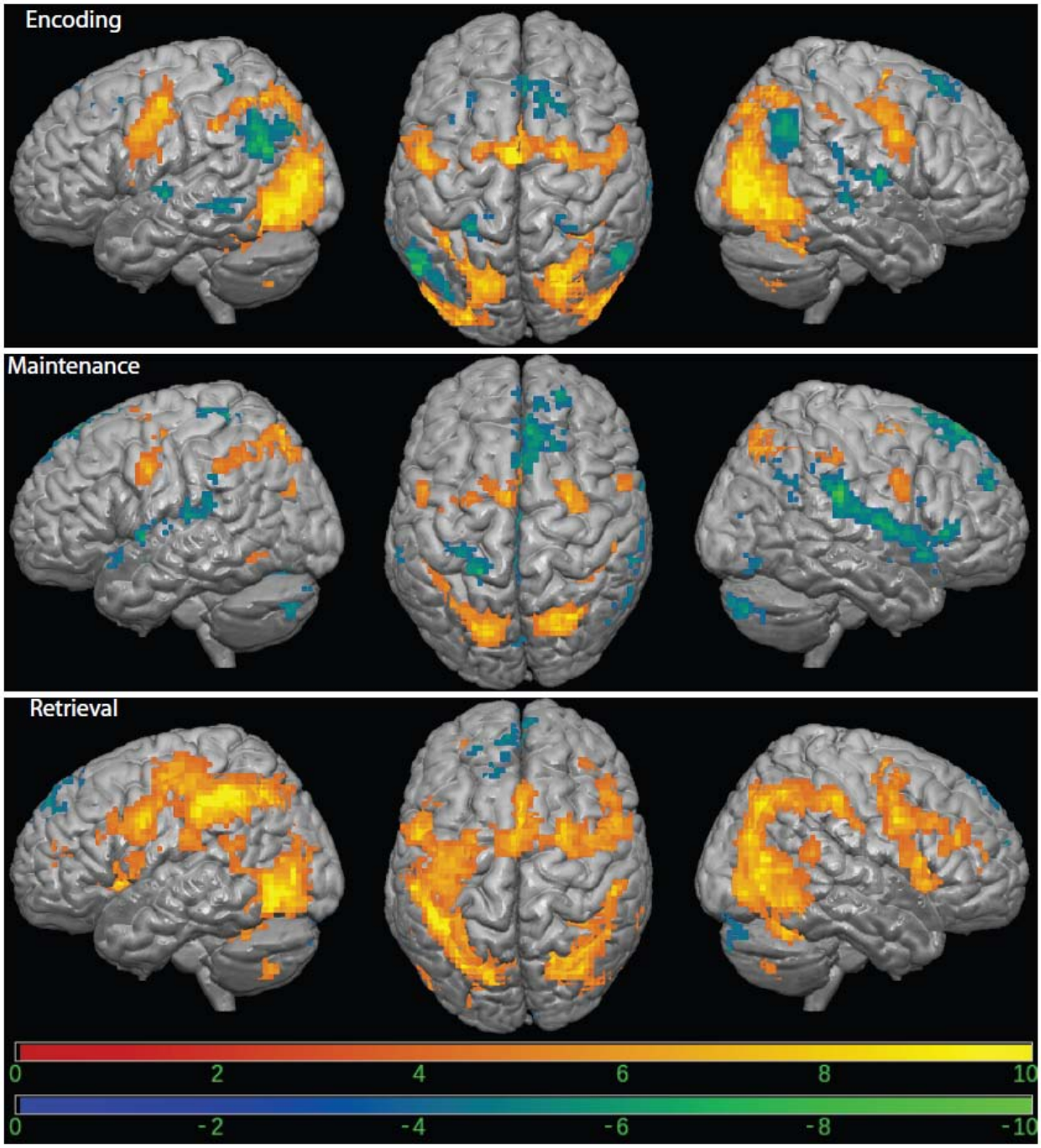

Figure 2.3: Completion of the bound working memory task resulted in robust activations at each working memory phase. Warm colors represent positive task activations compared to ITI and cool colors represent task deactivations compared to ITI. 3dClustSim was used to estimate the appropriate cluster size and threshold to meet statistical significance at family-wise error rate of 0.05 following Bonferroni correction.

Figure 2.4

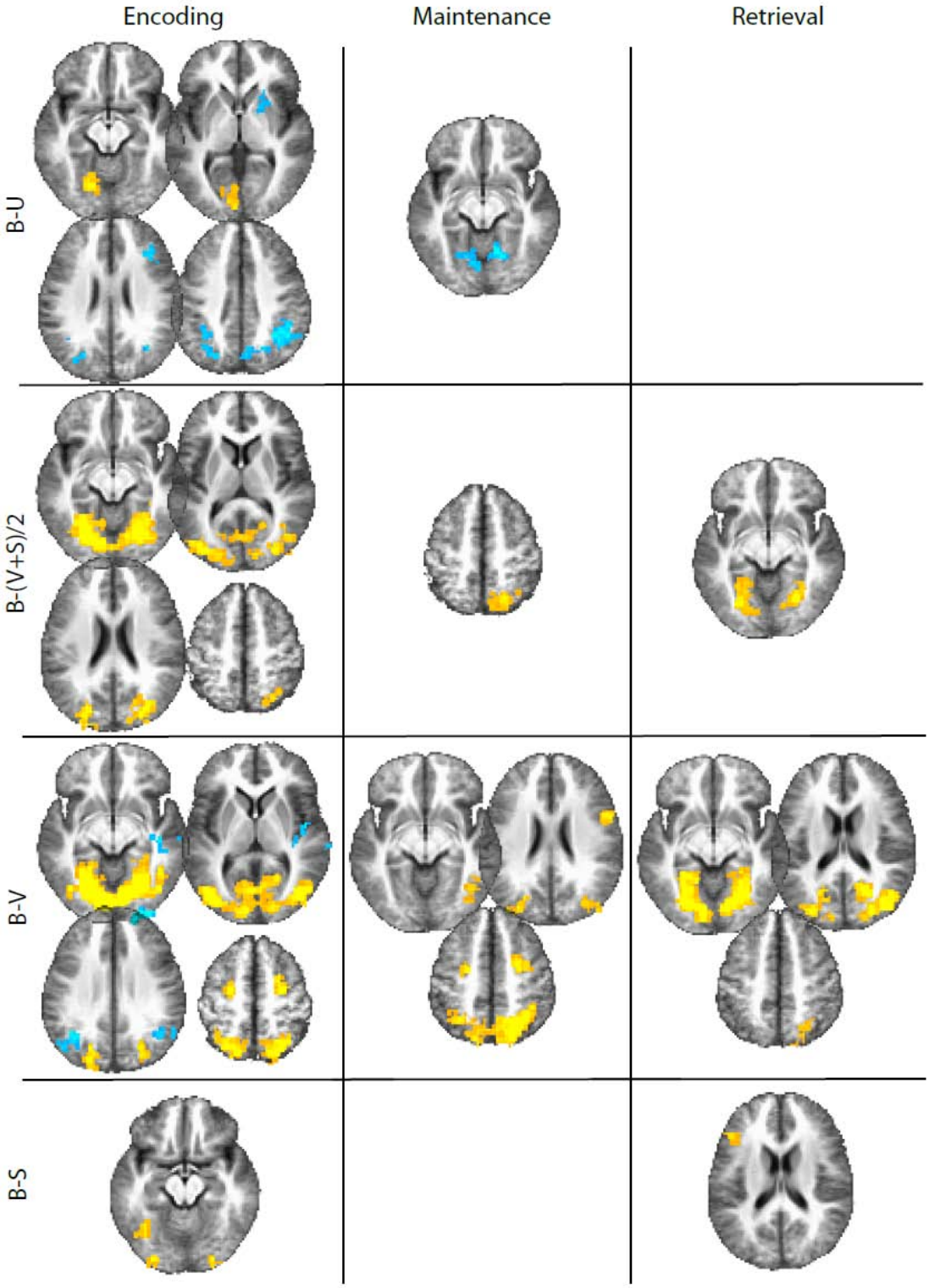

Figure 2.4: Significant differences in activation were observed in several contrasts of the bound working memory task. Warm colors represent greater activity in the bound task, while cool colors represent less activity (or greater deactivation) in the bound task compared to the respective contrast. 3dClustSim was used to estimate the appropriate cluster size and threshold to meet statistical significance at family-wise error rate of 0.05 following Bonferroni correction.

Figure 2.5

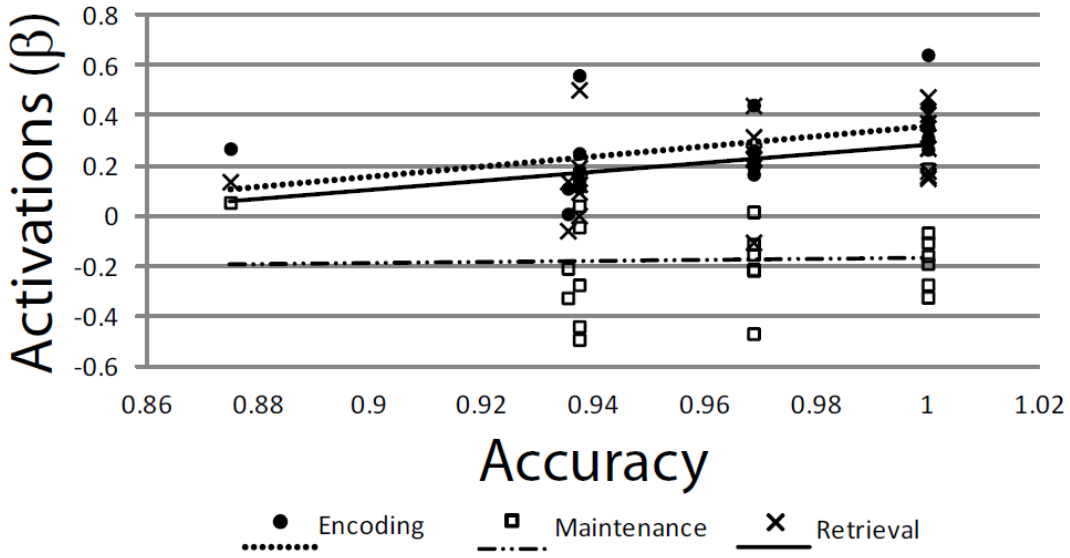
Activations (β)
0.8
0.6
0.4
0.2
0
-0.2
-0.4
-0.6
0.86
0.88
0.9
0.92
0.94
0.96
0.98
1
1.02
Accuracy
Encoding
Maintenance
Retrieval

Figure 2.5: Participants with greater encoding phase activity in the left lingual gyrus during the bound task performed more accurately in that task ($r(19) = .44$, $p < 0.05$). The positive correlation between retrieval phase activity during the bound task was not quite significant ($r(19) = .36$, $p = 0.11$). There was no relationship between maintenance phase activity in the lingual gyrus and accuracy on the bound task.

Figure 2.6

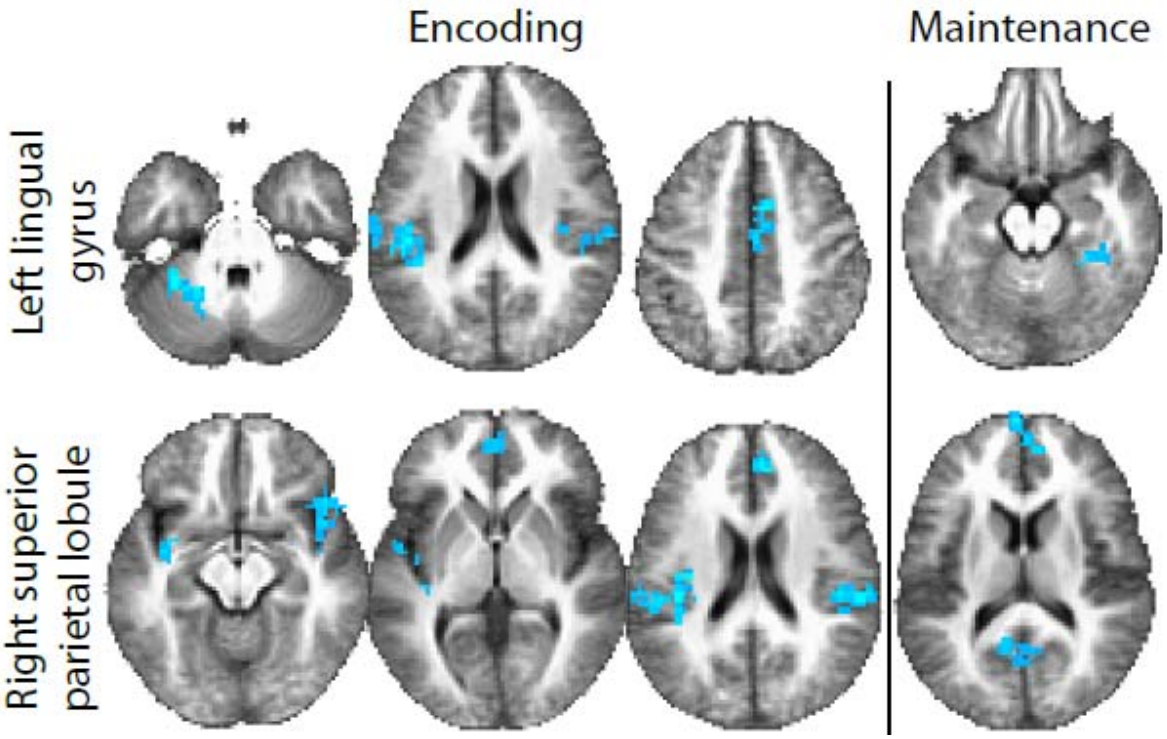
Encoding
Maintenance
Left lingual gyrus
Right superior parietal lobule

Figure 2.6: There were differences in functional connectivity to the left lingual gyrus and right superior parietal lobule during the bound task compared to the unbound task. For both seed-regions, connectivity was lower during the bound task compared to the unbound task to regions that displayed task-induced deactivations. Blue colors indicated greater connectivity in the unbound task than the bound task. 3dClustSim was used to estimate the appropriate cluster size and threshold to meet statistical significance at family-wise error rate of 0.05 following Bonferroni correction.

Reference

Aguirre, G.K., Zarahn, E., D'Esposito, M., 1998. An area within human ventral cortex sensitive to "building" stimuli: evidence and implications. Neuron 21, 373-383.

Azulay, H., Striem, E., Amedi, A., 2009. Negative BOLD in sensory cortices during verbal memory: a component in generating internal representations? Brain Topogr 21, 221-231.

Baddeley, A., 2000. The episodic buffer: a new component of working memory? Trends Cogn Sci 4, 417-423.

Buckner, R.L., Andrews-Hanna, J.R., Schacter, D.L., 2008. The brain's default network: anatomy, function, and relevance to disease. Ann N Y Acad Sci 1124, 1-38.

Campo, P., Maestu, F., Capilla, A., Morales, M., Fernandez, S., del Rio, D., Ortiz, T., 2008. Temporal dynamics of parietal activity during word-location binding. Neuropsychology 22, 85-99.

Chang, C., Crottaz-Herbette, S., Menon, V., 2007. Temporal dynamics of basal ganglia response and connectivity during verbal working memory. Neuroimage 34, 1253-1269.

Cox, R.W., 1996. AFNI: Software for analysis and visualization of functional magnetic resonance neuroimages. Computers and Biomedical Research 29, 162-173.

D'Esposito, M., Aguirre, G.K., Zarahn, E., Ballard, D., Shin, R.K., Lease, J., 1998. Functional MRI studies of spatial and nonspatial working memory. Brain Res Cogn Brain Res 7, 1-13.

Epstein, R., Kanwisher, N., 1998. A cortical representation of the local visual environment. Nature 392, 598-601.

Finke, C., Braun, M., Ostendorf, F., Lehmann, T.N., Hoffmann, K.T., Kopp, U., Ploner, C.J., 2008. The human hippocampal formation mediates short-term memory of colour-location associations. Neuropsychologia 46, 614-623.

Fox, M.D., Snyder, A.Z., Vincent, J.L., Corbetta, M., Van Essen, D.C., Raichle, M.E., 2005. The human brain is intrinsically organized into dynamic, anticorrelated functional networks. Proc Natl Acad Sci U S A 102, 9673-9678.

Friedman-Hill, S.R., Robertson, L.C., Treisman, A., 1995. Parietal contributions to visual feature binding: evidence from a patient with bilateral lesions. Science 269, 853-855.

Gallant, J.L., Shoup, R.E., Mazer, J.A., 2000. A human extrastriate area functionally homologous to macaque V4. Neuron 27, 227-235.

Habeck, C., Rakitin, B.C., Moeller, J., Scarmeas, N., Zarahn, E., Brown, T., Stern, Y., 2005. An event-related fMRI study of the neural networks underlying the encoding, maintenance, and retrieval phase in a delayed-match-to-sample task. Brain Res Cogn Brain Res 23, 207-220.

Hannula, D.E., Ranganath, C., 2008. Medial temporal lobe activity predicts successful relational memory binding. J Neurosci 28, 116-124.

Jonides, J., Smith, E.E., Koeppe, R.A., Awh, E., Minoshima, S., Mintun, M.A., 1993. Spatial working memory in humans as revealed by PET. Nature 363, 623-625.

Kapur, S., Rose, R., Liddle, P.F., Zipursky, R.B., Brown, G.M., Stuss, D., Houle, S., Tulving, E., 1994. The role of the left prefrontal cortex in verbal processing: semantic processing or willed action? Neuroreport 5, 2193-2196.

Kochan, N.A., Valenzuela, M., Slavin, M.J., McCraw, S., Sachdev, P.S., Breakspear, M., 2011. Impact of load-related neural processes on feature binding in visuospatial working memory. PLoS One 6, e23960.

Koivisto, M., Silvanto, J., 2012. Visual feature binding: the critical time windows of V1/V2 and parietal activity. Neuroimage 59, 1608-1614.

Liebe, S., Hoerzer, G.M., Logothetis, N.K., Rainer, G., 2012. Theta coupling between V4 and prefrontal cortex predicts visual short-term memory performance. Nat Neurosci 15, 456-462, S451-452.

Luck, D., Danion, J.M., Marrer, C., Pham, B.T., Gounot, D., Foucher, J., 2010. The right parahippocampal gyrus contributes to the formation and maintenance of bound information in working memory. Brain Cogn 72, 255-263.

Luck, S.J., Vogel, E.K., 1997. The capacity of visual working memory for features and conjunctions. Nature 390, 279-281.

Macaluso, E., Driver, J., 2005. Multisensory spatial interactions: a window onto functional integration in the human brain. Trends Neurosci 28, 264-271.

Macaluso, E., Frith, C.D., Driver, J., 2000. Modulation of human visual cortex by crossmodal spatial attention. Science 289, 1206-1208.

Mayer, J.S., Roebroeck, A., Maurer, K., Linden, D.E., 2010. Specialization in the default mode: Task-induced brain deactivations dissociate between visual working memory and attention. Hum Brain Mapp 31, 126-139.

McKiernan, K.A., D'Angelo, B.R., Kaufman, J.N., Binder, J.R., 2006. Interrupting the "stream of consciousness": an fMRI investigation. Neuroimage 29, 1185-1191.
McKiernan, K.A., Kaufman, J.N., Kucera-Thompson, J., Binder, J.R., 2003. A parametric manipulation of factors affecting task-induced deactivation in functional neuroimaging. J Cogn Neurosci 15, 394-408.

Mitchell, K.J., Johnson, M.K., Raye, C.L., D'Esposito, M., 2000. fMRI evidence of age-related hippocampal dysfunction in feature binding in working memory. Brain Res Cogn Brain Res 10, 197-206.

Morey, C.C., 2009. Integrated cross-domain object storage in working memory: evidence from a verbal-spatial memory task. Q J Exp Psychol (Hove) 62, 2235-2251.

Mumford, J.A., Turner, B.O., Ashby, F.G., Poldrack, R.A., 2012. Deconvolving BOLD activation in event-related designs for multivoxel pattern classification analyses. Neuroimage 59, 2636-2643.

Munk, M.H., Linden, D.E., Muckli, L., Lanfermann, H., Zanella, F.E., Singer, W., Goebel, R., 2002. Distributed cortical systems in visual short-term memory revealed by event-related functional magnetic resonance imaging. Cereb Cortex 12, 866-876.

Narayanan, N.S., Prabhakaran, V., Bunge, S.A., Christoff, K., Fine, E.M., Gabrieli, J.D., 2005. The role of the prefrontal cortex in the maintenance of verbal working memory: an event-related FMRI analysis. Neuropsychology 19, 223-232.

Olson, I.R., Page, K., Moore, K.S., Chatterjee, A., Verfaellie, M., 2006. Working memory for conjunctions relies on the medial temporal lobe. J Neurosci 26, 4596-4601.

Owen, A.M., Stern, C.E., Look, R.B., Tracey, I., Rosen, B.R., Petrides, M., 1998. Functional organization of spatial and nonspatial working memory processing within the human lateral frontal cortex. Proc Natl Acad Sci U S A 95, 7721-7726.

Paulesu, E., Frith, C.D., Frackowiak, R.S., 1993. The neural correlates of the verbal component of working memory. Nature 362, 342-345.

Piekema, C., Kessels, R.P., Mars, R.B., Petersson, K.M., Fernandez, G., 2006. The right hippocampus participates in short-term memory maintenance of object-location associations. Neuroimage 33, 374-382.

Piekema, C., Kessels, R.P., Rijpkema, M., Fernandez, G., 2009. The hippocampus supports encoding of between-domain associations within working memory. Learn Mem 16, 231-234.

Prabhakaran, V., Narayanan, K., Zhao, Z., Gabrieli, J.D., 2000. Integration of diverse information in working memory within the frontal lobe. Nat Neurosci 3, 85-90.

Raichle, M.E., MacLeod, A.M., Snyder, A.Z., Powers, W.J., Gusnard, D.A., Shulman, G.L., 2001. A default mode of brain function. Proc Natl Acad Sci U S A 98, 676-682.
Rissman, J., Gazzaley, A., D'Esposito, M., 2004. Measuring functional connectivity during distinct stages of a cognitive task. Neuroimage 23, 752-763.

Rombouts, S.A., Scheltens, P., Machielson, W.C., Barkhof, F., Hoogenraad, F.G., Veltman, D.J., Valk, J., Witter, M.P., 1999. Parametric fMRI analysis of visual encoding in the human medial temporal lobe. Hippocampus 9, 637-643.

Shafritz, K.M., Gore, J.C., Marois, R., 2002. The role of the parietal cortex in visual feature binding. Proc Natl Acad Sci U S A 99, 10917-10922.

Shulman, G.L., Astafiev, S.V., McAvoy, M.P., d'Avossa, G., Corbetta, M., 2007. Right TPJ deactivation during visual search: functional significance and support for a filter hypothesis. Cereb Cortex 17, 2625-2633.

Shulman, G.L., McAvoy, M.P., Cowan, M.C., Astafiev, S.V., Tansy, A.P., d'Avossa, G., Corbetta, M., 2003. Quantitative analysis of attention and detection signals during visual search. J Neurophysiol 90, 3384-3397.

Smith, E.E., Jonides, J., Koeppe, R.A., 1996. Dissociating verbal and spatial working memory using PET. Cereb Cortex 6, 11-20.

Todd, J.J., Marois, R., 2004. Capacity limit of visual short-term memory in human posterior parietal cortex. Nature 428, 751-754.

Tomasi, D., Ernst, T., Caparelli, E.C., Chang, L., 2006. Common deactivation patterns during working memory and visual attention tasks: an intra-subject fMRI study at 4 Tesla. Hum Brain Mapp 27, 694-705.

Treisman, A., 1996. The binding problem. Curr Opin Neurobiol 6, 171-178.

Treisman, A., 2006. Object tokens, binding and visual memory. In: Zimmer, H.D., Mecklinger, A., Lindenberger, U. (Eds.), Handbook of binding and memory: Perspectives from Cognitive Neuroscience. Oxford University Press, New York, pp. 315-338.

Treisman, A.M., Gelade, G., 1980. A feature-integration theory of attention. Cogn Psychol 12, 97-136.

Wheeler, M.E., Treisman, A.M., 2002. Binding in short-term visual memory. J Exp Psychol Gen 131, 48-64.

Wu, X., Chen, X., Li, Z., Han, S., Zhang, D., 2007. Binding of verbal and spatial information in human working memory involves large-scale neural synchronization at theta frequency. Neuroimage 35, 1654-1662.

Xu, Y., 2007. The role of the superior intraparietal sulcus in supporting visual short-term memory for multifeature objects. J Neurosci 27, 11676-11686.

Chapter 3

Age-related differences in the neural correlates of letter-location binding

Timothy B. Meier, Rasmus M. Birn, Mary E. Meyerand, Vivek Prabhakaran

In preparation

Abstract:

In this study we investigated age-related differences in the binding of verbal and spatial information in event-related working memory tasks. Twenty-one younger adults and twenty-one older adults performed two combined verbal and spatial working memory tasks. In the *unbound* version letters and locations were presented in a simultaneous, but separate fashion, while in the *bound* version each letter was paired with a specific location. In order to identify binding-specific differences, mixed-effects ANOVAs were run with the interaction of age and task as the effect of interest. Although older adults performed worse in the bound task, there was no interaction between task and age on working memory performance, meaning that there was no age-related deficit in binding, *per se*. However, interactions of age and task were observed in brain activity and functional connectivity analyese. For brain activity, older adults did not display the greater unbound than bound task activity that younger adults did. In the functional connectivity analyses, older adults did not display the greater dissociation between connectivity of task-positive regions to task-negative regions in the bound task compared to the unbound task that younger adults did. We conclude that the binding of letters and locations in working memory is not as efficient in older adults as it is in younger adults, possibly due to the inability to suppress brain regions not directly involved in working memory binding.

Introduction

Age-related decline in working memory has been hypothesized as being the core cause of higher-order cognitive decline that is associated with normal aging (Verhaeghen and Salthouse, 1997). However, the mechanisms behind age-related deficits in working memory are not well understood. One theory, known as the associative deficit hypothesis, is that deficits observed in memory with advancing age are due to the increased inability to form, maintain, and retrieve associations between different types of information (Chalfonte and Johnson, 1996; Naveh-Benjamin, 2000). Forming associations, or binding information, is particularly important in working memory, as the capacity of working memory is limited by the number of bound objects and not the total amount of separate information that may be presented (Luck and Vogel, 1997).

Several studies have demonstrated the existence of a binding deficit in episodic memory (Chalfonte and Johnson, 1996; Naveh-Benjamin, 2000; Naveh-Benjamin et al., 2004; Naveh-Benjamin et al., 2003; Plancher et al., 2010), but evidence supporting a binding deficit in working memory has been conflicting. For example, in studies by Mitchell et al. older adults were not able to bind objects and locations in working memory as successfully as younger adults, possibly due to the binding-specific hippocampal activity that was observed in younger adults but not in older adults (Mitchell et al., 2000a; Mitchell et al., 2000b). Similarly, Cowan et al. found that older adults were less able to identify changes in bound items in working memory than

younger adults (Cowan et al., 2006). In contrast, other studies suggest that there are no age-related deficits in working memory binding (Brockmole et al., 2008; Gilchrist et al., 2008; Parra et al., 2009). Furthermore, few studies, to our knowledge, has attempted to characterize age-related differences brain activation during working memory binding (Mitchell 2000). Thus, the nature of age-related changes in working memory binding, and the brain basis behind these changes remain unresolved.

In a previous study using event-related fMRI in young adults only, we have shown that the binding of letters and locations in working memory is more efficient than the simultaneous working memory of separate letters and locations (Chapter 2). Working memory of bound information was more efficient in that participants performed better in the bound condition and also had less brain activation in classic working memory regions during the bound task compared to the separate condition. However, this efficiency was at the cost of greater task-induced deactivations during the bound task, which we contributed to a form of cognitive control. Here, using the same event-related fMRI design, we test the hypothesis that older adults have deficits in binding in working memory performance, and investigate age-related difference in brain activation during working memory binding. Specifically, by using two combined spatial and verbal working memory tasks we investigate the interaction between age group and task type to see if there are age effects on the difference between activations during task in which letter-location binding is possible and during a task in which letters and locations must be remembered separately.

Methods

Subjects

Twenty-one young adults (13 male, 8 female; 24.6 ± 0.69 years old) and twenty-one older adults (11 male, 10 female; 57.8 ± 1.49 years old) were enrolled for this study after providing informed consent. All subjects were confirmed to be strongly right-handed based on the Edinburgh Handedness Inventory, had normal or corrected to normal vision, and had at least some college education. Younger adults and older adults each had an average of 17 years of education (some graduate or professional education). Participants reported no use of neuroactive medications and no history of mental illness. All aspects of this study were approved by the University of Wisconsin-Madison Health Sciences Institutional Review Board. Data from the younger subjects in this study have been previously reported (Chapter 2).

Task Design

Participants performed four versions of an item-recognition task in the MR-scanner. Stimuli were presented in the center of a back-projected screen and participants responded using a MR-compatible button box. Each task consisted of 32 trials each with an encoding phase of two seconds, a six second maintenance phase, a two second retrieval phase, and a varying inter-trial interval. Participants were instructed to indicate whether or not a probe stimuli presented at the retrieval phase was included in the encoding phase they had just seen. Task order was randomized across subjects

and each task type included an equal number of positive probes (requiring a ‘yes’ response) and negative probes (requiring a ‘no’ response).

Subjects performed a verbal and spatial working memory task, and two combined verbal and spatial working memory tasks. Only the combined verbal and spatial tasks are included in this study. In the *unbound* combined spatial and verbal working memory task, subjects were simultaneously presented with three upper-case letters at the center of the screen and three locations indicated by parentheses around an imaginary clock-face during the encoding phase. At the retrieval phase, a single lower-case letter was presented at a single location and participants had to decide whether or not both the letter and location were included in the encoding set.

In the *bound* combined spatial and verbal working memory task, subjects were presented with three upper-case letters presented at three locations around an imaginary clock face during the encoding phase. During the retrieval phase, subjects were presented with a single lower-case letter at a single location and had to determine whether or not both were presented during the encoding phase. However, the letter and location presented at the retrieval phase did not necessarily have had to been paired together during the encoding phase, as long as they each were presented in the encoding phase. Therefore, there were two types of positive probe trials in the bound task. In *congruent* trial, the single letter presented at the retrieval phase was in the exact same location that was in during the encoding phase. In *incongruent* trials, the letter presented at the retrieval phase was not in the exact same location as it was at the

encoding phase, but was in one of the other two locations presented at the encoding phase. The comparison of congruent and incongruent trials can be used to confirm subjects were binding the letters and locations.

Participants practiced the task outside of the scanner until it was deemed that they understood the task rules. Prior to each specific scan, subjects were reminded of the rules for the task version they were about to complete.

Behavioral analysis

Percent accuracy and response time for the bound task versus the unbound task, and congruent bound trials versus incongruent bound trials, were compared using mixed design analyses of variance with task as within-subjects factor and subjects nested in the between-subjects factor of age. Only trials in which participants attempted were included in the analyses.

fMRI acquisition and preprocessing

Scans were collected on a 3T MRI scanner (GE Healthcare, Waukesha, WI) using gradient-echo echo-planar imaging with the following parameters: TR = 2.6 s, TE = 22 ms, field of view = 22.4 cm, flip angle = 60°, 40 sagittal slices, acquisition matrix = 64 x 64, 3.5 mm isotropic voxel size, 231 time-points. T1-weighted anatomical images were collected using a FSPGR BRAVO sequence (TR = 8.132 ms, TE = 3.18 ms) over a 256 x 256 matrix and 156 slices (flip angle = 12°, FOV = 25.6 cm, slice thickness = 1 mm). For each working memory task variation a separate scan consisting of 185

volumes was collected, with approximately ten seconds of baseline signal were acquired before and after each scan. All working memory scans were collected during the same visit.

The first three volumes from each scan were removed to allow for magnet stabilization. Each functional scan was then despiked, registered to its first volume for motion correction, slice time corrected, spatially smoothed with a 4 mm FWHM Gaussian kernel, and converted to percent signal change. All preprocessing and analysis of imaging data was done in the AFNI program suite (Cox, 1996).

As done in Chapter 2, a fixed-effect model was used at the subject level for each task variation. Functional data were modeled using the general linear model in which the encoding, maintenance, and retrieval phases were modeled separately by convolving a 2 second, 6 second, and 2 second block stimulus to each event, respectively, with a canonical hemodynamic response function. Incorrect trials were modeled separately, but only correct trials were carried into the group analyses. For each task version, beta parameters were estimated for each phase. In order to allow comparison across subjects, each subject's anatomical scan was aligned to their functional scan and then both the aligned anatomical and the statistical images were normalized to a standard template space and resampled to 3 x 3 x 3 mm voxel size.

Univariate fMRI analysis

The primary goal of this work was to indentify age-related differences in the neural basis of letter and location binding. To do so, separate mixed-design analyses of

variance were run for each phase with task as a within-subjects factor and the random factor subjects nested in the between-subjects factor of age. Previously, in younger adults, we showed that the comparison of brain activity in the bound task to the unbound task identifies brain regions that display bound-specific activations (or deactivations), as the only difference between these tasks is the ability to bind letters and locations in the bound task (Chapter 2). Here, we were primarily interested in the interaction of task by age. That is, we wanted to identify the effects of age on the difference between bound task activity and unbound task activity. The approximate smoothness of our data was estimated via 3dFWHMx program in AFNI, and 3dClustSim was used to estimate the appropriate cluster size and threshold to meet statistical significance at family-wise error rate of 0.05 following Bonferroni correction for the number of ANOVAs performed.

Task functional connectivity analysis

Functional connectivity can proved complementary information regarding brain networks responsible for working memory. Here, we used a multivariate method, a modified beta-series correlation, to assess functional connectivity at each phase of the bound task. In beta-series correlation, each event is separately modeled as a regressor of interest in the general linear model (GLM) (Rissman et al., 2004). Beta values for each event type can then be concatenated in time and seed-based correlation analyses can be run on the subsequent beta-series. A modification of this method has recently been proposed, referred to by the authors as the Least Squares Separate (LSS) method

(Mumford et al., 2012). For LSS beta-series regression, a separate GLM is run for each event in which that event is modeled as a regressor of interest and all other events are modeled as regressors of no interest. The motivation behind separately modeling events is the reduction of collinearity between regressors in the GLM, a common problem in event-related working memory designs.

For this study we applied LSS beta-series correlation, performing separate GLMs for each phase of each trial in which all other phases and trials were modeled as regressors. The beta values were then grouped according to phase and concatenated over time. This resulted in three series of beta values (beta-series), one for each phase of both bound and unbound working memory tasks. Seed-based connectivity analyses were performed on the beta-series for each phase of both tasks. Four seed regions were selected for analysis. Two seed-regions, the right superior parietal lobule (MNI 18 -68 55) and the left lingual gyrus (MNI -18 -71 -15) were selected based on our previous study of binding in young adults which implicated these regions in working memory binding (Chapter 2). In addition, two seed-regions, the medial frontal gyrus (MNI 0 50 24) and the posterior cingulate (MNI 0 -55 25), were selected based on the local minimum of deactivation from a one-sample t-tests of bound task activity across both groups and all phases of the bound task. These regions were selected based on our previous research implicating the importance of the relationship between activations and deactivations during performance of the bound task (Chapter 2), and on the fact that they represent two common hubs of the default mode network which often displays task-induced deactivation (Raichle et al., 2001). The beta-series of every voxel within a

5mm radius sphere were averaged for each seed-region and the resultant series was then correlated with the beta-series of every other voxel in the brain. Correlation coefficients were Fisher-transformed and normalized to a z-score to allow for group level statistics. Mixed-effects analyses of variance identical to those used in the univariate analyses were performed at each phase for each seed-region. Again, we were interested in brain regions that displayed an interaction of task by age to identify brain regions in which there was an effect of age on the contrast of bound versus unbound task connectivity. 3dClustSim was used to estimate the appropriate cluster size and threshold to meet statistical significance at family-wise error rate of 0.05 following Bonferroni correction for the number of ANOVAs performed.

Results

Behavioral data

Mixed-design analyses of variance were run on response time and accuracy. For response time, neither the main effect of task ($F(1, 40) = 1.23$, $MSE = 8134.21$, $p > .1$), nor the interaction of task by age ($F, 1, 40) = 2.13$, $MSE = 8134.21$, $p > .1$), were significant. The main effect of age on response time was significant ($F, 1, 40) = 5.91$, $MSE = 123411.27$, $p < .05$), with younger adults responding faster than older adults (**Figure 3.1a)**. Similarly, for accuracy, neither the main effect of task ($F(1, 40) = 1.76$, $MSE = .003$, $p > .1$), nor the interaction between task and age ($F(1, 40) = .147$, $MSE = .003$, $p > .1$), were significant. However, the effect of age on accuracy was significant (F

(1, 40) = 11.78, MSE = .007, p < .005), with younger adults performing more accurately than older adults (**Figure 3.1a**).

Identical analyses of variance were performed on accuracy and response time for the different types of positive bound trials. There was a significant effect of task (F (1, 40) = 29.83, MSE = 15084.18, p < .001) and age (F (1, 40) = 29.83, MSE = 15084.18, p < .001) on response time. Younger adults responded faster than older adults for both congruent and incongruent bound trials, and both younger and older adults responded faster for congruent trials than incongruent trials (**Figure 3.1b**). There was no interaction between age and task for response time (F (1, 40) = .98, MSE = 15084.18, p > .1). For accuracy, both the main effect of task (F (1, 40) = 5.68, MSE = .009, p < .05) and the main effect of age F (1, 40) = 4.286, MSE = .028, p < .05) were significant. Both younger and older adults were more accurate in congruent trials than incongruent trials, indicated that both groups were binding letters and locations together. Younger adults were more accurate in both trials types compared to older adults (**Figure 3.1b**). There was no interaction between the factors of task and age (F (1, 40) = 1.62, MSE = .009, p > .1).

fMRI data – Interaction of age and task type

Previously, we identified binding-specific activations (and deactivations) in younger adults by comparing bound activity to unbound activity at each phase (Chapter 2). The unbound task serves as an appropriate contrast to the bound task, as the total amount of information presented for both tasks is the same. The primary goal of this

study was to investigate the effect of age on the difference between bound activity and unbound activity (B-U) (**Figure 3.2, Table 3.2**). There were three clusters in which older adults had significantly greater B-U activity during the encoding phase of the bound task compared to younger adults. These included a cluster in the right inferior parietal lobule (BA 40, 39), a cluster in the left inferior parietal lobule (BA 40, 39), and a cluster in the right putamen and globus pallidus. For these regions, younger adults display significantly more activity during the unbound task than during the bound task, which we have contributed to the relative efficiency of binding (Chapter 2). However, older adults do not show this difference in activity between the bound and unbound tasks.

For the maintenance phase, there was a significant cluster located in the left cerebellum in which older adults had greater B-U activity than younger adults. Whereas younger adults displayed greater unbound than bound activity, older adults displayed greater bound than unbound activity in this region (**Figure 3.2**). There were no significant interactions for the retrieval phase.

Effect of age on task functional connectivity

Investigation of functional connectivity can provide an additional insight into the neural basis of binding. We investigated the interaction of age and task for functional connectivity to four seed-regions. Previous research in our lab has implicated the right superior parietal lobule and the left lingual gyrus in the binding of letters and locations in working memory (Chapter 2). In addition, we also have shown that the bound task requires greater deactivation in certain regions compared to the unbound task.

Therefore, the right superior parietal lobule (MNI 18 -68 55) and left lingual gyrus (MNI -18 -71 -15) seed-regions were selected based on the univariate analysis of our previous study on binding in younger adults. Seed-region in the medial frontal gyrus (MNI 0 50 24) and the posterior cingulate (MNI 0 -55 25) were selected based on the extreme minima of deactivation observed across all phases of the bound task across both young and old subjects.

There was no interaction between task and age for functional connectivity to the lingual gyrus seed-region at any phase, meaning that there were no age differences in the comparison between connectivity during the bound task and connectivity during the unbound task. For the right superior parietal lobule seed-region, there was an interaction of age and task during the encoding phase in a cluster located in the right insula and inferior parietal lobule extending into the postcentral gyrus (**Figure 3.3, Table 3.3**). Younger adults had greater unbound than bound encoding phase connectivity to this region, which displayed deactivation during bound task, while older adults did not (**Figure 3.3**). There were no interactions between age and task for the right superior parietal seed-region at the maintenance or retrieval phases.

There was a significant interaction of age and task during the encoding phase for connectivity to the medial frontal gyrus in a cluster located at the right precentral gyrus (BA 6; **Figure 3.3, Table 3.3**). Again, for this region, which displayed task positive activation during the bound task, younger adults had greater unbound than bound

connectivity, while older adults did not. There were no interactions between age and task for the medial frontal gyrus seed-region at the maintenance or retrieval phases.

There were several regions that had significant interactions of age and task for connectivity to the posterior cingulate seed-region (**Figure 3.3, Table 3.3**). For all of these regions, younger adults had greater connectivity to the posterior cingulate during the unbound task than the bound task, while older adults did not. At the encoding phase, these included regions that displayed positive bound-task activity, including the right precentral gyrus (BA 6) extending into the postcentral gyrus (BA 4), the right precuneus (BA 7), the left cerebellum, and the right thalamus. In addition, the right postcentral gyrus (BA 3), which displayed task-induced deactivation during the bound task, also had a significant interaction at the encoding phase.

Two clusters had significant interactions of age and task for posterior cingulate connectivity during the maintenance phase (**Figure 3.3, Table 3.3**). These included the left postcentral and postcentral gyrus (BA 3, 4) and the left paracentral lobule and postcentral gyrus. For these regions, younger adults again had greater unbound than bound task connectivity to the posterior cingulate while older adults did not. There were no interactions between task and age for posterior cingulate seed-region connectivity at the retrieval phase.

Discussion

In this study, we investigated the effects of age on the neural basis of letter-location binding using event-related fMRI working memory tasks. Both older and

younger adults performed better in the bound working memory task than in the unbound working memory task. In addition, both older and younger adults performed better in congruent bound trials than in incongruent bound trials, suggesting that both age-groups were actually binding letter and locations during the bound task.

Younger adults performed better than older adults in both the bound and unbound tasks. However, at the behavioral level, there were no interactions between task and age. Therefore, our data suggest that although older adults were impaired in the binding working memory task, this impairment is not due to a specific deficit in binding, *per se*, but instead is due to a general decline in working memory. These results are consistent with previous behavioral studies that have also found a lack of binding deficit in working memory with advancing age (Brockmole et al., 2008; Gilchrist et al., 2008; Parra et al., 2009). However, other studies of binding in working memory have demonstrated an effect of age (Cowan et al., 2006; Mitchell et al., 2000a; Mitchell et al., 2000b). Discrepancies between studies could possibly be explained by different types of stimuli used in each study, or by the control task used to compare binding performance. We compare letter-location binding in working memory to a working memory task containing the same number of letters and locations in a separate fashion. Therefore, any differences should be due to the ability to bind information together. Our data suggest that, at the behavioral level, the binding deficit often observed in episodic memory (Chalfonte and Johnson, 1996; Naveh-Benjamin, 2000; Naveh-Benjamin et al., 2004; Naveh-Benjamin et al., 2003; Plancher et al., 2010) is not present in working memory.

Univariate analysis

The primary goal of this study was to investigate the effect of age on the neural basis of working memory binding. To do so, we investigated the effect of age on the difference between brain activity during the bound working memory task and the unbound working memory task, the interaction of age by task, at each phase of working memory. The unbound task is an appropriate control for the bound task, as both task involve the same amount of spatial and verbal information. However, while letters and locations have to be remembered separately in the unbound task, bound pairs of letters and locations can be remembered together in the bound task. Previously, in younger adults, we showed that at the encoding phase the bound working memory task requires less brain activity than the unbound working memory task in bilateral parietal regions, which we attributed to the relative efficiency of encoding bound items compared to separate items (Chapter 2). Here, we found that older adults did not display this difference in bound and unbound inferior parietal lobule activity at the encoding phase. In addition, older adults did not have differences in bound and unbound activity in the right putamen and globus pallidus that younger adults had. Finally, at the maintenance phase older adults did not have the greater unbound activity than bound activity in the cerebellum that younger adults had. These data suggest that the encoding and maintenance of bound information in working memory is not as efficient in older adults as it is in younger adults in terms of the amount of brain resources needed. Prior studies have found similar effects of age on cognition, with older adults displaying greater

activity in task-positive areas than younger adults (Grady et al., 2010). In this study, we observe this for the bound task relative to the unbound task.

Connectivity analyses

Functional connectivity analyses can provide additional information regarding the nature of age-related changes in the neural basis of binding in working memory. In younger adults we have shown that the right superior parietal lobule and left lingual gyrus are involved in the binding of letters and location in working memory (Chapter 2). Additionally, we demonstrated the importance of interactions between regions displaying bound-related activations and bound-related deactivations. In this study, we were interested in the interaction of age and task on functional connectivity to two binding-related seed-regions and two task-negative seed-regions during the encoding, maintenance, and retrieval phases to better characterize age-related deficits in binding-specific brain patterns.

A consistent pattern of age-related differences emerged from the analysis of functional connectivity. For every seed-region that displayed an interaction of age and task, this interaction was a result of older adults not having the greater unbound task connectivity than bound task connectivity that younger adults had. Moreover, differences in connectivity to the task positive right superior parietal seed-region were found in a task negative region, while nearly all clusters having differences in connectivity to the task negative seed-regions (medial frontal gyrus and posterior cingulate) were located in areas that displayed task positive activation.

In our previous study in younger adults only, we showed that the bound working memory task required more task deactivations than the unbound working memory task, which we attributed to an increase need for cognitive, or attentional, control during the binding letters and locations (Chapter 2). This interpretation is consistent with several studies that have shown greater deactivations in the default mode network for more demanding cognitive tasks (Hampson et al., 2006; McKiernan et al., 2003). In addition, previous studies have demonstrated that older adults are less capable of suppressing activity in task-negative regions than younger adults, possibly due to a reduction in cognitive control with advancing age (Grady et al., 2006; Lustig et al., 2003; Persson et al., 2007; Sambataro et al., 2010). We take this a step further and show that older adults do not have the dissociation in functional connectivity between task-positive and task-negative areas in the bound compared to the unbound task that younger adults.

Limitations

This study has limitations that must be considered. The primary limitation is that, due to the nature of event-related working memory task used, it is possibility of collinearities existing between the encoding, maintenance, and retrieval phases of our task. Although inter-trial intervals were jittered, the length of each phase was held constant in order to have comparable duty cycles for every task and trial type, similar to several previous working memory studies (Kochan et al., 2011; Narayanan et al., 2005). Furthermore, at the group level, phases were not compared to each other, but rather to the same phase of a different task. Finally, for the functional connectivity analyses, an

updated version of the beta-series correlation method that reduces collinearity between regressors was used in an attempt to attenuate the collinearity problem (Mumford et al., 2012; Rissman et al., 2004).

Summary

We investigated the effects of age on the difference in working memory tasks with and without letter-location binding. At the behavioral level, although older adults performed worse than younger adults in the bound working memory task, there was no interaction of age and task type, meaning that the deficit was likely due to a general age deficit in working memory and not specifically in the ability to binding letters and locations together. However, interactions of age and task were observed in brain activity and functional connectivity. For brain activity, older adults did not display the greater unbound than bound task activity that younger adults did. In the functional connectivity analyses, older adults did not display the greater dissociation between connectivity of task-positive regions to task-negative regions in the bound task compared to the unbound task that younger adults did. Therefore, we conclude that the binding of letters and locations in working memory is not as efficient in older adults as it is in younger adults, possibly due to the inability to suppress brain regions not directly involved in working memory binding.

Table 3.1

Interaction of age and task - univariate activity

Phase	Volume	Peak Voxel			Hemisphere	Brodmann	Regions
		x	y	z			
Encoding	1836	48	-45	37	Right	39,40	Inferior parietal lobule
Encoding	1593	-34	-68	38	Left	39,40	Inferior parietal lobule
Encoding	1242	20	2	0	Right	--	Putamen, globus pallidus
Maintenance	1377	-30	-58	-39	Left	--	Cerebellum

Table 3.1: There were four clusters that had a significant interaction of task and phase. For every cluster, the interaction was a result of older adults not having the greater unbound than bound activity that younger adults had. Volume of clusters is in mm^3 and coordinates are in MNI space.

Table 3.2

Interaction of age and task - functional connectivity

Seed-region	Phase	Volume	Peak Voxel			Hemisphere	BA	Regions
			x	y	z			
Superior parietal lobule	Encoding	1647	57	-30	20	Right	13, 40	Inferior parietal lobule, insula, postcentral gyrus
Medial frontal gyrus	Encoding	756	44	-8	45	Right	6	Precentral gyrus, middle frontal gyrus
Posterior cingulate	Encoding	4968	44	-18	34	Right	6, 4	Precentral gyrus, postcentral gyrus
		4644	-16	-71	-26	Left	--	Cerebellum
		2268	20	-32	64	Right	7, 5, 3	Postcentral gyrus, precuneus
		972	18	-23	-1	Right	--	Thalamus
	Maintenance	1512	-34	-33	50	Left	4, 3	Postcentral gyrus, precentral gyrus
		1026	-6	-45	76	Left	4, 5	Postcentral gyrus, paracentral lobule

Table 3.2: There were eight clusters that had a significant interaction of task and phase on functional connectivity to various seed-regions. For every cluster, the interaction was a result of older adults not having the greater unbound than bound connectivity that younger adults had. Volume of clusters is in mm^3 and coordinates are in MNI space.

Figure 3.1

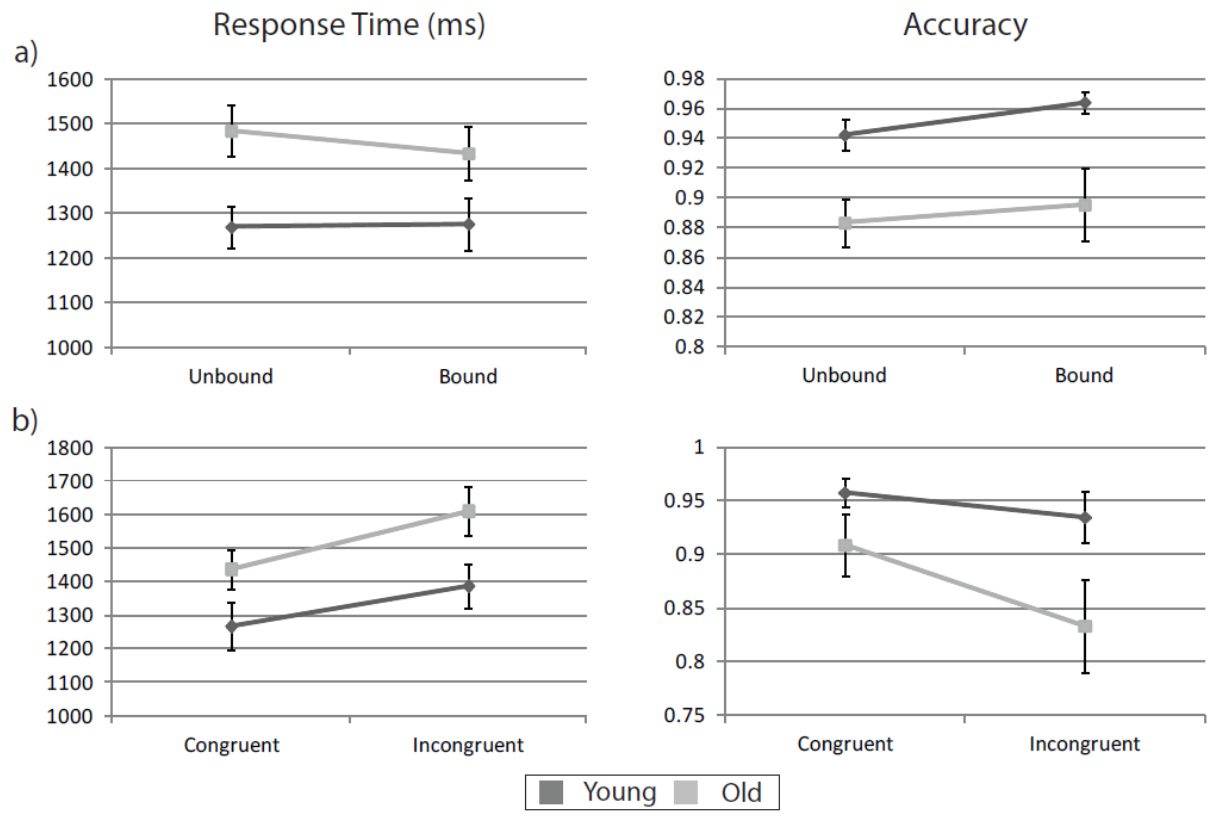
Response Time (ms)
Accuracy
a)
1600
1500
1400
1300
1200
1100
1000
Unbound
Bound
0.98
0.96
0.94
0.92
0.9
0.88
0.86
0.84
0.82
0.8
Unbound
Bound
b)
1800
1700
1600
1500
1400
1300
1200
1100
1000
Congruent
Incongruent
1
0.95
0.9
0.85
0.8
0.75
Congruent
Incongruent
Young
Old

Figure 3.1: For overall task performance (*a*) there was a significant effect of age on response time ($p < .05$) and accuracy ($p < .005$), with younger adults performing better on both measures. Neither the effect of task, nor the interaction of task and age were significant. For positive bound trials (*b*) there was a significant effect of task and age on both response time ($p < .001$ for both) and accuracy ($p < .05$ for both). Younger adults performed better on both measures, while both older and younger adults performed better on congruent trials than incongruent trials. There was no interaction between task and age.

Figure 3.2

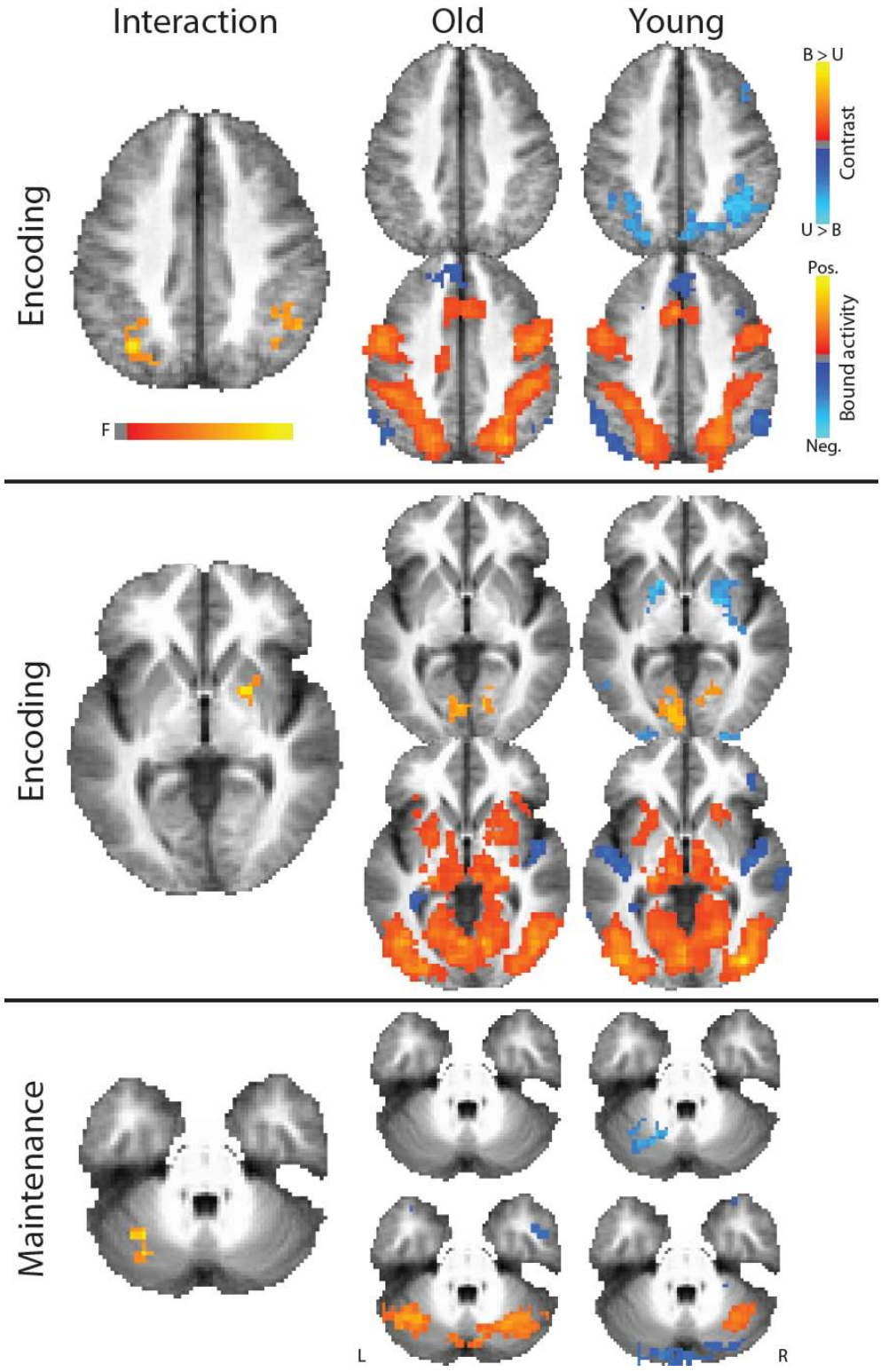
Interaction
Old
Young
B > U
Contrast
U > B
Pos.
Bound activity
Neg.
F
Encoding
Encoding
Maintenance
L
R

Figure 3.2: There were significant interactions between age and task in brain activity. The phase at which each interaction occurred is indicated to the left of each image. The top row of the images to the right of each interaction includes the contrasts of bound minus unbound for each age group to illustrate the differences driving the interaction. The lower row of images to the right of each interaction are the bound task activity for each age group to illustrate regions that were task positive and task negative. Interaction images are displayed at a multiple comparison corrected level of 0.05, while the other images are displayed at an uncorrected level of 0.01 for illustrative purposes only.

Figure 3.3

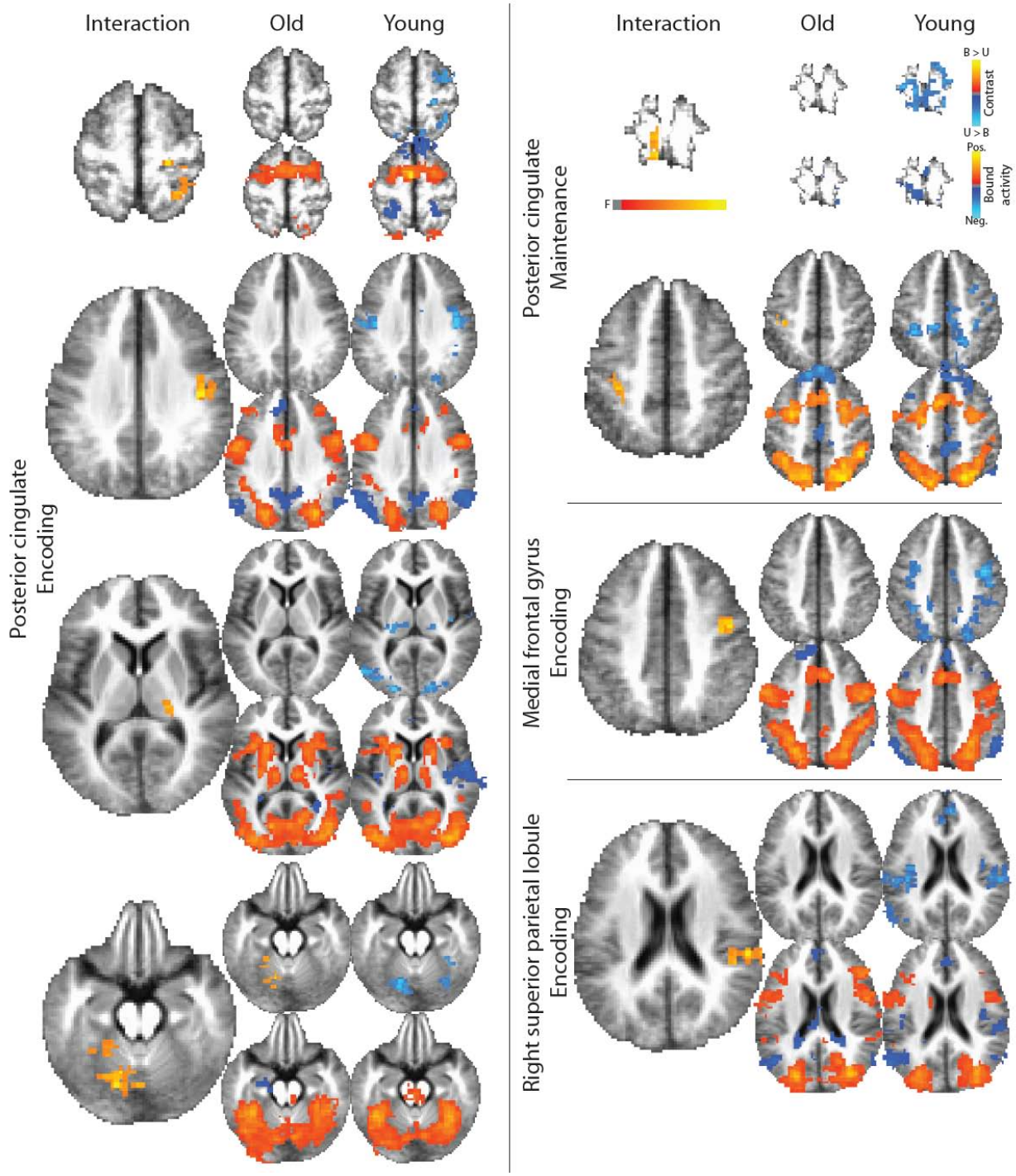
Interaction
Old
Young
Posterior cingulate
Encoding
Interaction
Old
Young
B > U
Contrast
U > B
Pos.
Bound activity
Neg.
F
Posterior cingulate
Maintenance
Medial frontal gyrus
Encoding
Right superior parietal lobule
Encoding

Figure 3.2: There were significant interactions between age and task in functional connectivity to multiple seed-regions. The seed-region and phase at which each interaction occurred is indicated to the left of each image. The top row of images to the right of each interaction includes the contrasts of bound connectivity minus unbound connectivity for each age group to illustrate the differences driving the interaction. The lower row of images to the right of each interaction are the bound task activity for each age group to illustrate regions that were task positive and task negative. Interaction images are displayed at a multiple comparison corrected level of 0.05, while the other images are displayed at an uncorrected level of 0.01 for illustrative purposes only.

References

Brockmole, J.R., Parra, M.A., Della Sala, S., Logie, R.H., 2008. Do binding deficits account for age-related decline in visual working memory? Psychon Bull Rev 15, 543-547.

Chalfonte, B.L., Johnson, M.K., 1996. Feature memory and binding in young and older adults. Mem Cognit 24, 403-416.

Cowan, N., Naveh-Benjamin, M., Kilb, A., Saults, J.S., 2006. Life-span development of visual working memory: when is feature binding difficult? Dev Psychol 42, 1089-1102.

Cox, R.W., 1996. AFNI: Software for analysis and visualization of functional magnetic resonance neuroimages. Computers and Biomedical Research 29, 162-173.

Gilchrist, A.L., Cowan, N., Naveh-Benjamin, M., 2008. Working memory capacity for spoken sentences decreases with adult ageing: recall of fewer but not smaller chunks in older adults. Memory 16, 773-787.

Grady, C.L., Protzner, A.B., Kovacevic, N., Strother, S.C., Afshin-Pour, B., Wojtowicz, M., Anderson, J.A., Churchill, N., McIntosh, A.R., 2010. A multivariate analysis of age-related differences in default mode and task-positive networks across multiple cognitive domains. Cereb Cortex 20, 1432-1447.

Grady, C.L., Springer, M.V., Hongwanishkul, D., McIntosh, A.R., Winocur, G., 2006. Age-related changes in brain activity across the adult lifespan. Journal of cognitive neuroscience 18, 227-241.

Hampson, M., Driesen, N.R., Skudlarski, P., Gore, J.C., Constable, R.T., 2006. Brain connectivity related to working memory performance. J Neurosci 26, 13338-13343.

Kochan, N.A., Valenzuela, M., Slavin, M.J., McCraw, S., Sachdev, P.S., Breakspear, M., 2011. Impact of load-related neural processes on feature binding in visuospatial working memory. PLoS One 6, e23960.

Luck, S.J., Vogel, E.K., 1997. The capacity of visual working memory for features and conjunctions. Nature 390, 279-281.

Lustig, C., Snyder, A.Z., Bhakta, M., O'Brien, K.C., McAvoy, M., Raichle, M.E., Morris, J.C., Buckner, R.L., 2003. Functional deactivations: change with age and dementia of the Alzheimer type. Proceedings of the National Academy of Sciences of the United States of America 100, 14504-14509.

McKiernan, K.A., Kaufman, J.N., Kucera-Thompson, J., Binder, J.R., 2003. A parametric manipulation of factors affecting task-induced deactivation in functional neuroimaging. J Cogn Neurosci 15, 394-408.
Mitchell, K.J., Johnson, M.K., Raye, C.L., D'Esposito, M., 2000a. fMRI evidence of age-related hippocampal dysfunction in feature binding in working memory. Brain Res Cogn Brain Res 10, 197-206.

Mitchell, K.J., Johnson, M.K., Raye, C.L., Mather, M., D'Esposito, M., 2000b. Aging and reflective processes of working memory: binding and test load deficits. Psychol Aging 15, 527-541.

Mumford, J.A., Turner, B.O., Ashby, F.G., Poldrack, R.A., 2012. Deconvolving BOLD activation in event-related designs for multivoxel pattern classification analyses. Neuroimage 59, 2636-2643.

Narayanan, N.S., Prabhakaran, V., Bunge, S.A., Christoff, K., Fine, E.M., Gabrieli, J.D., 2005. The role of the prefrontal cortex in the maintenance of verbal working memory: an event-related FMRI analysis. Neuropsychology 19, 223-232.

Naveh-Benjamin, M., 2000. Adult age differences in memory performance: tests of an associative deficit hypothesis. J Exp Psychol Learn Mem Cogn 26, 1170-1187.

Naveh-Benjamin, M., Guez, J., Kilb, A., Reedy, S., 2004. The associative memory deficit of older adults: further support using face-name associations. Psychol Aging 19, 541-546.

Naveh-Benjamin, M., Hussain, Z., Guez, J., Bar-On, M., 2003. Adult age differences in episodic memory: further support for an associative-deficit hypothesis. J Exp Psychol Learn Mem Cogn 29, 826-837.

Parra, M.A., Abrahams, S., Logie, R.H., Sala, S.D., 2009. Age and binding within-dimension features in visual short-term memory. Neurosci Lett 449, 1-5.

Persson, J., Lustig, C., Nelson, J.K., Reuter-Lorenz, P.A., 2007. Age differences in deactivation: a link to cognitive control? Journal of cognitive neuroscience 19, 1021-1032.

Plancher, G., Gyselinck, V., Nicolas, S., Piolino, P., 2010. Age effect on components of episodic memory and feature binding: A virtual reality study. Neuropsychology 24, 379-390.

Raichle, M.E., MacLeod, A.M., Snyder, A.Z., Powers, W.J., Gusnard, D.A., Shulman, G.L., 2001. A default mode of brain function. Proc Natl Acad Sci U S A 98, 676-682.

Rissman, J., Gazzaley, A., D'Esposito, M., 2004. Measuring functional connectivity during distinct stages of a cognitive task. Neuroimage 23, 752-763.

Sambataro, F., Murty, V.P., Callicott, J.H., Tan, H.Y., Das, S., Weinberger, D.R., Mattay, V.S., 2010. Age-related alterations in default mode network: impact on working memory performance. Neurobiol Aging 31, 839-852.

Verhaeghen, P., Salthouse, T.A., 1997. Meta-analyses of age-cognition relations in adulthood: estimates of linear and nonlinear age effects and structural models. Psychol Bull 122, 231-249.

Chapter 4

Parallel ICA identifies sub-components of resting state networks that covary with behavioral indices

Timothy B. Meier, Joseph C. Wildenberg, Jingyu Liu, Jiayu Chen, Vince D. Calhoun, Bharat B. Biswal, Mary E. Meyerand, Rasmus, M. Birn, Vivek Prabhakaran

In preparation

Abstract

Parallel Independent Component Analysis (para-ICA) is a multivariate method that can identify complex relationships between different data modalities by simultaneously performing Independent Component Analysis on each data set while finding mutual information between the two data sets. We use para-ICA to test the hypothesis that spatial sub-components of common resting state networks (RSNs) covary with specific behavioral measures. Resting state scans and a battery of behavioral indices were collected from 24 younger adults. Group ICA was performed and common RSNs were identified by spatial correlation to publically available templates. Nine RSNs were identified and para-ICA was run on each network with a matrix of behavioral measures serving as the second data type. Five networks had spatial sub-components that significantly correlated with behavioral components. These included a sub-component of the temporo-parietal attention network that differentially covaried with different trial-types of a sustained attention task, sub-components of default mode networks that covaried with attention and working memory tasks, and a sub-component of the bilateral frontal network that split the left inferior frontal gyrus into three clusters according to its cytoarchitecture that differentially covaried with working memory performance. Additionally, we demonstrate the validity of para-ICA in cases with unbalanced dimensions using simulated data.

Introduction

There has been a recent explosion of interest in the neuroscience community in identifying individual or group differences in intrinsic functional connectivity that correlate with specific behaviors or traits. To date, traditional analyses have been mostly univariate in nature. However, such analyses cannot identify complex relationships between data types. In order to understand the complex relationships between data types, such as behavior and neuroimaging, data need to be evaluated simultaneously in a multivariate fashion. A relatively new method, parallel independent component analysis (para-ICA), has been introduced as a multimodal data fusion tool that allows simultaneous multivariate analysis of two data types collected in the same subjects (Liu et al., 2008). As with other fusion methods that have been developed, such as joint ICA, para-ICA is a data-driven, second level analysis tool that can be used to investigate hidden relationships between data types such as activation maps from tasks, connectivity measures, and structural measures (Calhoun et al., 2009). The advantage of para-ICA over joint ICA is that para-ICA identifies the relationship between two fundamentally different types of data, whereas joint ICA is best suited for different data types that are assumed to modulate in the exact same manner (e.g., derived from the same spatial structure). Previously, para-ICA has been used to identify linear combinations of single nucleotide polymorphisms (SNPs) that covary with fMRI activations during an auditory oddball task or grey matter volume in schizophrenia patients (Jamadar et al., 2011; Liu et al., 2009), and spatial patterns of Amyloid-β that covary with rates of brain atrophy in MCI patients (Tosun et al., 2011).

In this study, we test the hypothesis that common resting state networks can be spatially decomposed into sub-components that covary with specific behavioral profiles. It has been proposed that every functional network that is available during task performance is present during resting conditions as low frequency fluctuations in neural activity (Smith et al., 2009). Differences in functional connectivity in RSNs have been found to correlate with several different behavioral measures, including measures of intelligence (Song et al., 2008), reading competence (Koyama et al., 2011), risky behavior (Cox et al., 2010), working memory (Sala-Llonch et al., 2011), and spatial navigation (Wegman and Janzen, 2011). To our knowledge, no study has investigated whether sub-components of resting state networks can be identified based on their covariance with different behavioral indices in a multivariate manner. Here, using simulated data we first demonstrate the ability of para-ICA to identify valid relationships between data modalities, even in cases in which the two data sets have unbalanced dimensionality. Finally, we use para-ICA to investigate the covariance between sub-components of several resting state networks, including the attention, default, and frontal network, to linear combinations of a matrix of behavioral indices that require brain regions associated with these networks.

Materials and Methods

Participants

Twenty-four healthy young adults (14 male; age 25 ± 0.67 years) provided informed consent to participate in three separate visits for this study. Twenty

participants were right handed, one was left handed, and three were ambidextrous based on the Edinburgh Handedness Inventory. All aspects of this study were approved by the University of Wisconsin-Madison Health Sciences Institutional Review Board.

Behavioral data acquisition

Participants completed a series of behavioral tasks and questionnaires outside of the scanner during a separate visit completed after the first scan visit, and inside the scanner during the second scan visit. Tasks performed outside the scanner included a computerized Stroop test (Stroop, 1935), a computerized Eriksen flanker task (Eriksen and Eriksen, 1974), digit and spatial forward and backward spans (Wechsler, 1997), Raven's Advanced Progressive Matrices (Raven et al., 1998), and a processing speed task (Wechsler, 2008). Tasks performed inside the scanner included a simple motor response task, a spatial working memory task, a verbal working memory task, and two combined spatial and verbal working memory tasks that our lab has previously used (Prabhakaran et al., 2000; Prabhakaran et al., 2011). In the 'bound' version of the combined spatial and verbal working memory task, the spatial and verbal information is presented together, essentially allow subjects to encode a letter and location as one item (**Supp. Figure 4.1**). In the 'unbound' combined working memory task, the verbal and spatial information are presented separately, just requiring the letters and locations be encoded separately. Behavioral indices such as response time, accuracy, and rate were measured for each behavioral task as applicable (**Supp. Table 4.1**). Detailed explanations of each task used can be found in the supplement.

Resting state fMRI acquisition

Each participant completed nine, ten-minute resting state scans, six of which were collected in the first visit and three were collected during a visit at least two months after the first visit. Of these nine scans, three were collected with the participants instructed to have their eyes closed, three were collected with the participants instructed to have their eyes open, and three were collected with the participants instructed to fixate their gaze on a fixation cross projected to the center of a MR-safe screen. Resting state scans were collected on a 3T MRI scanner (GE Healthcare, Waukesha, WI) using gradient-echo echo-planar imaging with the following parameters: TR = 2.6 s, TE = 22 ms, field of view = 22.4 cm, flip angle = 60°, 40 sagittal slices, acquisition matrix = 64 x 64, 3.5 mm isotropic voxel size, 231 time-points. T1-weighted anatomical images were collected at each scan visit using a FSPGR BRAVO (TR = 8.132 ms, TE = 3.18 ms) over a 256 x 256 matrix and 156 slices (flip angle = 12°, FOV = 25.6 cm, slice thickness = 1 mm).

Resting state fMRI preprocessing

The first three time points of each scan were removed, and images were slice time corrected and motion corrected using AFNI (Cox, 1996). Participants' anatomical scans were registered to each functional scan and then normalized to standard MNI space in SPM8. This transformation was then used to map the functional scans to MNI space with a resampling to 3 x 3 x 3 mm^3. Functional scans were then temporally

bandpass filtered (0.01-0.1 Hz) and spatially smoothed with an 8 mm^3 full width half maximum isotropic Gaussian kernel in AFNI.

First-level analysis: Group Independent Component Analysis

An overview of the different analysis steps performed for this study can be seen in **Figure 4.1**. Before para-ICA can be run, a first level analysis identifying resting state networks is necessary. In order to do so, group ICA was performed using temporal concatenation as implemented in the GIFT 1.3i program (Calhoun et al., 2009). Group ICA, as implemented in the GIFT program, is a completely data-driven method that can be used to identify spatially distinct, temporally coherent components from resting state data. One attractive feature of this program is that it provides back-reconstruction steps that produce subject, or session, specific spatial maps for each independent component extracted at the group level. This allows the spatial extent of each network to vary across subjects or sessions making post-analysis comparisons of network extent possible.

The entire dataset of 216 resting state runs was masked to include only brain structures, temporally concatenated, and two rounds of Principal Component Analyses (PCA) were performed prior to ICA to reduce the dimensionality of the data. Forty independent components were estimated using the Infomax algorithm to maximize the spatial independence of the components (Obradovic and Deco, 1998). Five iterations of the ICA were performed to verify consistency of the components and the resulting IC

spatial maps were back reconstructed and scaled to z-scores. This resulted in back-reconstructed components for each of the nine resting state scans for every subject.

The resulting group components were then spatially correlated at a z-score threshold of 3.0 ($p < 0.005$) with templates of established resting state networks provided online by the developers of the GIFT program at a threshold of $t = 35.5$ (t value based on suggestion of template providers; Allen et al., 2011). In their original study, Allen et al performed group ICA on over 600 subjects and identified 28 components as being resting state networks. These templates were used to confirm that the networks carried over for our para-ICA in the second level analyses are consistent with established common RSNs. In addition, the identification of common networks in our data provides verification that the number of independent components we estimated for the group ICA was appropriate. We limited our investigation to *a priori* selected networks in order to limit the total number of comparisons performed. For this study, we were interested in the attention networks, the default networks, and the frontal networks (**Figure 4.2**) as these networks involve brain regions thought to be responsible for many of the behavioral tasks performed by our subjects (Buckner et al., 2008; Corbetta and Shulman, 2002; Koechlin and Summerfield, 2007). In addition, we identified the auditory network as a negative control, with the hypothesis that variations in this network at rest should not correlate with our behavioral tasks.

Only components that spatially correlated with the provided templates at a correlation coefficient of 0.4 ($p < 0.001$) or greater were considered in order to limit our

analyses to statistically significant correlations and moderate-to-strong correlations. This identified nine RSN's: a left frontal-parietal attention network, a right frontal-parietal attention network, a bilateral temporo-parietal attention network, an auditory network, a posterior-superior component of the default mode network consisting of the precuneus, a posterior-inferior component of the default mode network consisting of the posterior cingulate, a medial frontal default mode network component, a bilateral frontal network, and a frontal pole network (**Figure 4.2**). These networks were carried out for second-level para-ICA analyses.

Second-level analysis: Parallel Independent Component Analysis

Separate parallel ICA (para-ICA) analyses were carried out for each of the nine RSNs identified in the group ICA using the Fusion ICA Toolbox (http://icatb.sourceforge.net). Para-ICA is a second-level analysis that allows investigation of cross information between two different data types (Liu et al., 2009). Essentially, two ICAs are run simultaneously, one on the subject specific back-reconstructed resting state network and one on the matrix of behavioral measures, with a term in each mixing matrix that describes the relationship between the two ICAs (**Figure 4.1**). The two un-mixing matrices are iteratively updated while the components from each modality with the highest correlation are selected and used to modify the de-mixing matrix until a stopping criteria is reached. This process results in a number of components for each data type that are differentially expressed in each subject which is quantified by a loading parameter per component for each subject. The variation of the

expression (loading parameter) of a single component for one data type is correlated across subject with the expression of a single component from the second data type, resulting in pairs of correlated components (**Figure 4.3**) from each data modality (Calhoun et al., 2009; Liu et al., 2008).

There are three parameter settings within the para-ICA software that influence how the correlations between the two modalities are derived. The *constrained connection* parameter is the level of correlation between modalities at which the para-ICA selectively updates the de-mixing matrix. The *constrained components* parameter is the maximum number of paired components that can be updated based on the constrained connections threshold. Finally, the *endurance* parameter is the maximally allowed descending trend of entropy. More details regarding these parameters can be found elsewhere (Liu et al., 2008). Here, we use the default values of 0.3, 3, and -1e-3, respectively, for these three parameters.

The RSN data entered into each para-ICA was derived from the first functional scan during the visit where subjects were instructed to fixate their gaze on a fixation cross. For the other data type, a total of 39 behavioral and demographic measures, such as response time, accuracy, gender, and handedness were provided as input.

PCA was performed on each data set separately to approximate the number of components to estimate for each data type. Approximately 90% of the variance was explained by retaining 10 components for both the behavioral data and each resting state component. Therefore, 10 components were extracted for each data type. Each

para-ICA was repeated 20 times to ensure consistency of the components. For each para-ICA, analysis of each resting state network was limited to areas within a mask of that particular RSN at a threshold of $z > 1.96$ ($p < 0.05$) to limit our search to areas that contributed strongly to the RSN.

Simulations

The primary goal of this research was to identify sub-components of common RSNs (high dimension data) that specifically covary with sub-components of behavioral indices (low dimension data). To alleviate potential concerns about the performance of para-ICA in the null case in which no relationship exist between data modalities, and to assess the robustness of para-ICA in scenarios with unbalanced data dimensions, simulations were performed. For the simulations a 100 sample dataset was created. To reflect the unbalanced dimensions the fMRI data were simulated to span 10,000 voxels and involve 8 independent components, while the behavioral data were simulated to consist of 5 variables and involve 4 independent components. Thus, the resulting dimension was 100-by-10,000 for the simulated fMRI data and 100-by-5 for the simulated behavioral data. The two modalities were connected with different levels of randomly ranging correlations that served as the ground truth. Para-ICA was then applied to the simulated dataset and the results compared with the ground truth to investigate the use of para-ICA in the null scenario of no relationship between data modalities. Each simulation was run 100 times, and default para-ICA parameters were used.

Results

Simulations

The performance of para-ICA on simulated data in several scenarios of ground truth correlation between components is displayed in **Figure 4.4**. For each graph, the highest correlation between each of the eight simulated fMRI components and any one of the four simulated behavioral components is plotted against the ground truth correlation between that pair of components. The dotted horizontal line reflects the constrained connections parameter (r_th) used, and any component pair with correlation above r_th is circled, indicating that this pair (maximum three pairs) was updated based on the correlation constraint (see methods). **Figure 4.4*a*** illustrates the performance of para-ICA in cases in which there are no inter-modal correlations that exceed r_th, resulting in the acceptance of the null hypothesis that the data modalities are not connected. **Figure 4.4*b*** summarizes the performance of para-ICA in cases of varying supra-threshold (r_th) correlations between modalities.

At the default parameter settings para-ICA only enhances the correlations of the top three pairs of components whose natural correlations are higher than 0.3. In null scenarios where no correlations exceed this threshold para-ICA essentially works as two separate ICAs. When the true correlation is near the 0.3 threshold, a larger deviation of derived correlations is seen due to the para-ICA correlation-based updating of the de-mixing matrix on pairs just above the threshold, but not on those just below the threshold. At higher true correlations, the para-ICA performs relatively precisely. These

simulations demonstrate the validity of para-ICA in identifying correlations between components from two data modalities in cases of unbalanced data dimensionality.

Resting state and behavioral data

To control for multiple comparison, only components with an absolute correlation coefficient greater than 0.653 are reported ($p < 0.05$, Bonferonni FWE correction). For the spatial components, only clusters greater than 100 mm^3 in volume (at least 4 contiguous voxels) are reported (**Figure 4.5**). Four of the nine para-ICA analyses did not have any IC pairs meet this criterion. These include the auditory network, the frontal pole network, and the two lateralized attention networks.

The para-ICA procedure produces pairs of components from each data type (**Table 4.1**). The components from the RSN are spatial maps of z-scaled loading parameters at each voxel. The components coming from the behavioral matrix consists of z-scaled loading parameters for each behavioral measure. For visualization, only voxels with a z-scaled loading parameter $z > 1.96$ ($p < 0.05$) are displayed. Likewise, only behavioral indices with a z-scaled loading parameter $z > 1.96$ ($p < 0.05$) are presented and discussed.

Temporo-parietal attention network

A significant negative correlation (CC = -0.67; **Table 4.1**) was found between a sub-component of the temporo-parietal attention (**Figure 4.5**) network consisting of a 351 mm^3 cluster located in the precuneus with a negative loading parameter and a behavioral component consisting of response time in congruent ($z = 2.55$) and

incongruent (z = -2.13) trials of the Stroop test. Less connectivity of this area of the precuneus to the temporo-parietal attention network negatively covaried with response time in congruent Stroop trials, but positively covaried with greater response time in incongruent Stroop trials.

Posterior-superior default mode network

For the posterior-superior default mode network, a significant negative correlation (CC = -0.67; **Table 4.1**) was found between a positively weighted 2133 mm^3 cluster (**Figure 4.5**) located in the cuneus and a behavioral component consisting of response time in the spatial working memory task (z = -3.75) and response time in incongruent trials of the bound working memory task (z = -2.02), which requires simultaneous retention of both spatial and verbal information. This indicates that greater connectivity of this region of the cuneus to the posterior-superior default mode network negatively covaries with faster response times in two separate tasks involving spatial working memory.

Posterior-inferior default mode network

A significant positive correlation (CC = 0.759; **Table 4.1**) was found between a behavioral component that includes response time in the unbound working memory task of both spatial and verbal information (z = -2.90) and response time in congruent trials of the Stroop task (z = 2.19) to a 108 mm^3 cluster located in the right middle occipital gyrus with positive loading (**Figure 4.5**). Thus, greater connectivity of the right middle occipital gyrus to the posterior-inferior default mode network positively covaries with

slower response time in congruent trials of the Stroop task and faster response time in the unbound spatial and verbal working memory task.

A significant negative correlation (CC = -0.697) was found between a 513 mm^3 cluster in the cerebellum (**Figure 4.5**) and a behavioral component consisting of response time in both incongruent Stroop trials (z = 4.13) and all to the average response time to all Stroop trial types (z = 2.50). This can be interpreted as less connectivity of this area in the cerebellum to the posterior-inferior default mode network negatively covaried with slower response time in incongruent trials of the Stroop task and in all trials in the Stroop task.

Medial frontal default mode network

A significant negative correlation (CC = -0.73; **Table 4.1**) was found between a behavioral component including response time in the verbal working memory task (z = -4.02) and response time in the unbound working memory task involving both spatial and verbal information (z = 2.23) to a 783 mm^3 cluster in the mid-cingulate cortex and a 243 mm^3 cluster in the brainstem (**Figure 4.5**). Greater connectivity of mid-cingulate cortex and less connectivity of the brainstem to the medial frontal default mode network is negatively covaried to faster response time in the verbal working memory task and slower response time in the unbound working memory task, which requires the simultaneous retention of separate spatial and verbal information.

Bilateral frontal network

A significant negative correlation (CC = -0.70) was found between a behavioral component including response time in the bound working memory task (z = -3.9) to spatial clusters in the left inferior frontal gyrus (**Table 4.1**). The spatial component included a 135 mm^3 cluster with negative loading in the left frontal pars orbitalis, a 324 mm^3 cluster with positive loading in the left frontal par triangularis, and a 999 mm^3 cluster in the left frontal opercularis with positive loading (**Figure 4.5**). This indicates that greater connectivity of the left frontal opercularis and triangularis, and less connectivity of the left frontal orbitalis, are negatively covaried with faster response time in the bound spatial and verbal working memory task.

Discussion

Using simulation data we first demonstrate that para-ICA results in realistic correlations between data sets with large differences in dimensionality. The validity of para-ICA on datasets with more balanced dimensions has been previously established (Liu et al., 2008). Based on our simulated data, we conclude that para-ICA performs well in the null scenario, where there is no relationship between modalities, as well as in cases with varying levels of correlations between modalities even when applied to datasets with unbalanced dimensions. This is because, under the Infomax-ICA framework, the performance of para-ICA depends on the dimensionality of the samples (e.g. subjects), and not on the dimensionality of the data modalities (Liu et al., 2008).

Furthermore, we demonstrate that common resting state networks can be spatially decomposed into sub-components that covary with specific behavioral profiles.

Of the nine networks we performed para-ICA on, four did not result in significant correlations between the spatial components and behavior components. As hypothesized, there were no sub-components of the auditory network that significantly covaried with any of the behavioral indices collected. This was expected, as the behavioral indices were mostly cognitive in nature, and there were no tasks with auditory information. In addition, no significantly correlated pairs of components were observed for the two lateralized attention networks and the frontal pole network. However, as hypothesized, other RSNS including the default mode networks, the bilateral frontal network, and an attention network did have sub-components that covaried with specific cognitive measures.

Temporo-parietal attention network

The para-ICA on the temporo-parietal attention network identified a spatial sub-component located in the precuneus that differentially covaried with response time in congruent and incongruent Stroop task trials. In congruent Stroop trials, the color of the word and the word spelled out are the same; for example, a trial where the word ‘red’ appears in red font is a congruent trial. In contrast, a trial in which the color of the word does not match the word spelled out is an incongruent trial; for example, the word ‘red’ in green font. Less connectivity of this area in the precuneus to temporo-parietal attention RSN negatively covaried with better performance (faster response time) in incongruent trials, but worse performance (slower response time) in congruent trials.

The precuneus has previously been implicated in visuo-spatial processes, including attention (Beauchamp et al., 2001; Cavanna and Trimble, 2006; Simon et al., 2002). In addition, the precuneus has been shown to be preferentially activated in a color-word Stroop task with a hypothesized role of selecting task relevant information together with the dorsolateral PFC (Banich et al., 2000). Here, we show that the level of involvement of a cluster of the precuneus to the temporo-parietal attention networks has different effects on incongruent and congruent trials in the Stroop task, a task often used to measure selective attention.

Posterior-superior default network

For the posterior-superior default network, greater connectivity from a sub-component in the cuneus was found to negatively covary with two separate working memory tasks that require the retention of spatial information. Subjects with more cuneus involvement in this RSN had slower response times in a spatial working memory task, and a combined spatial and verbal working memory task. This area of the primary visual cortex is essential for visuo-spatial processing, including working memory (for review, see Kravitz et al., 2011). In addition, previous studies have shown that the ability to suppress areas of the default mode network, including the cuneus, during working memory tasks is correlated with performance on those tasks (Anticevic et al., 2010; Hampson et al., 2006). Here we found a sub-component of the default mode network at rest that negatively covaries specifically with two tasks involving spatial working memory.

Posterior-inferior default network

There were two sub-components of the posterior-inferior default network that covaried with specific behavioral components. The first sub-component consisted of a small cluster in the right middle occipital gyrus (BA 19) that differentially covaried with congruent Stroop task trials and a combined verbal and spatial working memory task. Greater connectivity of this area to the posterior-inferior default network positively covaried with faster response time in the working memory task and slower response time in the Stroop congruent task trials. Therefore, the connectivity of this region to this RSN has different effects on selective attention and working memory tasks.

The second sub-component of the posterior-inferior default network included a region in the vermis of the cerebellum that negatively covaried with response time to all Stroop trial types, as well as response time to incongruent Stroop trial types. Less connectivity to this RSN by the cerebellum, which has previous been implicated in Stoop task performance (Egner and Hirsch, 2005), was inversely related to slower response times in these Stroop trial types.

The identification of a sub-component of the default mode network that covaried differently to an attention task and a working memory task, and the fact that a second sub-component specifically covaried with just a selective attention task, is not without precedent. Although regions that deactivate during cognitive tasks are generally similar across task type, subtle task-dependent deactivations have been reported (Tomasi et al., 2006). Interestingly, a recent study by Mayer and colleagues found that task induced

deactivations of the default mode network differed between an attention task and a working memory task (2010).

Medial frontal default network

The para-ICA on the medial frontal default network identified a spatial component consisting of the brainstem and mid-cingulate cortex that differentially covaried with two working memory tasks. The greater connectivity of the mid-cingulate and less connectivity of the brainstem to this default network was inversely related to faster response time in the verbal working memory tasks, but slower response time in a combined verbal and spatial working memory task. For the medial frontal default network, we again see regions of the default mode network that differentially respond to different tasks. However, in contrast to our findings for the posterior-inferior default network, here we identify regions of the medial frontal default network that responds differently to two working memory tasks, one involving just spatial information and one involving both verbal and spatial information.

Bilateral frontal network

The para-ICA performed on the bilateral frontal network resulted in a spatial sub-component that split the left inferior frontal gyrus into three separate clusters that were negatively covaried with response time in a combined spatial and verbal working memory task (bound). These three clusters included the pars opercularis (BA 44), pars triangularis (BA 45), and pars orbitalis (BA 47). Greater connectivity of pars opercularis and pars triangularis, which together are generally thought to make up Broca's Area

(Keller et al., 2009), and less connectivity of pars orbitalis, was inversely related to faster response time in the combined spatial and verbal working memory task. This is especially interesting in light of the hypothesis put forward by Badre and colleagues that a dual system of cognitive control exists in the left inferior frontal gyrus (2005). According to this model, for any cognitive task requiring retrieval and selection of mnemonic information, such as a working memory task, the anterior portion of the left ventrolateral prefrontal cortex (pars orbitalis; BA 47) is responsible for the controlled retrieval of information while the mid-ventrolateral prefrontal cortex is responsible for post-retrieval selection of task-relevant representations (Badre and Wagner, 2007). Here, we show a similar dissociation between the left anterior ventrolateral prefrontal cortex (pars orbitalis) and the left mid-ventrolateral prefrontal cortex (pars opercularis and pars triangularis), as the involvement of these areas to the bilateral frontal resting state network covaried differently with performance in a dual spatial and verbal working memory task.

Limitations

This study has several limitations. One common issue with ICA analyses, including para-ICA analyses, is the number of components that are estimated. However, we believe that the 40 components estimated in the group ICA is appropriate due to the high degree of spatial correlation between our components and the common RSN templates. For the para-ICA, we based our decision by identifying the number of components that explained approximately 90% of the variance for both the behavioral

data and each resting state component. Finally, this study is limited by a relatively small sample size, a larger sample size would provide more detection power, and by the fact that nine separate para-ICAs were performed. Several steps were taken in attempts to control for this issue as several different levels of the analyses (**Figure 4.1**). In addition, this study is intended as an exploratory study to show the feasibility of indentifying sub-components of RSNs that covary with specific behaviors.

Conclusion

In this study, we first demonstrate the utility of a para-ICA in identifying real inter-modal relationships in data with unbalanced dimensions using simulated data. We then use this simultaneous multivariate method to demonstrate that sub-components of common resting state networks covary with specific behavioral measures. Importantly, the regions of these sub-components were found to covary with tasks that have previously been associated with those regions. For the temporo-parietal attention resting state network, para-ICA identified a sub-component that covaried differently for two different trial types in a common sustained attention task. Likewise, for the bilateral frontal resting state network, the para-ICA identified a sub-component that split the left inferior frontal gyrus into three clusters according to its cytoarchitecture that differentially covaried with performance on a working memory task. In addition, the separation of these regions of the left inferior frontal gyrus is consistent with a prominent model of dual cognitive control in the ventrolateral prefrontal cortex (Badre and Wagner, 2007). Finally, the para-ICA identified several sub-components of the default mode networks

investigated that covaried differently with specific cognitive tasks, consistent with previous studies that have demonstrated task-dependent differences in deactivations of default mode regions (Mayer et al., 2010). In summary, para-ICA identified specific sub-components of common resting state networks that covaried with different behavioral profiles, shedding light on the complex relationship between behavior and spontaneous brain activity.

Table 4.1

RSN	"+" sub-component areas			"-" sub-component areas			Behavior	behavior z-score	CC
	Area	*MNI coordinates*	*Volume (mm^3)*	*Area*	*MNI coordinates*	*Volume (mm^3)*			
Temporo-parietal attention				R precun.	3, -55, 58	351	Stroop Con. RT	2.55	-0.67
							Stroop Incon. RT	-2.13	
Posterior-superior default mode	Cuneus	0, -77, 38	2133				Spatial RT	-3.75	-0.67
							Bound Incon. RT	-2.02	
Posterior-inferior default mode	R mid. occ. gyr. BA 19	48, -82, 22	108				Unbound RT	-2.9	0.76
							Stroop Con. RT	2.19	
Posterior-inferior default mode				L vermis	-3, -49, 4	513	Stroop Incon. RT	4.13	-0.70
							Stroop RT	2.5	
Medial frontal default mode	M cing. BA 24	0, 2, 34	783	R brainst.	3, -28, -53	243	Verbal RT	-4.02	-0.72
							Unbound RT	2.23	
Bilateral frontal	L inf. front. oper. BA 44	-51, 23, 34	999	L inf. front. orb. BA 47	-51, 38, -11	135	Bound RT	-3.9	-0.70
	L inf. front. tri. BA 45	-48, 41, 13	324						

Table 4.1: Displayed above are the RSNs that had pairs of components from the para-ICA that were significantly correlated ($r > .653$). Only behaviors and spatial clusters with loading parameter $z > 1.96$ ($p < 0.05$) are displayed. In addition, only spatial clusters with a minimum 100 mm^3 volume were included for this analysis in order to limit analysis of extremely small clusters (must have at least 4 contiguous voxels).

Figure 4.1

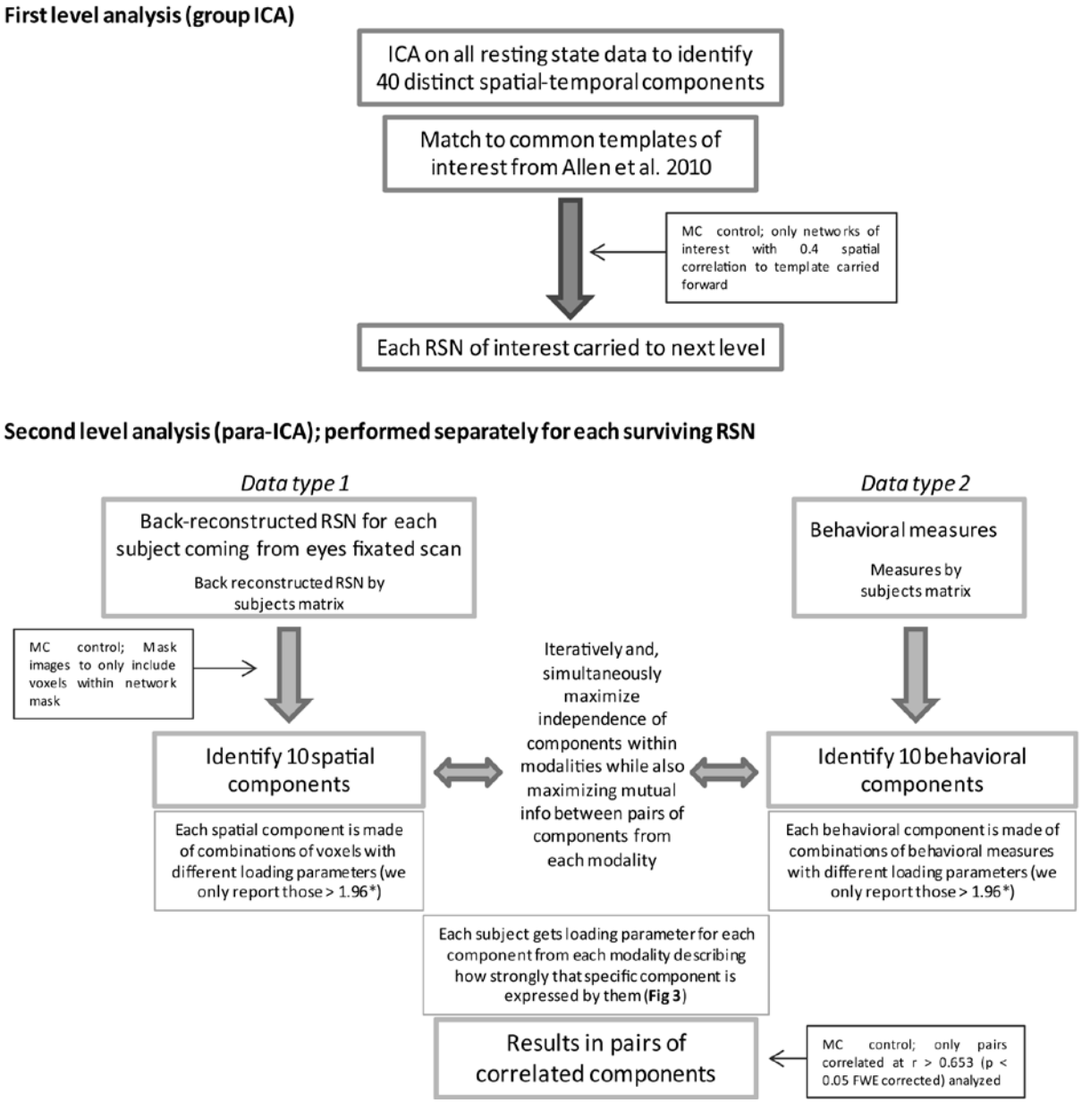
First level analysis (group ICA)
ICA on all resting state data to identify 40 distinct spatial-temporal components
Match to common templates of interest from Allen et al. 2010
MC control; only networks of interest with 0.4 spatial correlation to template carried forward
Each RSN of interest carried to next level
Second level analysis (para-ICA); performed separately for each surviving RSN
Data type 1
Back-reconstructed RSN for each subject coming from eyes fixated scan
Back reconstructed RSN by subjects matrix
MC control; Mask images to only include voxels within network mask
Identify 10 spatial components
Each spatial component is made of combinations of voxels with different loading parameters (we only report those > 1.96*)
Iteratively and, simultaneously maximize independence of components within modalities while also maximizing mutual info between pairs of components from each modality
Data type 2
Behavioral measures
Measures by subjects matrix
Identify 10 behavioral components
Each behavioral component is made of combinations of behavioral measures with different loading parameters (we only report those > 1.96*)
Each subject gets loading parameter for each component from each modality describing how strongly that specific component is expressed by them (Fig 3)
Results in pairs of correlated components
MC control; only pairs correlated at r > 0.653 (p < 0.05 FWE corrected) analyzed

Figure 4.1: Displayed is a flow chart of the methods used for this study. MC and * indicate where steps were taken to limit multiple comparisons (MC). For in depth description of para-ICA analysis see the following papers (Calhoun et al., 2009; Liu et al., 2009).

Figure 4.2

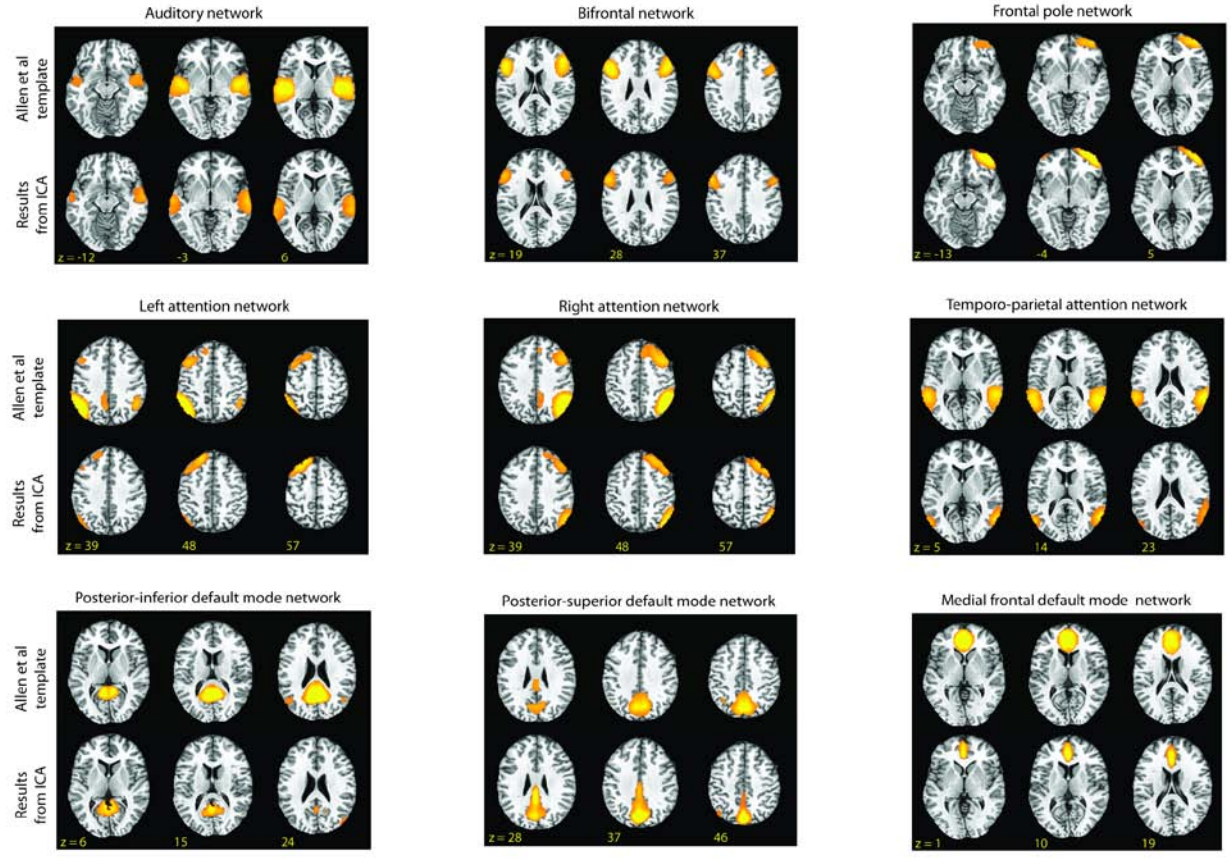
Auditory network
Allen et al template
Results from ICA
z = -12
-3
6
Bifrontal network
z = 19
28
37
Frontal pole network
z = -13
-4
5
Left attention network
Allen et al template
Results from ICA
z = 39
48
57
Right attention network
z = 39
48
57
Temporo-parietal attention network
z = 5
14
23
Posterior-inferior default mode network
Allen et al template
Results from ICA
z = 6
15
24
Posterior-superior default mode network
z = 28
37
46
Medial frontal default mode network
z = 1
10
19

Figure 4.2: Shown above are the RSNs identified by Allen et al. and the component from our group ICA that had the highest spatial correlation to the Allen et al. templates (2011). In this figure, for the templates the threshold is set at t = 45 and for the matching components from our data the threshold is set at z = 3.0.

Figure 4.3

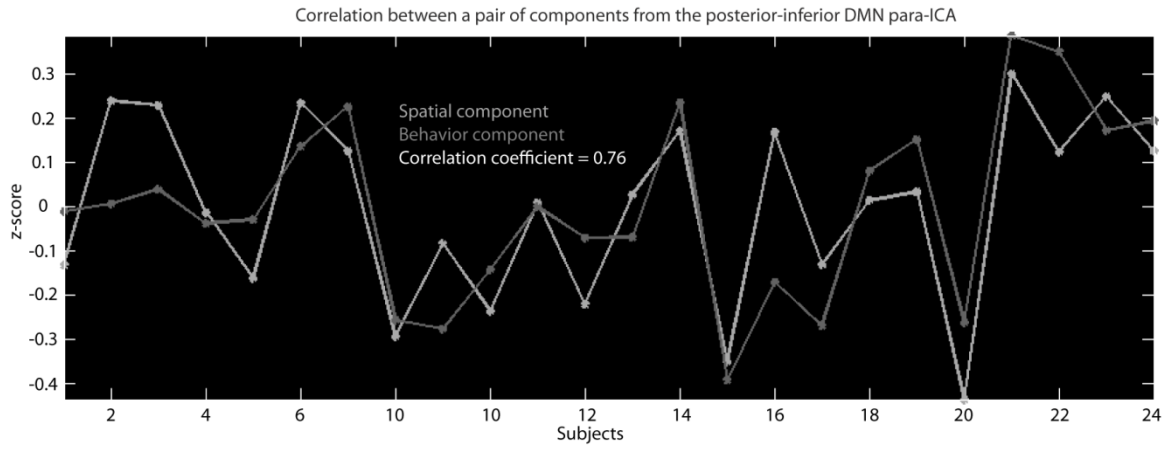
Correlation between a pair of components from the posterior-inferior DMN para-ICA
Spatial component
Behavior component
Correlation coefficient = 0.76
z-score
0.3
0.2
0.1
0
-0.1
-0.2
-0.3
-0.4
2
4
6
10
10
12
14
16
18
20
22
24
Subjects

Figure 4.3: This is an example of the correlation across subjects between the z-scaled loading parameters for a behavioral component and the z-scaled loading parameters of a spatial component that resulted from the para-ICA run for the posterior-inferior default mode network.

Figure 4.4

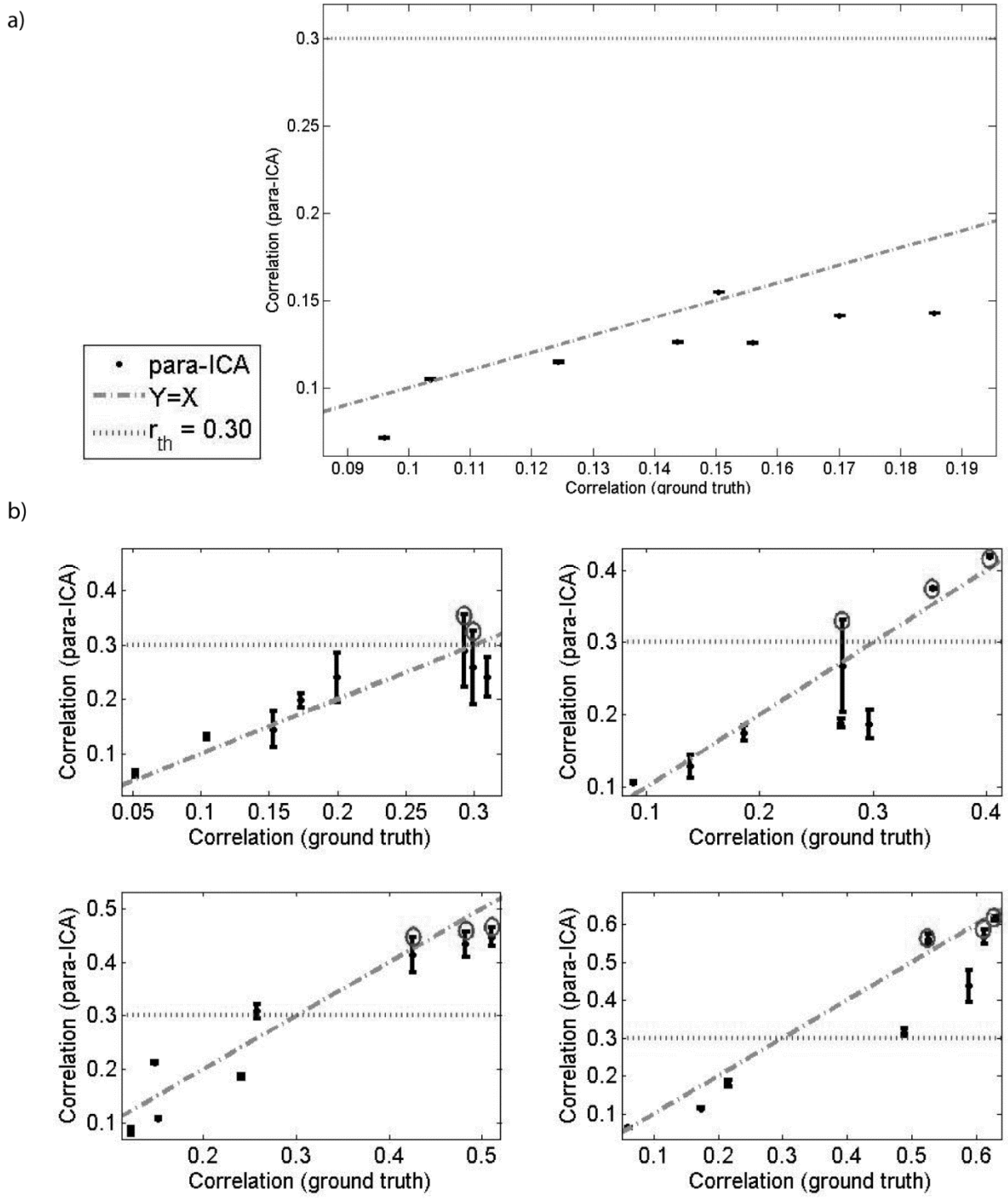
a)
para-ICA
Y=X
r_{th} = 0.30
Correlation (para-ICA)
Correlation (ground truth)
b)
Correlation (para-ICA)
Correlation (ground truth)

Figure 4.4: Displayed are the simulated data results comparing the correlations derived from para-ICA to the ground truth correlations in data with highly unbalanced data dimensions in cases of sub-threshold correlations between data modalities (*a*) and in cases with varying supra-threshold correlations between modalities (*b*). The dotted horizontal line reflects the constrained connections parameter (r_th) and the dotted diagonal line reflects a perfect match between the ground truth and the para-ICA derived correlations. Para-ICA treats data-modalities with only sub-threshold correlations as having no inter-modal relationship (as seen in *a*). When the correlation between pairs of components exceeds r_th, these components are updated in the para-ICA algorithm (as circled in *b*). A maximum of three sub-threshold pairs can be updated in the para-ICA framework. Error bars represent standard deviation based on 100 iterations. Note that error bars of (*a*) overlap with the data points and are hard to see due to low standard deviations.

Figure 4.5

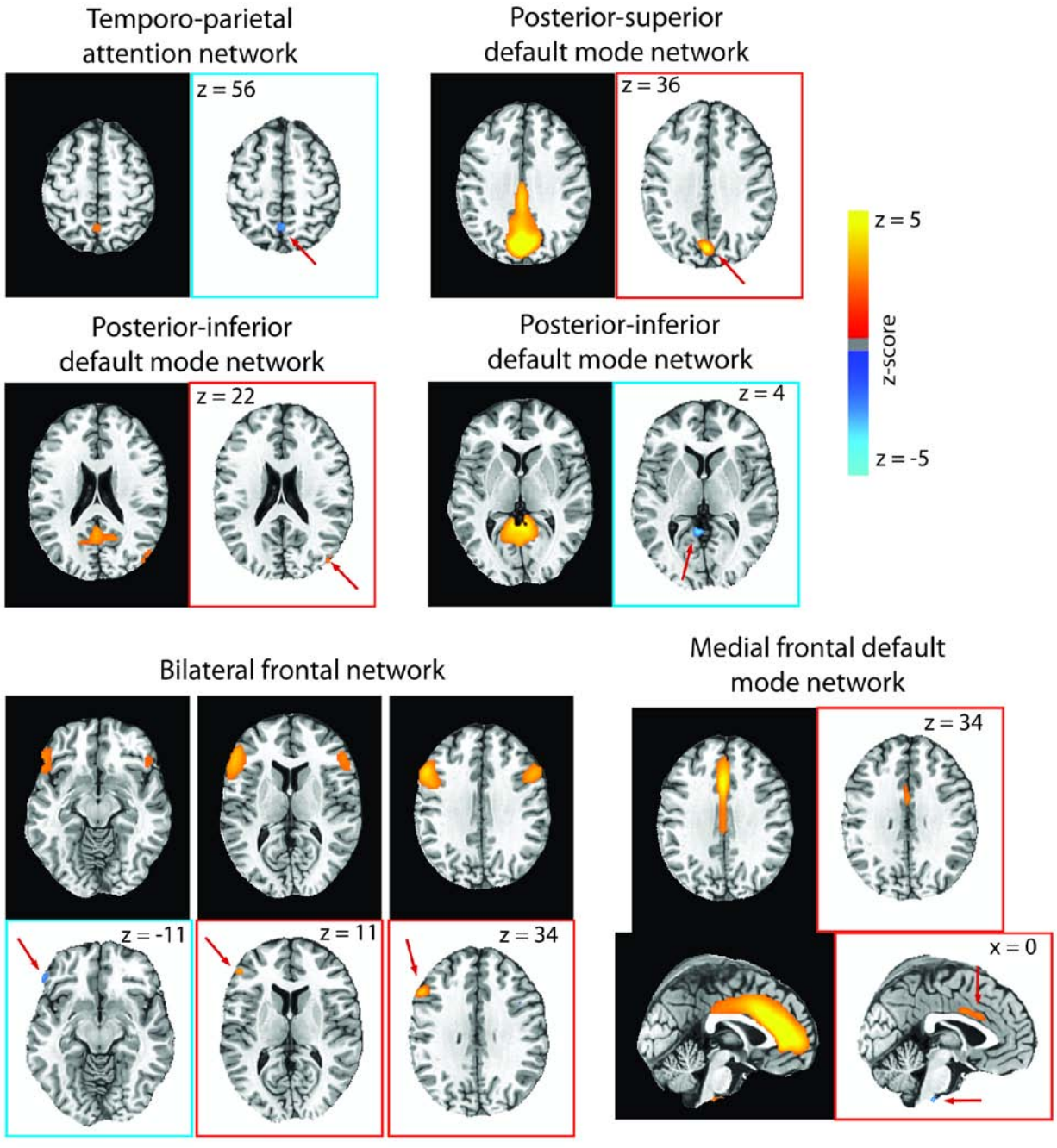
Temporo-parietal attention network
z = 56
Posterior-superior default mode network
z = 36
z = 5
z-score
z = -5
Posterior-inferior default mode network
z = 22
Posterior-inferior default mode network
z = 4
Bilateral frontal network
z = -11
z = 11
z = 34
Medial frontal default mode network
z = 34
x = 0

Figure 4.5: For each RSN that had significant para-ICA correlations, the RSN from our group ICA is displayed on black background, while the spatial component resulting from the para-ICA is displayed on white background. Spatial components with blue borders represent components with negative loadings while those with red borders represent components with positive loadings. Red arrows are included to direct the reader to the spatial components. Only voxels with loading parameter $z > 1.96$ ($p < 0.05$) are shown.

References

Allen, E.A., Erhardt, E.B., Damaraju, E., Gruner, W., Segall, J.M., Silva, R.F., Havlicek, M., Rachakonda, S., Fries, J., Kalyanam, R., Michael, A.M., Caprihan, A., Turner, J.A., Eichele, T., Adelsheim, S., Bryan, A.D., Bustillo, J., Clark, V.P., Feldstein Ewing, S.W., Filbey, F., Ford, C.C., Hutchison, K., Jung, R.E., Kiehl, K.A., Kodituwakku, P., Komesu, Y.M., Mayer, A.R., Pearlson, G.D., Phillips, J.P., Sadek, J.R., Stevens, M., Teuscher, U., Thoma, R.J., Calhoun, V.D., 2011. A baseline for the multivariate comparison of resting-state networks. Front Syst Neurosci 5, 2.

Anticevic, A., Repovs, G., Shulman, G.L., Barch, D.M., 2010. When less is more: TPJ and default network deactivation during encoding predicts working memory performance. Neuroimage 49, 2638-2648.

Badre, D., Poldrack, R.A., Pare-Blagoev, E.J., Insler, R.Z., Wagner, A.D., 2005. Dissociable controlled retrieval and generalized selection mechanisms in ventrolateral prefrontal cortex. Neuron 47, 907-918.

Badre, D., Wagner, A.D., 2007. Left ventrolateral prefrontal cortex and the cognitive control of memory. Neuropsychologia 45, 2883-2901.

Banich, M.T., Milham, M.P., Atchley, R., Cohen, N.J., Webb, A., Wszalek, T., Kramer, A.F., Liang, Z.P., Wright, A., Shenker, J., Magin, R., 2000. fMri studies of Stroop tasks reveal unique roles of anterior and posterior brain systems in attentional selection. J Cogn Neurosci 12, 988-1000.

Beauchamp, M.S., Petit, L., Ellmore, T.M., Ingeholm, J., Haxby, J.V., 2001. A parametric fMRI study of overt and covert shifts of visuospatial attention. Neuroimage 14, 310-321.

Buckner, R.L., Andrews-Hanna, J.R., Schacter, D.L., 2008. The brain's default network: anatomy, function, and relevance to disease. Ann N Y Acad Sci 1124, 1-38.

Calhoun, V.D., Liu, J., Adali, T., 2009. A review of group ICA for fMRI data and ICA for joint inference of imaging, genetic, and ERP data. Neuroimage 45, S163-172.

Cavanna, A.E., Trimble, M.R., 2006. The precuneus: a review of its functional anatomy and behavioural correlates. Brain : a journal of neurology 129, 564-583.

Corbetta, M., Shulman, G.L., 2002. Control of goal-directed and stimulus-driven attention in the brain. Nat Rev Neurosci 3, 201-215.

Cox, C.L., Gotimer, K., Roy, A.K., Castellanos, F.X., Milham, M.P., Kelly, C., 2010. Your resting brain CAREs about your risky behavior. PLoS One 5, e12296.

Cox, R.W., 1996. AFNI: Software for analysis and visualization of functional magnetic resonance neuroimages. Computers and Biomedical Research 29, 162-173.

Egner, T., Hirsch, J., 2005. The neural correlates and functional integration of cognitive control in a Stroop task. Neuroimage 24, 539-547.

Eriksen, B.A., Eriksen, C.W., 1974. Effects of noise letters upon identification of a target letter in a non-search task. Perception and Psychophysics 16, 143-149.

Hampson, M., Driesen, N.R., Skudlarski, P., Gore, J.C., Constable, R.T., 2006. Brain connectivity related to working memory performance. J Neurosci 26, 13338-13343.

Jamadar, S., Powers, N.R., Meda, S.A., Gelernter, J., Gruen, J.R., Pearlson, G.D., 2011. Genetic influences of cortical gray matter in language-related regions in healthy controls and schizophrenia. Schizophr Res 129, 141-148.

Keller, S.S., Crow, T., Foundas, A., Amunts, K., Roberts, N., 2009. Broca's area: nomenclature, anatomy, typology and asymmetry. Brain Lang 109, 29-48.

Koechlin, E., Summerfield, C., 2007. An information theoretical approach to prefrontal executive function. Trends Cogn Sci 11, 229-235.

Koyama, M.S., Di Martino, A., Zuo, X.N., Kelly, C., Mennes, M., Jutagir, D.R., Castellanos, F.X., Milham, M.P., 2011. Resting-state functional connectivity indexes reading competence in children and adults. J Neurosci 31, 8617-8624.

Kravitz, D.J., Saleem, K.S., Baker, C.I., Mishkin, M., 2011. A new neural framework for visuospatial processing. Nat Rev Neurosci 12, 217-230.

Liu, J., Demirci, O., Calhoun, V.D., 2008. A Parallel Independent Component Analysis Approach to Investigate Genomic Influence on Brain Function. IEEE Signal Process Lett 15, 413-416.

Liu, J., Pearlson, G., Windemuth, A., Ruano, G., Perrone-Bizzozero, N.I., Calhoun, V., 2009. Combining fMRI and SNP data to investigate connections between brain function and genetics using parallel ICA. Hum Brain Mapp 30, 241-255.

Mayer, J.S., Roebroeck, A., Maurer, K., Linden, D.E., 2010. Specialization in the default mode: Task-induced brain deactivations dissociate between visual working memory and attention. Hum Brain Mapp 31, 126-139.

Obradovic, D., Deco, G., 1998. Information maximization and independent component analysis; is there a difference? Neural Comput 10, 2085-2101.

Prabhakaran, V., Narayanan, K., Zhao, Z., Gabrieli, J.D., 2000. Integration of diverse information in working memory within the frontal lobe. Nat Neurosci 3, 85-90.

Prabhakaran, V., Rypma, B., Narayanan, N.S., Meier, T.B., Austin, B.P., Nair, V.A., Naing, L., Thomas, L.E., Gabrieli, J.D., 2011. Capacity-speed relationships in prefrontal cortex. PLoS One 6, e27504.

Raven, J.C., Raven, J., Court, J.H., 1998. A manual for Raven's Progressive Matrices and Vocabulary Scales. H.K. Lewis, London.
Sala-Llonch, R., Pena-Gomez, C., Arenaza-Urquijo, E.M., Vidal-Pineiro, D., Bargallo, N., Junque, C., Bartres-Faz, D., 2011. Brain connectivity during resting state and subsequent working memory task predicts behavioural performance. Cortex.

Simon, S.R., Meunier, M., Piettre, L., Berardi, A.M., Segebarth, C.M., Boussaoud, D., 2002. Spatial attention and memory versus motor preparation: premotor cortex involvement as revealed by fMRI. J Neurophysiol 88, 2047-2057.

Smith, S.M., Fox, P.T., Miller, K.L., Glahn, D.C., Fox, P.M., Mackay, C.E., Filippini, N., Watkins, K.E., Toro, R., Laird, A.R., Beckmann, C.F., 2009. Correspondence of the brain's functional architecture during activation and rest. Proc Natl Acad Sci U S A 106, 13040-13045.

Song, M., Zhou, Y., Li, J., Liu, Y., Tian, L., Yu, C., Jiang, T., 2008. Brain spontaneous functional connectivity and intelligence. Neuroimage 41, 1168-1176.

Stroop, J.R., 1935. Studies of interference in serial verbal reactions. Journal of Experimental Psychology 18, 643-662.

Tomasi, D., Ernst, T., Caparelli, E.C., Chang, L., 2006. Common deactivation patterns during working memory and visual attention tasks: an intra-subject fMRI study at 4 Tesla. Hum Brain Mapp 27, 694-705.

Tosun, D., Schuff, N., Mathis, C.A., Jagust, W., Weiner, M.W., 2011. Spatial patterns of brain amyloid-beta burden and atrophy rate associations in mild cognitive impairment. Brain 134, 1077-1088.

Wechsler, D., 1997. Wechsler Memory Scale - Third edition (WMS--III). Harcourt Assessment, San Antonio, TX.

Wechsler, D., 2008. Wechsler Adult Intelligence Scale - 4th Edition (WAIS--IV). Harcourt Assessment, San Antonio, TX.

Wegman, J., Janzen, G., 2011. Neural encoding of objects relevant for navigation and resting state correlations with navigational ability. J Cogn Neurosci 23, 3841-3854.

Supplementary Information: Parallel ICA identifies sub-components of resting state networks that covary with behavioral indices

Behavioral Measures

Stroop task

All participants performed an in-house computerized Stroop test (Stroop, 1935) in which names of colors were presented on the screen for 1500 ms followed by 500 ms ITI. Participants were instructed to indicate the font color of the word by pressing the appropriate key marked with colored tape. For example, if the word ‘green’ was presented in red font color, then the correct response would be to select the red taped key on the keyboard. This is an example of an incongruent trial. If the word ‘green’ was presented in green font color then the correct response would be to select the green tapes key on the keyboard. This is an example of a congruent trial. Response time and accuracy were recorded for all trials, and the average response time and accuracy for all trials, congruent trials only, and incongruent trials only for each subject were entered into the behavioral matrix for the parallel ICA.

Flanker task

For the computerized flanker task (Eriksen and Eriksen, 1974), an arrow and four distracters were presented on the screen for 1000 ms followed by 500 ms ITI. Subjects were instructed to focus on the arrow in the middle and press the arrow key pointing towards the same direction (left or right) on the keyboard. In congruent trials, all arrows pointed in the same direction (>>>>>). In incongruent trials, the distracters were arrows

pointed in the opposite direction than the middle arrow (>><>>). In neutral trials, the middle arrow was flanked by four crosses (++>++). Average response time and accuracy for all trials, congruent trials only, incongruent trials only, and neutral trials only for each subject were each included in the behavioral matrix for the parallel ICA.

Digit span

Forward, backward, and total digit span were recorded for each participant (Wechsler, 1997). In this task, increasingly longer strings of numbers were read aloud to participants. For the forward digit span, subjects were instructed to repeat the numbers in the same order as they were read to them. For the backwards digit span, subjects were instructed to repeat the numbers in reverse order that they were read. Tests were administered and scores calculated according to the WMS-III (Wechsler, 1997), with the total span measure equaling the sum of the scores on the forward and backward spans. Total, forward, and backward digit span for each subject were included in the behavioral matrix for the parallel ICA.

Spatial span

Forward, backward, and total spatial span were recorded for each participant (Wechsler, 1997). In this task, increasingly longer sequences of blocks on a standard board were touched by the experimenter. For the forward spatial span, subjects were instructed to repeat the sequence in the same order as they were touched by the experimenter. For the backward spatial span, subjects were instructed to repeat the sequence of touched blocks in reverse order than they were pressed by the experimenter. Tests were administered and scores calculated according to the WMS-III

(Wechsler, 1997), with the total span measure equaling the sum of the scores on the forward and backward spans. Total, forward, and backward spatial span for each subject were included in the behavioral matrix for the parallel ICA.

Verbal working memory

Participants completed a verbal working memory task inside the scanner. For each trial, three upper case letters (excluding vowels and 'L') were presented in the center of a back projected screen for 2 seconds. Following a delay period of 6 seconds a single lower case letter was presented in the center of the screen for 2 seconds. Trials were separated by varying ITI. Changing the case of the letter ensured subjects were encoding the information verbally. Subjects responded using a MR-safe button pad whether or not the lower case letter was one of the three letters they had previously seen. Average response time and accuracy for each subject were included in the behavioral matrix for the parallel ICA.

Spatial working memory

In the spatial working tasks, three locations indicated by parentheses presented around an imaginary clock face case letters were presented in the center of a back projected screen for 2 seconds. Following a delay period of 6 seconds a single location was presented on the screen for 2 seconds. Trials were separated by varying ITI. Subjects responded using a MR-safe button pad whether or not that location was one of the three locations they had previously seen. Average response time and accuracy for each subject were included in the behavioral matrix for the parallel ICA.

Bound spatial and verbal working memory

Subject also performed two combined verbal and spatial working memory tasks designed to identify the neural substrates of working memory feature binding (Prabhakaran et al., 2000; Prabhakaran et al., 2011). In the bound task three upper case letters were presented in three different locations around an imaginary clock face on a back projected screen for 2 seconds. Following a delay period of 6 seconds a single lower case letter at a single location around the clock face was presented on the screen for 2 seconds. Trials were separated by varying ITI. Subjects responded using a MR-safe button pad whether or not *both* the letter and location were included in the previous screen. However, subjects were informed that the letter and location did not necessarily had to have been paired together initially in order for the trial to be a 'match' trial. These are examples of incongruent match trials. In congruent match trials the letter and location presented in the retrieval phase were also paired together in the encoding phase (**Supplementary Figure 4.1**). Average response time and accuracy for congruent trials, incongruent trials, and all trials from each subject were used as input to the behavioral matrix for the parallel ICA.

Separate spatial and verbal working memory

In the separate, or unbound, working memory task, three upper case letters were presented in the center of the screen and three different locations indicated by parentheses were presented on an imaginary clock face around the center of the back projected screen for 2 seconds. Following a delay period of 6 seconds a single lower

case letter at a single location around the clock face was presented on the screen for 2 seconds. Trials were separated by varying ITI. Subjects responded using a MR-safe button pad whether or not *both* the letter and location were included in the previous screen (**Supplementary Figure 4.1**). Average response time and accuracy on all trials for each subject were used as input to the behavioral matrix for the parallel ICA.

Digit symbol substitution task

Participants also completed the digit symbol substitution task (Wechsler, 2008). In this task, subjects were given 120 seconds to write the appropriate symbol associated with each specific number based on a key presented at the top of the page. The number of symbols corrected drawn per second for each subject was included in the behavioral matrix for the parallel ICA.

Motor task

During the scanning session participants performed a simple block design motor task in which they sequentially pressed four buttons on a MR-safe button pad with their four fingers when the word ‘Tap’ appeared on the screen. Subjects were to stop and rest when the word ‘Rest’ appeared on the screen. Twenty second long ‘Rest’ and ‘Tap’ blocks were alternated for 3 minutes and 20 seconds (4 ‘Rest’ blocks, 3 ‘Tap’ blocks). The average response time for each button press and the number of total presses per second from each subject were included as variables in the behavioral matrix for the parallel ICA.

Raven’s advanced progressive matrices

Sets 1 and 2 of Raven's advanced progressive matrices, a canonical reasoning task, were completed by each subject (Raven et al., 1998). The 12 questions of set 1 were given as an untimed practice session, and each question answered incorrectly was reviewed and explained by the experimenter. Following this, subjects were given 40 minutes to complete the 36 questions in set 2. The total number of correctly answered questions from set 2 for each subject was entered into the behavioral matrix for the parallel ICA.

Supplementary Table 4.1

Task	Measure	Mean	SEM	Task	Measure	Mean	SEM
Verbal WM	RT	1045.13	50.77	**DSST**	Items/sec	0.74	0.03
	Accuracy	0.98	0.01	**Finger Tap**	RT	386.98	22.60
Spatial WM	RT	1124.37	43.8		Rate	2.86	0.21
	Accuracy	0.93	0.01	**Flanker**	RT	502.07	9.82
Unbound WM	RT	1298.54	47.55		Accuracy	0.98	0.00
	Accuracy	0.93	0.02	*Congruent*	RT	478.63	10.09
Bound WM	RT	1284	50.45		Accuracy	0.99	0.00
	Accuracy	0.96	0.01	*Incongruent*	RT	521.6	11.67
Congruent	RT	1263.57	56.75		Accuracy	0.97	0.01
	Accuracy	0.95	0.01	*Neutral*	RT	499.43	11.53
Incongruent	RT	1406.05	57.48		Accuracy	0.99	0.00
	Accuracy	0.91	0.02	**Stroop**	RT	844.84	24.52
Digit Span	Forward	11.5	0.5		Accuracy	0.97	0.01
	Backward	9.21	0.74	*Congruent*	RT	826.45	23.45
	Total	20.29	0.96		Accuracy	0.99	0.01
Spatial Span	Forward	9.38	0.36	*Incongruent*	RT	863.92	26.75
	Backward	9.42	0.36		Accuracy	0.95	0.01
	Total	18.79	0.52	**Raven's APM**	Items	27.38	0.77

Supplementary Table 4.1: Displayed are the averages and SEMs across all subjects for the items included in the behavioral matrix for the parallel ICA. *Handedness* (20 R, 1 L, 3 Amb) scores from the Edinburgh Handedness Inventory*, gender* (14M/10F), and *age* (25 ± 0.67 yrs) for each subject were also included in the behavioral matrix for the parallel ICA. RT = response time, measured in milliseconds. WM = working memory, DSST = digit symbol substation task, APM = advanced progressive matrices.

Supplementary Figure 4.1

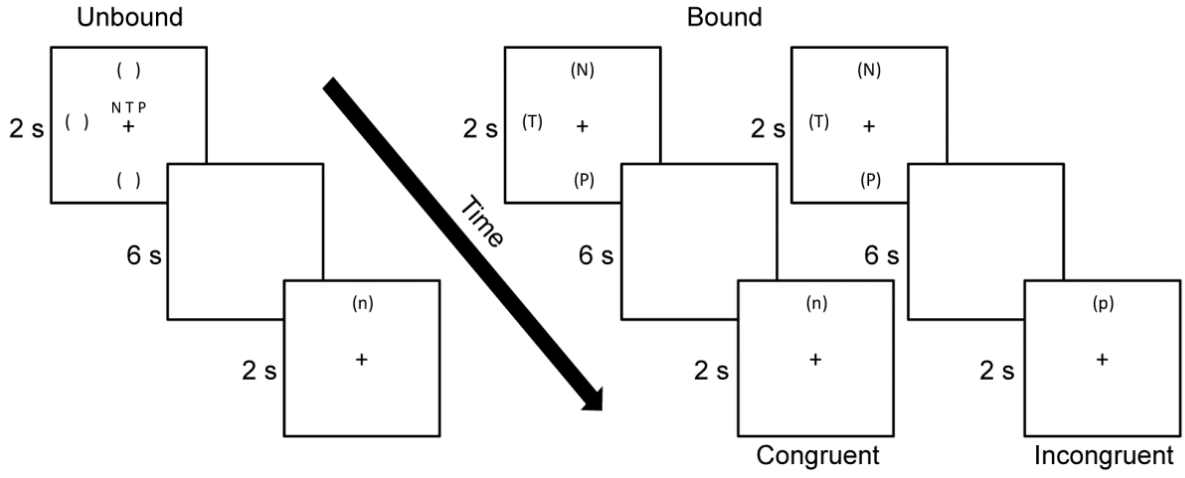

Supplementary Figure 4.1: Displayed above are examples of the two combined spatial and verbal working memory tasks. For both tasks participants were instructed to respond ‘yes’ or ‘no’ by pressing the appropriate button on a button pad whether both the letter and location in the retrieval phase were included in that trial’s encoding phase. In the ‘unbound’ version (*left*), the letters and locations are presented separately. Shown is an unbound trial requiring a ‘yes’ response. In the ‘bound’ version, each letter is presented in a specific location. There were two bound ‘yes’ trial types. In congruent trials the letter is in the same location in the retrieval phase that it was in during the encoding phase. In the retrieval phase of incongruent trials the probe letter is associated with one of the three other locations that were present during the encoding phase.

Supplementary References

Eriksen, B.A., Eriksen, C.W., 1974. Effects of noise letters upon identification of a target letter in a non-search task. Perception and Psychophysics 16, 143-149.

Prabhakaran, V., Narayanan, K., Zhao, Z., Gabrieli, J.D., 2000. Integration of diverse information in working memory within the frontal lobe. Nat Neurosci 3, 85-90.

Prabhakaran, V., Rypma, B., Narayanan, N.S., Meier, T.B., Austin, B.P., Nair, V.A., Naing, L., Thomas, L.E., Gabrieli, J.D., 2011. Capacity-speed relationships in prefrontal cortex. PLoS One 6, e27504.

Raven, J.C., Raven, J., Court, J.H., 1998. A manual for Raven's Progressive Matrices and Vocabulary Scales. H.K. Lewis, London.

Stroop, J.R., 1935. Studies of interference in serial verbal reactions. Journal of Experimental Psychology 18, 643-662.

Wechsler, D., 1997. Wechsler Memory Scale - Third edition (WMS--III). Harcourt Assessment, San Antonio, TX.

Wechsler, D., 2008. Wechsler Adult Intelligence Scale - 4th Edition (WAIS--IV). Harcourt Assessment, San Antonio, TX.

Chapter 5

Support vector machine classification and characterization of age-related reorganization of functional brain networks

Timothy B. Meier, Alok S. Deshpande, Svyatoslav Vergun, Veena A. Nair, Jie Song, Bharat B. Biswal, Mary E. Meyerand, Rasmus M. Birn, Vivek Prabhakaran

Published in:

NeuroImage, 60(1): 601-613 (2012).

Abstract

Most of what is known about the reorganization of functional brain networks that accompanies normal aging is based on neuroimaging studies in which participants perform specific tasks. In these studies, reorganization is defined by the differences in task activation between young and old adults. However, task activation differences could be the result of differences in task performance, strategy, or motivation, and not necessarily reflect reorganization. Resting-state fMRI provides a method of investigating functional brain networks without such confounds. Here, a support vector machine (SVM) classifier was used in an attempt to differentiate older adults from younger adults based on their resting-state functional connectivity. In addition, the information used by the SVM was investigated to see what functional connections best differentiated younger adult brains from older adult brains. Three separate resting-state scans from 26 younger adults (18-35 yrs) and 26 older adults (55-85) were obtained from the International Consortium for Brain Mapping (ICBM) dataset made publically available in the 1000 Functional Connectomes project www.nitrc.org/projects/fcon_1000. 100 seed-regions from four functional networks with 5 mm^3 radius were defined based on a recent study using machine learning classifiers on adolescent brains. Time-series for every seed-region were averaged and three matrices of z-transformed correlation coefficients were created for each subject corresponding to each individual's three resting-state scans. SVM was then applied using leave-one-out cross-validation. The SVM classifier was 84% accurate in classifying older and younger adult brains. The majority of the connections used by the classifier to distinguish subjects by age came from seed-regions belonging to the

sensorimotor and cingulo-opercular networks. These results suggest that age-related decreases in positive correlations within the cingulo-opercular and default networks, and decreases in negative correlations between the default and sensorimotor networks, are the distinguishing characteristics of age-related reorganization.

Introduction

Until relatively recently, most of our knowledge regarding the age-related reorganization of functional networks in the human brain has been based on neuroimaging studies comparing differences in task activity between younger and older adults. However, following an explosion of research into resting-state functional connectivity, it has been proposed that all functional networks that are utilized for task performance are present during rest in the form of correlations between low frequency fluctuations (Biswal et al., 1995; Smith et al., 2009). Resting-state fMRI allows the investigation of age-related changes in functional networks without confounds of task studies, such as performance, motivation, and the use of divergent strategies.

Relatively few studies have attempted to characterize age-related reorganization of functional networks at the brain-wide level using resting-state functional connectivity (Biswal et al., 2010). In one such study, Meunier et al. completed a graph theoretical analysis on resting-state data investigating the effects of aging on the modular organization of functional networks (2009). They found that large modules, or networks, observed in young healthy adults were split up into smaller modules in older adults. In addition, they observed a shift in the hubs of modular connectivity, where the hubs for older adults were located in more posterior regions compared to younger adults (Meunier et al., 2009). A separate study investigating global functional connectivity differences in homotopic regions of the brain between younger and older adults found that functional connectivity between homotopic areas decreases from adolescence to adulthood, and then increases again with advancing age in adulthood (Zuo et al., 2010).

However, several questions regarding the exact nature of the changes in brain networks that accompany age remain.

One powerful method available to investigate the age-related reorganization of functional networks is the use of machine learning classifiers (Pereira et al., 2009). Machine learning classifiers, such as support vector machines (SVM), entail selecting independent variables, known as features, and using these features to predict the class membership of an individual example. The features are assigned parameters, called weights, by applying the SVM algorithm to a training dataset with known class labels. In essence, the feature weight corresponds to the relative contribution of a specific feature to the classifier's ability to successfully differentiate the two groups. After feature weights are calculated, the classifier can then be applied to a separate dataset, known as the testing dataset, and the performance of the classifier can be assessed in terms of its accuracy in classifying examples to the correct class.

The use of SVM on resting-state fMRI data has several advantages over traditional univariate methods. For example, the robustness of findings on group differences can be measured in terms of the accuracy in which these findings classify individual subjects. Importantly, SVM allows the identification of features that contributed the most to subject classification, providing insight into the defining differences between two groups.

Machine learning classifiers, including SVM, have been successfully applied to resting-state fMRI data in the classification of major depressive disorder, schizophrenia, and adolescent brains from normal adult brains (Craddock et al., 2009; Shen et al., 2010; Supekar et al., 2009). A recent study by Dosenbach and colleagues used SVM

(and a related method support vector regression) to classify adolescent and adult brains based on resting-state functional connectivity (2010). They observed that the distinguishing characteristic for successful classification between child and adult brains was a decrease in correlations among short-range connections, along with an increase in correlations among long-range connections with increasing age.

In this study, a commonly used machine learning method namely the SVM was used to discriminate healthy younger and older adults based on their resting-state functional connectivity. We hypothesized that older and younger adult brains could be successfully classified based on their resting-state functional connectivity with the use of binary SVM. In addition, the major goal of this study was to use the information provided by SVM to identify what features (in our case functional connections) contributed the most to the success of the classifier. It is our hope that by thoroughly investigating these features we can identify patterns of network and seed-region differences that represent the distinguishing functional network changes that occur with normal aging.

Materials and Methods

Resting-state data from 26 right-handed younger adults (18-35 yrs, mean = 24.7 yrs ± 0.9 SEM, 12 male, 14 females) and 26 right-handed older adults (55-85 yrs, mean = 64.7 yrs ± 1.56 SEM, 11 male, 15 female) were obtained from the International Consortium for Brain Mapping (ICBM) dataset made publically available in the 1000 Functional Connectomes project www.nitrc.org/projects/fcon_1000 (Biswal et al., 2010). This dataset includes three separate resting-state scans for each subject in which 23 axial slices were acquired on a 3T scanner and comprised of 128 time points using a gradient-echo EPI sequence with TR = 2 seconds where subjects lied in the scanner

with their eyes closed. Out of 78 total scans in older adults, 42 were acquired with spatial resolution of 4 x 4 x 5.5 mm, while 36 were acquired with spatial resolution of 4 x 4 x 4 mm. Out of the 78 total scans in younger adults, 36 were acquired with spatial resolution of 4 x 4 x 5.5 mm, while 42 were acquired with spatial resolution of 4 x 4 x 4 mm. Information regarding this dataset is available at www.nitrc.org.

Preprocessing

Functional data were preprocessed using slightly modified scripts included in the 1000 Functional Connectomes Project using a combination of FSL and AFNI (Biswal et al., 2010; Cox, 1996; Smith et al., 2004; Woolrich et al., 2009). All images were first deobliqued and reoriented to RPI orientation for use in FSL. EPIs were motion and slice-time corrected, spatially smoothed using a Gaussian kernel of 6 mm FWHM, and scaled to the grand mean. Time series were then band-pass filtered (0.005 – 0.1 Hz) and linear and quadratic trends were removed. The eighth image of each scan was used to register the EPI scan to the high resolution anatomical scan that was acquired during the same session of the particular EPI.

In order to control for participant movement and physiological processes, motion parameters, global signal, white matter signal, and CSF signal were regressed from the time series. The global signal was calculated by averaging across all voxels in the brain. White matter and CSF masks were created by the segmentation of each individual's structural image using FSL's FAST program and then applied to each EPI to extract the white matter and CSF signals. Following the removal of these nuisance variables, the residual time series for each scan were demeaned, re-sampled to 3 mm^3, and registered to MNI152 standard space using FSL's FLIRT program.

Seed-based connectivity

Time courses were extracted from predefined regions of interest derived from a series of meta-analyses of task-related fMRI studies, as described in Dosenbach et al. (2010). In their study, Dosenbach and colleagues investigated 160 total seed-regions from six different networks. We focused on seed-regions located in the default network, sensorimotor network, fronto-parietal network, and the cingulo-opercular network. **Figure 5.1** displays the seed-regions used. In order to calculate seed-regions that were common among all subjects, an inclusive mask of the spatially normalized residuals was created and applied to every EPI. This insured that seed-regions in which some or all participants had no signal or EPI brain coverage were not included in our analysis.

The time series from 100 five mm^3 radius spherical seed-regions that survived the inclusive mask were extracted from the spatially standardized residuals for every EPI scan. The resulting time series for each seed-region from each of the three EPI scans per subject were then imported into Matlab (Mathworks) and correlated against every other seed-region, resulting in the creation of three 100 x 100 matrices of correlation coefficients for each individual. Correlation coefficients were z-transformed using Fisher's r-to-z transformation to normalize the distribution.

Binary SVM classification and leave-one-out cross-validation

Soft-margin SVM classification (with regularization parameter C = 0.5) was performed using the Spider Machine Learning Toolbox (Weston et al., 2005) implemented in Matlab (Mathworks). A radial basis function was used as the underlying kernel to map the data in higher-dimension vector space and apply a linear decision function to classify individual scans as being from either the younger or older adult

group. Leave-one-out cross-validation (LOOCV) was used for tuning the SVM hyper-parameters and estimating the classifier's accuracy. The benefit of LOOCV is that the same dataset can be used for both the training and testing of the classifier (Pereira et al., 2009). For each round of LOOCV, a subject's data was removed (all three scans to avoid twinning bias) and the top 200 features (connections) were selected using two-sample t-tests (not assuming equal variance) on the training set and ranked according to their absolute t-statistics in descending order. The criterion of retaining top 200 features was based upon the fact that approximately the same number of features survived the same t-test on the whole data after False Discovery Rate correction. The classifier was then trained, and feature weights were estimated on the remaining subjects' datasets (serving as the training dataset). The three scans of the subject that were left out of the training set served as the testing dataset, and were each separately classified as being either young or old. This process was repeated for every subject and the total accuracy of the classifier was determined by the percent of scans which were correctly categorized.

Results

Overall classifier performance

The classifier successfully discriminated older adults from younger adults at an accuracy of 84%. Given the equal number of older and younger adults in our sample, chance performance of the classifier would have yielded an accuracy of 50% (the null hypothesis). Therefore, we treated each fold of the leave one out cross validation as a Bernoulli trial with success probability of 0.5, as specified by Pereira et al. (2009). By comparing the number of true positives to the total number of examples (scans to be

classified as young or old) we observed the probability of our measured accuracy occurring by chance. The 84% accuracy of the classifier was highly significant, having a p value < 0.0000001.

Consensus features

Two-hundred features, defined as the functional connectivity between two seed-regions, were obtained from each round of LOOCV. From these, 126 features, known as consensus features, were found to be common across every round. **Table 5.1** lists the consensus features with negative predictor weights corresponding to seed-region pairs in which older adults had significantly higher correlation coefficients than younger adults. **Table 5.2** lists consensus features with positive predictor weights corresponding to seed-region pairs in which younger adults had significantly higher correlation coefficients than older adults.

The goal of the present study was to identify the functional connections that distinguish older adult brains from younger adult brains. To identify brain regions that undergo significant age-related changes in functional connectivity, the contribution of each seed-region to the overall ability of the classifier to accurately discriminate between age groups can be assessed by summing one-half of the feature weights associated with that seed-region. For this study, we used a non-linear radial basis function as the kernel for the SVM classification, to be consistent with the study by Dosenbach and colleagues (2010). The use of a non-linear kernel limits the interpretation of the SVM weights in high dimensional feature space, and also prevents the exact transformation of feature weights from feature space back to input space (Scholkopf et al., 1999). Therefore, we find an approximation of feature weight by

performing a two sample t-test between the young and old age groups for each connection (feature) and use the resulting t-score as our feature weight.

The single seed-region with the greatest amount of feature weight associated with it was a seed-region located in the left precuneus, near the border of the cingulate (MNI coordinates -3 -38 45). **Table 5.3** displays the top ten seed-regions when ranked by total feature weight. The seed-region that contributed to the second-most feature weights was located in the right post-central gyrus (MNI coordinates 46 -20 45). The third and fourth largest contributions came from the right pre-SMA (MNI coordinates 0 5 51) and SMA (0 -1 52), respectively.

The z-transformed correlation coefficients from the consensus features for both the younger and older adult groups were analyzed to determine the exact nature of the functional connectivity changes that contributed to the total feature weight used in the SVM classification (**Tables 5.1 and 5.2**). Of the total feature weight entered into the SVM, 37% came from pairs of seed-regions that displayed a decrease in correlation coefficients with age, where older adults displayed a significantly lower correlation between seed-region pairs than younger adults (**Figure 5.2a**). Positive correlations that were significantly higher in older adults than younger adults accounted for 31% of the total feature weight. Negative correlations that were significantly less negative in older adults than younger adults contributed to 32% of the total feature weight. **Figure 5.3** is an illustration of the consensus features connected to their associated see-regions. Although in terms of SVM performance decreases in negative correlations and increases in positive correlations with age were equivalent (i.e., both resulted in negative weights), we differentiated the patterns in this nature because of the

hypothesized physiological significance of a positive correlation and a negative correlation (anti-correlation) between two regions (Fox et al., 2005).

The seed-regions used in this study have been previously classified as belonging to four different functional networks by Dosenbach et al. (2010). Seed-regions from the fronto-parietal, cingulo-opercular, sensorimotor, and default network were investigated here. In order to identify what functional networks display the greatest amount of age-related change, the contribution of each network to the SVM classification was compared by summing the weight from all of the seed-regions classified as belonging to a certain network. As seen in **Figure 5.2b**, seeds from the sensorimotor network contributed the highest percentage of the feature weight, although all four networks contributed. We were able to further characterize each seed-region pair as either being between two different networks or being within a single network. Based on our SVM results, the majority of seed-region pairs that were significantly more connected in older adults (or less negatively correlated) were between network connections. Conversely, the majority of seed-region pairs that were significantly less connected in older adults were approximately half within network connections and half between network connections.

To get an in depth understanding of what types of age-related changes each network underwent, the contribution of each individual network to each of the above-mentioned scenarios was calculated.

Increased positive correlations with age

Between networks

Sixty-three percent of the weight from seed-region pairs that had an increase positive correlation with age were from connections between two different networks (**Figure 5.4a**). Of these, the majority (57%) of the weight came from connections between seed-regions in the sensorimotor and cingulo-opercular networks, 16% was between seed-regions in the sensorimotor and fronto-parietal networks, 14% was between seed-regions in the default and the fronto-parietal networks, 10% was between seed-regions in the fronto-parietal and cingulo-opercular, and 3% was between seed-regions in the cingulo-opercular and default networks.

Within networks

Thirty-seven percent of the weight coming from connections that were more positively correlated in older adults than younger adults was from within network connections. Of these, sensorimotor made up 79%, default made up 14%, and fronto-parietal made up 7%.

Decreased negative correlations with age

Between networks

All of the seed-region pairs that were significantly less negatively connected in older adults than in younger adults were between networks (**Figure 5.4b**). The majority of the feature weight from these seed-regions (70%) was between the seed-regions in the sensorimotor and default networks. Connections between the cingulo-opercular network and the default network accounted for 20% of the feature weight, while connections between the fronto-parietal and sensorimotor networks contributed 7% of the weight, and the cingulo-opercular and the fronto-parietal networks contributed 3% of the weight.

Decreased positive correlations with age

Between networks

Just over half (51%) of the weight from seed-region correlations that became less positive with age was from between network connections (**Figure 5.4c**). Of these, 73% were between the sensorimotor and cingulo-opercular networks, 15% were between the fronto-parietal and cingulo-opercular networks, 8% were between the fronto-parietal and sensorimotor networks, and 4% were between the default and sensorimotor networks.

Within networks

Within network connections contributed 49% of the weight coming from connections that were less positively correlated in older adults than younger adults. Of the within network connections 49% of the weight came from the cingulo-opercular network, 30% came from the sensorimotor network, 17% came from the default network, and 4% came from the fronto-parietal network.

Analysis by network

The feature weights belonging to each individual network was also classified by what type of connections they were and by what other networks they were connected to in order to understand the exact nature of the changes each network underwent.

Fronto-parietal

The connections accounting for the weight involving the fronto-parietal network were analyzed. Eighty-three percent of all of the weight coming from connections that included a fronto-parietal seed-region was from between network connections, whereas within network connections accounted for 17% (**Figure 5.5a**). Of the fronto-parietal connections that were between networks, 50% of the feature weight came from

connections that increased positive correlation with age, 29% came from decreased positive correlation with age, and 21% came from connections that decreased positive correlation with age. Of the fronto-parietal connections that were within network, 52% increased positive correlation with age and 48% decreased positive correlation with age.

Cingulo-opercular

From the features that included the cingulo-opercular network, 68% of the weight was from between network connections while 32% was from connections within the cingulo-opercular network (**Figure 5.5b**). Forty-four percent of the weight coming from between network connections decreased positive correlation with age, while 36% increased positive correlation with age and 20% decreased negative correlation with age. Of the weight coming from connections that were within the cingulo-opercular network, 100% decreased positive correlation with age.

Sensorimotor

Sixty-five percent of the weight coming from features that included the sensorimotor network was between network connections and 35% was within network connections (**Figure 5.5c**). Among the weight coming from between network connections that included the sensorimotor network, 45% decreased negative correlation with age, 26% increased positive correlation with age, and 29% decreased positive correlation with age. Among the weight derived from within sensorimotor connections, 63% increased positive correlation with age and 37% decreased positive correlation with age.

Default

The feature weight attributed to connections involving the default network were 78% between network connections and 22% within network connections (**Figure 5.5d**). Of the weight coming from between network connections that included the default network, 88% was from connections that decreased in negative correlation with age, 10% was from connections that increased in positive correlation with age, and 2% was from connections that decreased in positive correlation with age. Of the weight that came from within default network connections, 65% decreased positive correlation with age, 35% increased positive correlation with age.

Seed-to-seed distance

Consensus features were also characterized by the Euclidian distance between the seed-to-seed connections to determine if there were any patterns in the age-related functional connectivity differences. Connections were grouped according to the differences in correlation coefficients in the three general scenarios described above and the distances were compared using two sample t-tests with unequal variance (**Figure** 5.**6**). Connections that were significantly more positively correlated in older adults than younger adults (42.27 ± 3.87 mm SEM, n = 38) were significantly shorter than both connections that were less negatively correlated in older adults (56.33 ± 3.16 mm SEM, n = 40; $t(76) = -2.826$, $p < 0.01$), and connections that were less positively correlated in older adults (57.13 ± 2.95 mm SEM, n = 48; $t(84) = -3.112$, $p < 0.005$). There was no difference between connections that were less negatively correlated in older adults and connections that were less positively correlated with age.

Discussion

The goal of the current study was to identify the distinguishing age-related differences in resting state functional connectivity. The feature weights derived from SVM classification provide a means of doing so as the success of the SVM classification is dependent on the weights assigned to each feature. The contribution of individual seed-regions and networks to the success of the SVM can be assessed by summing the feature weight associated with each.

Based on our analysis of the feature weights, every single network as previously defined by Dosenbach et al. (2010) that we investigated made a large contribution to the SVM classification (**Figure 5.2b**). Interestingly, the greatest contribution came from seed-regions located in the sensorimotor network. This is reflected by the fact that five of the top ten seed-regions that contributed the most feature weight belonged to this network (**Table 5.3**). Although not as extensively studied as age-related changes in cognition, numerous studies have established that normal aging is accompanied by a general decline in simple sensorimotor function associated with varying levels of task-related increases in brain activation and functional connectivity (Calautti et al., 2001; Chen et al., 2009; Hutchinson et al., 2002; Mattay et al., 2002; Naccarato et al., 2006; Riecker et al., 2006; Ward and Frackowiak, 2003). In addition, decreases in functional connectivity and regional homogeneity of low frequency fluctuations at rest have also been reported in the motor network (Wu et al., 2007a; Wu et al., 2007b).

The greatest contribution from any one seed-region came from a region in the left precuneus of the default network (**Table 5.3**). The precuneus is thought to be involved in self-referential processing and, as part of the default mode network, is considered a major structural and functional hub of the brain (Cavanna and Trimble, 2006; Hagmann

et al., 2008). Age differences in task-related deactivation of the precuneus, and the default network as a whole, have been linked to difficulties in cognitive control that are often apparent in older adults (Grady et al., 2010; Grady et al., 2006; Lustig et al., 2003; Park et al., 2010; Persson et al., 2007; Sambataro et al., 2010). The effects of age on the default network are discussed below.

The differences in correlation coefficients between older adults and younger adults that contributed to the observed feature weights followed three different scenarios (visualized in **Figure 5.3**). First, there were those connections that were more positively correlated in older adults than in younger adults. Similar to this, there were those connections that were less negatively correlated in older adults than in younger adults. Finally, there were connections that were less positively correlated in older adults than in younger adults. Each of these scenarios contributed approximately one third of the total summed feature weight used for the SVM classification (**Figure 5.2a**). Importantly, connections that strengthened with age, which includes those that increase positive correlation and those that decrease negative correlation, accounted for two thirds of the total weight. This implies that connections that increase in strength with age are the distinguishing characteristics of age-related changes in connectivity, as the SVM classification relied heavily on these connections.

Stronger connections in older adults

A second significant observation from our SVM data presented here is that the connections that were stronger in older adults were mostly between network, or inter-network, connections (**Figure 5.4**). This included inter-network connections that became more positively correlated with age, which were mostly between the sensorimotor

network and the two networks previously defined as the task-control networks (the fronto-parietal and cingulo-opercular networks; (Dosenbach et al., 2007; Dosenbach et al., 2006), and also included inter-network connections that became less negatively correlated with age, which were mostly from connections between the default network and the sensorimotor network or the cingulo-opercular network (**Figure 5.4a-b**).

The observation that most of the feature weight used to classify older adult brains from younger adult brains came from increasingly positive connections between the sensorimotor network and the task-control networks is consistent with the hypothesis that cognitive systems must compensate in older adults for the general decline in sensorimotor abilities (Li and Lindenberger, 2002; Seidler et al., 2010). For example, Heuninchx et al. have shown that older adults display additional activations not observed in younger adults in cognitive areas including the frontal operculum, dorsolateral PFC, and the superior parietal cortex during simple motor tasks (Heuninckx et al., 2005; Heuninckx et al., 2008). Likewise, an increase in functional connectivity between sensorimotor areas and subcortical regions has been observed during simple motor tasks (Marchand et al., 2011). Our results suggest that the cognitive networks and the sensorimotor networks become less segregated in normal adult aging, possibly due to the greater functional inter-dependence of these networks in older adults. However, it is important to point out that some of the seed-regions classified as sensorimotor by Dosenbach et al. include regions such as the SMA, PMC, and dorsal frontal cortex regions that have previously been implicated in cognitive tasks (Dosenbach et al., 2010).

Another major contribution to our classifier came from connections that had decreases in negative correlations between regions in the default network and regions in the sensorimotor or cingulo-opercular network. It has been documented that the default network is negatively correlated with brain regions that are generally activated during attention-demanding cognitive tasks (Fox et al., 2005; Fransson, 2005). As previously mentioned, older adults often have difficulties in suppressing the default mode network compared to younger adults during cognitive task performance (Grady et al., 2010; Grady et al., 2006; Lustig et al., 2003; Park et al., 2010; Persson et al., 2007; Sambataro et al., 2010). Here, our finding of decreased negative correlations in older adults in connections between the default network and the cingulo-opercular network is consistent with this literature. However, the majority of the feature weight utilized by our classifier that came from decreased negative correlations were from seed-region pairs between the sensorimotor network and default network. It is plausible that this is one consequence of the previously described increased integration of the sensorimotor network and the task-control networks. Further research is needed to investigate the relationship between the default mode network and sensorimotor systems.

Weaker connections in older adults

In contrast to connections that became stronger in older adults, which were mostly inter-network connections, those that became weaker with age were roughly half inter-network and half intra-network, or within network, connections (**Figure 5.4c**). Although, as previously noted, much of the feature weight came from seed-regions pairs involving the sensorimotor and cingulo-opercular networks that were more positively correlated in older adults, there were a large number of seed-region pairs involving

these networks that became less positively correlated with age. This suggests that the increased involvement of cognition in sensorimotor tasks is a product of substantial reorganization of these two networks, including both increases and decreases in connectivity between the regions.

Our finding that nearly half of the connections that decreased with age were within network connections could reflect the dedifferentiation of these networks with advancing age. This seems to be the case in particular for the default mode network and the cingulo-opercular network, both of which had lower positive correlations in older adults than younger adults for within network connections (**Figure 5.5**). Age-related decreases in functional connectivity within the default network have been documented during task performance and at rest (Andrews-Hanna et al., 2007; Damoiseaux et al., 2008; Grady et al., 2010; Park et al., 2010). Reduced connectivity between areas of the cingulo-opercular network could be linked to difficulties of executive control that are often observed in older adults (for review, see Hedden and Gabrieli, 2004).

Connection distances

In the data presented here there is an age-related weakening of both long-range correlations and negative correlations, and an age-related strengthening of short-range correlations (**Figure 5.6**). Thus, the long-range positive and negative correlations that define normal brain organization in healthy adults become less defined in older adults. The reduced connectivity of long range connections observed in our study is in line with a study by Wang et al. that found that there are less long-range connections in older adults than in younger adults during a memory task (Wang et al., 2010). Interestingly,

the short-range connections with increasing connectivity with age were mostly between network connections, perhaps reflecting blurring of the functional networks.

Limitations

The present study does have limitations. The use of SVM requires several user decisions, including choosing the number of seed-regions to include and the manner in which seed-regions are defined. We selected seed-regions in an attempt to complement the recent Dosenbach paper that used support vector machines to classify adolescent brains from adult brains (Dosenbach et al., 2010). We also used the same network affiliations of the seed-regions as determined by Dosenbach and colleagues from their community detection analysis. However, the axial slice acquisition of the EPIs prevented the inclusion of the occipital and cerebellar networks in our analysis, as several subjects included in the ICBM dataset did not have coverage in these regions. The use of the entire Dosenbach seed-regions would have been ideal, but the accuracy of our predictor speaks to the robustness of our data. Additionally, although not a limitation, it is important to note that some of the seed-regions in the sensorimotor network have been implicated in cognitive tasks, which might explain the high level of interaction between the sensorimotor and cingulo-opercular networks observed here. It should also be noted that by using Euclidian distance between seed-regions as our measurement for connection length, some of the distances may not truly reflect the structural connective distance, such as for cases in which the measurement was between the hemispheres.

It is possible that factors associated with the scanning sessions themselves contributed to some of the differences observed. However, due to the fact that this

dataset was obtained from a data base, detailed information regarding potentially confounding factors such as differences in IQ or the degree to which subjects were able to stay awake during the scans is unfortunately unavailable.

Group differences in head motion

One major consideration regarding the current study is that group differences in head movement have been shown by Van Dijk and colleagues to significantly affect correlations between seed-regions (2011). To investigate this issue, a composite score of total motion for each subject was calculated as the square root of the sum of squares of the derivatives for each motion parameter, as suggested by Jones et al (2010). Older adults did have significantly more motion than younger adults (0.14 ± 0.013 in older adults, 0.07 ± .005 in younger adults; $t(50) = 4.37$, $p < 0.005$). Motion parameters were controlled for as nuisance regressors as is standard in the field, although this may not completely control effects introduced by motion as shown by Van Dijk et al (2011). Older subjects had consistently low movement from frame to frame rather than brief periods of large movement precluding frame by frame censoring of the data. We therefore performed three separate analyses to address this issue further (see supplement). First, we performed a second non-linear SVM using a subset of 16 younger subjects and 16 older subjects that were matched in the amount of head motion. This second SVM classified adults at an accuracy of 68%, which is still highly significant ($p < .0005$), and over one third of the consensus features from this analysis were identical to the original analysis (**Supplementary Table 5.1**). Second, we performed a non-linear support vector regression (SVR) on the original 52 subjects with each subjects' composite motion parameter estimate as a dependent variable in order

to extract features influenced by their total head motion. From this motion SVR, 76 features were identified of which 27 consensus features overlapped with consensus features derived from the original age SVM (indicated by an asterisk in **Tables 5.1 & 5.2**; listed in **Supplementary Table 5.2**). We interpret these 27 features as being sensitive to both age and motion (see a listing of these features as indicated by asterisks in **Tables 5.1 & 5.2**; listed in **Supplementary Table 5.2**). We also performed a third analysis of SVM identical to the primary age classifying SVM except without the 76 consensus features derived from the motion SVR. This classifier was 82% accurate, having 99 of its 126 consensus features identical to the original SVM along with 27 additional age-predicting features (see supplement). We interpret these 99 features as a robust set of features sensitive to age-related changes, since the accuracy change was minimal from the original SVM (84% accurate for original age SVM, 82% accurate for the SVM analysis without the 76 motion-influenced features). We also have made note of the 27 additional age-predicting features (**Supplementary Table 5.3**); essentially, the 27 features that overlapped between the motion SVR and the original age SVM were replaced with these 27 additional age-predicting features. However, it must be noted that simply removing the 76 features or connections that were most predictive of head movement does not completely remove the effect that head movement possibly has on the remaining features or connections.

These analyses suggest that motion may account for some of the differences in connectivity observed in this study; however, it is also important to note that for our motion-matched SVM there was a great reduction in power (loss of 10 subjects per group) as a result of matching our groups in terms of head motion. In addition,

regression of motion parameters was performed. Although this does not completely eliminate motion-related signal changes, it does reduce the influence of motion. The secondary SVM, and omitting overlapping features based on the motion classifying SVR, are conservative attempts to address the issues of head motion differences in the groups and may result in false negatives. Therefore the paper is mainly focused on all the age-related features, some of which were influenced by motion, and used the entire data set for this study. Certainly, the effect of head motion on functional connectivity analyses needs to be further explored to identify appropriate ways of controlling for group differences that might confound such studies.

Conclusion

These results show that SVM can successfully classify younger adult brains from older adult brains based on their resting-state functional connectivity. More importantly, the use of SVM allowed us to investigate the patterns of age-related connectivity changes that best differentiate older and younger adult brains with confounds typically associated with tasks. We observed three general patterns of resting state functional connectivity that differentiated younger adult brains from older adult brains. The first pattern we observed was that connections between the sensorimotor and cingulo-opercular networks contributed the most to the classifier's accuracy. The second pattern we observed is that there is a decrease in negative correlations between the default network and the sensorimotor and cingulo-opercular networks. Finally, we observed that within network connections of the cingulo-opercular and default networks were less positively correlated in older adults than in younger adults. These three patterns were observed in the main analysis as well as in the more conservative analyses provided in

the supplement in order to account for group differences in head motion (see supplement). Our observation that connections that were more positively correlated in older adults than younger adults were significantly shorter than both connections that were less negatively correlated in older adults and connections that were less positively correlated in older adults was not observed in our more conservative analyses, and it is uncertain whether this finding is due to group differences in head movement or the reduced power of these supplementary analyses.

This study complements the recent study by Dosenbach et al. in which machine learning classifiers were used to predict brain maturity during development (2010). This study also adds to the small body of literature that characterizes age-related reorganization of functional networks with the use of machine learning classifier on resting-state functional connectivity. Better understanding the structural and functional network changes that accompany aging may lead to strategies to ameliorate some of the behavioral consequences of normal aging.

Table 5.1

	Consensus Features				Weight	zCC	
	Network 1	Seed 1	Network 2	Seed 2		Young	Old
*	fronto-parietal	L_IPL_1	default	L_precuneus_1	-6.9637	0.026	0.324
*	sensorimotor	L_parietal_1	sensorimotor	R_parietal_3	-6.8139	0.14344	0.41574
	cingulo-opercular	L_parietal_8	fronto-parietal	L_IPL_3	-6.4236	0.4054	0.71477
	sensorimotor	L_parietal_5	default	L_precuneus_1	-6.3416	-0.07283	0.19833
*	cingulo-opercular	M_mFC	default	R_sup_frontal	-6.0915	-0.07322	0.19149
*	sensorimotor	R_parietal_1	default	L_precuneus_1	-6.037	-0.06051	0.23221
	sensorimotor	L_vFC_2	sensorimotor	L_precentral_gyrus_2	-5.9828	0.27595	0.49152
*	cingulo-opercular	R_precuneus_1	sensorimotor	R_dFC_3	-5.9076	0.00677	0.20285
	cingulo-opercular	R_basal_ganglia_2	default	L_post_cingulate_1	-5.8994	-0.04513	0.15182
*	sensorimotor	L_parietal_2	default	L_precuneus_1	-5.8611	-0.08508	0.1419
	cingulo-opercular	R_vFC_1	sensorimotor	L_mid_insula_1	-5.8045	0.05756	0.28137
	default	L_sup_frontal	default	R_sup_frontal	-5.785	0.31145	0.53908
*	sensorimotor	L_parietal_4	default	L_precuneus_1	-5.7482	-0.07106	0.18429
	cingulo-opercular	R_vFC_1	sensorimotor	R_vFC_2	-5.6727	0.10371	0.32266
	fronto-parietal	M_ACC_2	default	R_sup_frontal	-5.5557	0.12497	0.36098
*	sensorimotor	R_frontal_2	default	L_precuneus_1	-5.5424	-0.13916	0.09649
	cingulo-opercular	R_basal_ganglia_2	default	L_post_cingulate_2	-5.5077	-0.00997	0.19253
*	sensorimotor	L_parietal_1	sensorimotor	R_parietal_1	-5.443	0.11674	0.31418
	sensorimotor	L_parietal_1	sensorimotor	L_parietal_7	-5.4388	0.12552	0.38364
	sensorimotor	R_frontal_1	default	R_post_cingulate	-5.4126	-0.33475	-0.09609
	sensorimotor	L_precentral_gyrus_1	default	L_precuneus_1	-5.3767	-0.09455	0.13864
	cingulo-opercular	R_precuneus_1	sensorimotor	R_precentral_gyrus_3	-5.3665	0.09811	0.29391
*	cingulo-opercular	R_precuneus_1	sensorimotor	R_parietal_1	-5.3601	0.13225	0.34745
	cingulo-opercular	L_parietal_8	default	L_angular_gyrus_2	-5.3436	-0.02154	0.26414
*	sensorimotor	R_precentral_gyrus_3	default	L_precuneus_1	-5.3309	-0.05766	0.1785
*	sensorimotor	R_frontal_1	default	L_precuneus_2	-5.3051	-0.40751	-0.17159
*	sensorimotor	R_dFC_3	default	L_precuneus_1	-5.3008	-0.13199	0.08819
	fronto-parietal	L_dFC	sensorimotor	R_precentral_gyrus_3	-5.215	0.0284	0.20884
	sensorimotor	L_parietal_5	default	M_post_cingulate	-5.214	-0.186	0.00616
*	sensorimotor	R_frontal_1	default	R_precuneus_3	-5.1548	-0.38606	-0.17114

	sensorimotor	L_parietal_1	sensorimotor	R_precentral_gyrus_3	-5.0597	0.00014	0.17029
	sensorimotor	R_pre_SMA	default	L_precuneus_1	-5.0595	-0.01934	0.182
	cingulo-opercular	R_precuneus_1	sensorimotor	L_precentral_gyrus_1	-5.0434	0.03514	0.22223
*	sensorimotor	R_frontal_1	default	L_post_cingulate_1	-5.0271	-0.2892	-0.06083
	sensorimotor	L_mid_insula_1	default	R_precuneus_2	-4.9988	-0.11259	0.08349
	cingulo-opercular	R_precuneus_1	fronto-parietal	R_dFC_2	-4.9833	-0.02671	0.15223
*	sensorimotor	L_post_parietal_1	default	L_precuneus_1	-4.9758	-0.00006	0.22795
	sensorimotor	M_SMA	default	L_precuneus_1	-4.9607	-0.02843	0.19909
	sensorimotor	R_post_insula	default	M_post_cingulate	-4.9419	-0.09243	0.09829
	sensorimotor	L_parietal_1	sensorimotor	L_parietal_4	-4.9403	0.2186	0.43343
	fronto-parietal	L_vent_aPFC	sensorimotor	L_precentral_gyrus_3	-4.938	-0.08357	0.07917
	sensorimotor	L_precentral_gyrus_1	sensorimotor	L_parietal_1	-4.8991	0.24984	0.44281
	sensorimotor	R_vFC_2	default	R_post_cingulate	-4.8767	-0.15563	0.02577
	fronto-parietal	L_dFC	sensorimotor	M_SMA	-4.8728	-0.03186	0.13673
*	fronto-parietal	L_IPL_1	fronto-parietal	L_IPL_2	-4.8506	0.39204	0.59056
	cingulo-opercular	L_basal_ganglia_1	default	R_sup_frontal	-4.8298	-0.15502	0.02432
	fronto-parietal	R_dFC_2	sensorimotor	R_precentral_gyrus_3	-4.7777	0.07521	0.26542
*	sensorimotor	R_frontal_1	default	R_precuneus_2	-4.7749	-0.22408	-0.0175
	cingulo-opercular	M_mFC	default	L_sup_frontal	-4.7542	-0.08898	0.10304
	sensorimotor	L_mid_insula_2	default	R_precuneus_2	-4.7339	-0.04408	0.14061
*	sensorimotor	L_precentral_gyrus_1	sensorimotor	R_parietal_3	-4.6947	0.12362	0.30584
	cingulo-opercular	R_vFC_1	sensorimotor	R_mid_insula_1	-4.6941	0.06274	0.22645
*	sensorimotor	R_frontal_1	default	L_post_cingulate_3	-4.6882	-0.35517	-0.14138
*	cingulo-opercular	R_aPFC_2	default	M_mPFC	-4.6811	0.11098	0.34963
	sensorimotor	L_vFC_2	sensorimotor	R_precentral_gyrus_2	-4.6715	0.20328	0.36102
	sensorimotor	L_vFC_2	sensorimotor	L_parietal_2	-4.6594	0.1762	0.35079
	fronto-parietal	L_dFC	sensorimotor	L_parietal_5	-4.5916	0.02255	0.19673
*	cingulo-opercular	L_vFC_1	sensorimotor	L_precentral_gyrus_2	-4.5639	0.1151	0.26631
	cingulo-opercular	L_thalamus_1	sensorimotor	L_mid_insula_1	-4.5524	0.13101	0.34489
	cingulo-opercular	R_precuneus_1	sensorimotor	L_parietal_1	-4.541	0.10812	0.2848
	sensorimotor	L_parietal_1	sensorimotor	M_SMA	-4.5282	0.4107	0.59782
	cingulo-opercular	R_precuneus_1	fronto-parietal	L_IPL_1	-4.5181	0.08958	0.24964
	fronto-parietal	L_dFC	sensorimotor	R_parietal_1	-4.5076	-0.0236	0.1464
	sensorimotor	L_mid_insula_1	default	L_post_cingulate_1	-4.4725	-0.1563	0.02463

	cingulo-opercular	R_precuneus_1	sensorimotor	L_parietal_4	-4.4683	0.1485	0.31761
	cingulo-opercular	L_parietal_8	default	L_IPS_2	-4.4477	-0.13155	0.07914
	sensorimotor	L_parietal_5	default	L_post_cingulate_1	-4.4456	-0.22846	-0.08524
	sensorimotor	R_precentral_gyrus_1	default	R_post_cingulate	-4.4272	-0.1245	0.03998
	sensorimotor	L_parietal_2	default	M_post_cingulate	-4.4161	-0.16392	0.00723
	sensorimotor	L_parietal_5	default	R_precuneus_3	-4.4074	-0.1752	-0.01556
*	fronto-parietal	L_IPL_2	sensorimotor	L_post_parietal_1	-4.3931	0.03602	0.23119
	cingulo-opercular	R_precuneus_1	sensorimotor	L_parietal_2	-4.3759	0.0748	0.23352
	default	L_aPFC_2	default	R_sup_frontal	-4.3651	0.00635	0.19928
*	fronto-parietal	L_post_parietal_2	default	L_precuneus_1	-4.3286	0.06226	0.2472
*	sensorimotor	R_precentral_gyrus_1	default	R_precuneus_2	-4.3278	-0.16687	-0.00511
	cingulo-opercular	L_vFC_1	sensorimotor	L_mid_insula_2	-4.3116	0.14899	0.30957
	cingulo-opercular	R_dACC	default	R_sup_frontal	-4.2573	-0.10625	0.05787
	cingulo-opercular	R_vFC_1	sensorimotor	R_precentral_gyrus_1	-4.2376	0.01835	0.18367

Table 5.1: Information on consensus features with negative feature weights derived from connections that were more positively correlated (or less negatively correlated) in older adults than in younger adults. Shown are the seed-region pairs and their respective networks, the average feature weight for each seed-region pair, and the respective z-transformed correlation coefficients for both the younger and older adult groups. Features that overlap with features derived from the motion-SVR (see supplement) indicated with *. ROI seeds are coded for ease of visualization in Tables 1-3: fronto-parietal – yellow; sensorimotor – blue; default – red; cingulo-opercular – green.

Table 5.2

	Consensus Features				Weight	zCC	
	Network 1	Seed 1	Network 2	Seed 2		Young	Old
	cingulo-opercular	L_ant_insula	cingulo-opercular	M_mFC	7.0028	0.416	0.166
	cingulo-opercular	R_mid_insula_2	sensorimotor	R_parietal_3	6.2496	0.13351	-0.06179
	cingulo-opercular	R_basal_ganglia_1	cingulo-opercular	M_mFC	5.74	0.23981	0.05116
*	sensorimotor	L_temporal_2	sensorimotor	R_parietal_1	5.4257	0.16448	-0.03993
	cingulo-opercular	L_mid_insula_3	sensorimotor	R_parietal_3	5.3	0.07934	-0.09357
	default	L_post_cingulate_1	default	M_post_cingulate	5.2879	0.71585	0.50237
	cingulo-opercular	L_vFC_3	cingulo-opercular	L_basal_ganglia_1	5.1761	0.31143	0.11882
	sensorimotor	L_mid_insula_1	sensorimotor	L_parietal_5	5.1124	0.27156	0.06977
	cingulo-opercular	L_post_insula	cingulo-opercular	R_precuneus_1	5.1106	0.05066	-0.09328
	cingulo-opercular	M_ACC_1	sensorimotor	M_SMA	4.977	0.09544	-0.07402
	cingulo-opercular	M_ACC_1	sensorimotor	R_pre_SMA	4.9165	0.15591	-0.0049
	sensorimotor	R_vFC_2	sensorimotor	M_SMA	4.9102	0.29728	0.10816
	cingulo-opercular	R_basal_ganglia_1	sensorimotor	L_vFC_2	4.9018	0.065	-0.10551
	cingulo-opercular	L_ant_insula	sensorimotor	R_dFC_3	4.8627	0.12801	-0.06275
	cingulo-opercular	R_mid_insula_2	sensorimotor	R_pre_SMA	4.7979	0.16215	0.01979
	cingulo-opercular	L_basal_ganglia_2	sensorimotor	L_vFC_2	4.7975	0.13288	-0.01373
	cingulo-opercular	R_ant_insula	cingulo-opercular	M_mFC	4.7868	0.36379	0.19215
	fronto-parietal	L_IPL_1	sensorimotor	R_frontal_1	4.7661	0.24419	0.04502
	sensorimotor	L_mid_insula_2	sensorimotor	R_pre_SMA	4.7616	0.11863	-0.01357
	cingulo-opercular	R_basal_ganglia_2	sensorimotor	R_parietal_3	4.7302	0.09986	-0.05815
	cingulo-opercular	L_ant_insula	cingulo-opercular	L_basal_ganglia_1	4.6473	0.34985	0.16561
	sensorimotor	L_precentral_gyrus_1	default	L_aPFC_2	4.6358	0.0399	-0.12346
	default	R_ACC	default	M_post_cingulate	4.6356	0.34947	0.1559
	cingulo-opercular	L_thalamus_1	cingulo-opercular	M_mFC	4.6113	0.13332	-0.01663
	cingulo-opercular	L_ant_insula	fronto-parietal	M_ACC_2	4.6103	0.27293	0.10616
	cingulo-opercular	R_aPFC_2	sensorimotor	R_pre_SMA	4.5785	0.16879	0.00282
	cingulo-opercular	L_mid_insula_3	sensorimotor	R_pre_SMA	4.5591	0.09643	-0.03078

*	sensorimotor	L_temporal_3	sensorimotor	R_parietal_1	4.5587	0.15899	-0.0075
	cingulo-opercular	R_mid_insula_2	sensorimotor	M_SMA	4.5469	0.14311	-0.01256
	default	L_post_cingulate_1	default	R_precuneus_4	4.5457	0.26562	0.0622
	cingulo-opercular	L_ant_insula	cingulo-opercular	M_ACC_1	4.5381	0.28149	0.10303
	default	R_precuneus_2	default	R_precuneus_4	4.5077	0.30916	0.1291
	cingulo-opercular	M_mFC	sensorimotor	R_frontal_1	4.5062	0.24623	0.0819
	sensorimotor	L_post_parietal_1	sensorimotor	L_temporal_2	4.4753	0.14963	-0.02755
	cingulo-opercular	L_vFC_3	sensorimotor	L_parietal_5	4.4663	0.10568	-0.05657
	cingulo-opercular	R_temporal_2	sensorimotor	R_precentral_gyrus_3	4.4644	0.15667	0.00187
	fronto-parietal	L_dFC	fronto-parietal	R_vlPFC	4.4437	0.10913	-0.06178
	cingulo-opercular	R_ant_insula	fronto-parietal	R_dlPFC_1	4.4428	0.4023	0.1982
	cingulo-opercular	R_temporal_3	sensorimotor	R_precentral_gyrus_3	4.4342	0.0595	-0.08722
	sensorimotor	R_pre_SMA	sensorimotor	R_precentral_gyrus_1	4.4261	0.14524	0.01156
	fronto-parietal	R_IPL_1	sensorimotor	R_frontal_1	4.4176	0.31142	0.10737
	cingulo-opercular	L_ant_insula	fronto-parietal	R_dlPFC_1	4.4089	0.32468	0.13562
	cingulo-opercular	R_basal_ganglia_1	fronto-parietal	R_dFC_2	4.408	0.10857	-0.04004
	cingulo-opercular	L_vFC_3	cingulo-opercular	M_mFC	4.3863	0.25435	0.10965
	cingulo-opercular	R_vPFC	sensorimotor	R_dFC_3	4.3446	0.09467	-0.04865
	cingulo-opercular	L_post_insula	cingulo-opercular	M_mFC	4.3383	0.02779	-0.10139
	cingulo-opercular	L_ant_insula	sensorimotor	R_pre_SMA	4.3322	0.28154	0.11907
	cingulo-opercular	R_ant_insula	cingulo-opercular	R_dACC	4.323	0.35691	0.19289

Table 5.2: Information on consensus features with positive feature weights derived from connections that were more positively correlated in younger adults than in older adults. Shown are the seed-region pairs and their respective networks, the average feature weights for each seed-region pair, and the respective z-transformed correlation coefficients for both the younger and older adult groups. Features that overlap with features derived from the motion-SVR (see supplement) indicated with *.

Table 5.3

Network	Seed	X	Y	Z
default	L_precuneus_1	-3	-38	45
sensorimotor	R_parietal_1	46	-20	45
sensorimotor	R_pre_SMA	10	5	51
sensorimotor	M_SMA	0	-1	52
cingulo-opercular	R_precuneus_1	8	-40	50
cingulo-opercular	M_mFC	0	15	45
sensorimotor	R_frontal_1	58	11	14
sensorimotor	L_parietal_5	-55	-22	38
fronto-parietal	L_dFC	-42	7	36
cingulo-opercular	L_ant_insula	-36	18	2

Table 5.3: Listed are the top 10 seed-regions with their MNI coordinates and their respective networks ranked by the sum of 1/2 of all the feature weight coming from connections involving that seed-region.

Figure 5.1

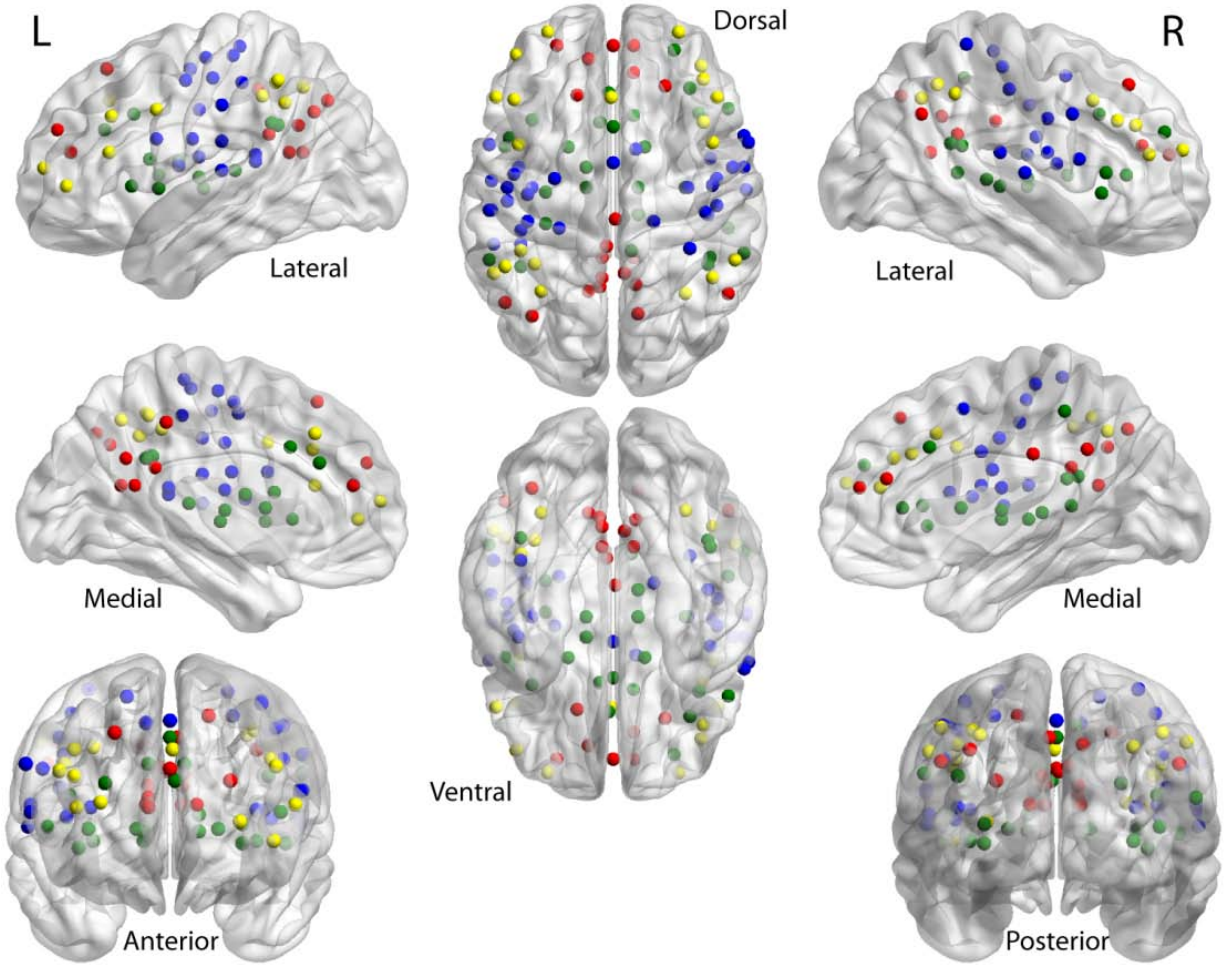
L
Lateral
Medial
Anterior
Dorsal
Ventral
R
Lateral
Medial
Posterior

Figure 5.1: Shown are the 100 seed-regions used in this study taken from Dosenbach et al. (2010). Fronto-parietal network is in yellow; sensorimotor in blue; default in red; cingulo-opercular in green.

Figure 5.2

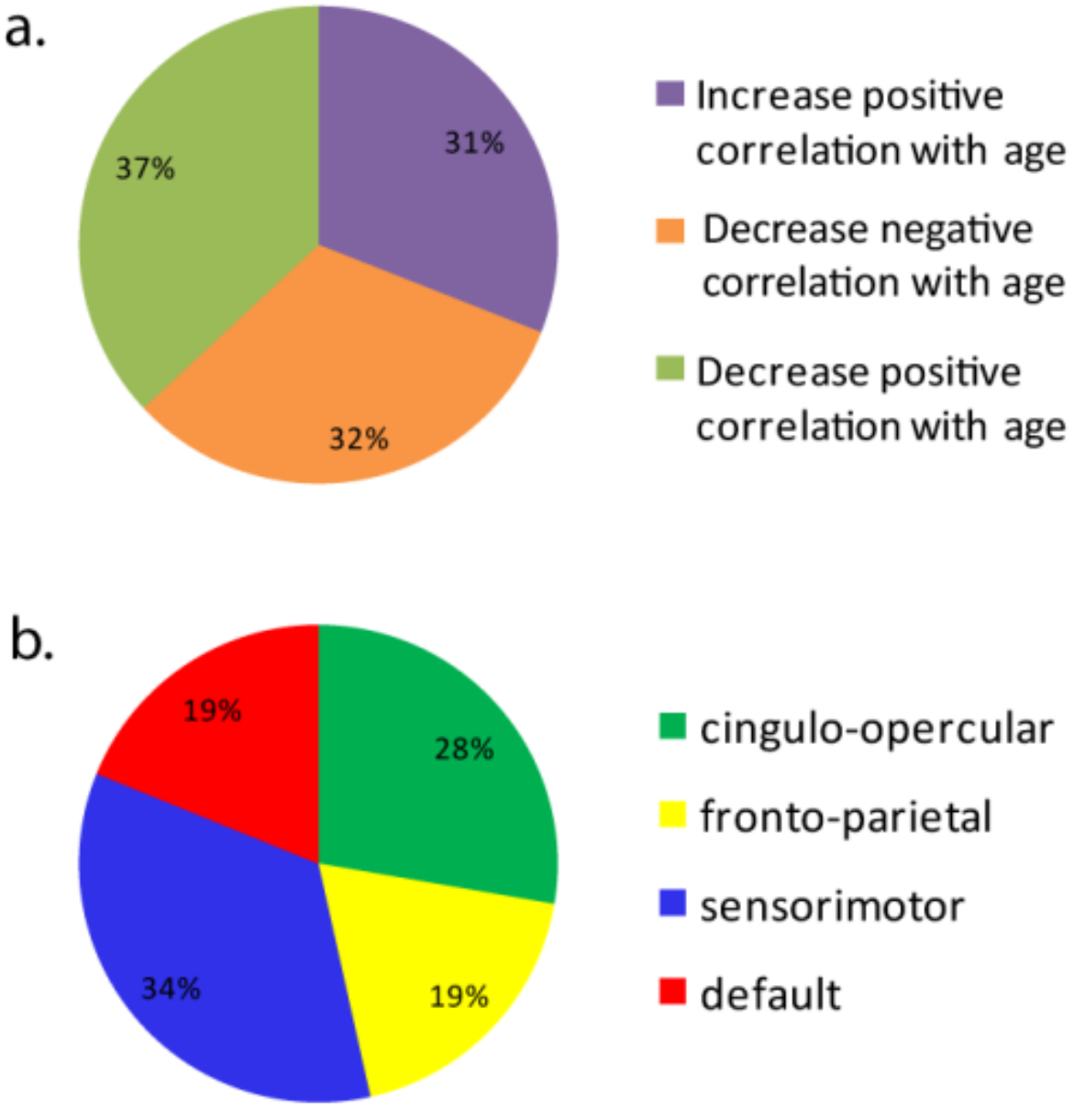
a.
31%
37%
32%
Increase positive correlation with age
Decrease negative correlation with age
Decrease positive correlation with age
b.
19%
28%
34%
19%
cingulo-opercular
fronto-parietal
sensorimotor
default

Figure 5.2: Pie charts illustrating the percentage of the total weight that came from each (*a*) scenario observed and (*b*) network studied.

Figure 5.3

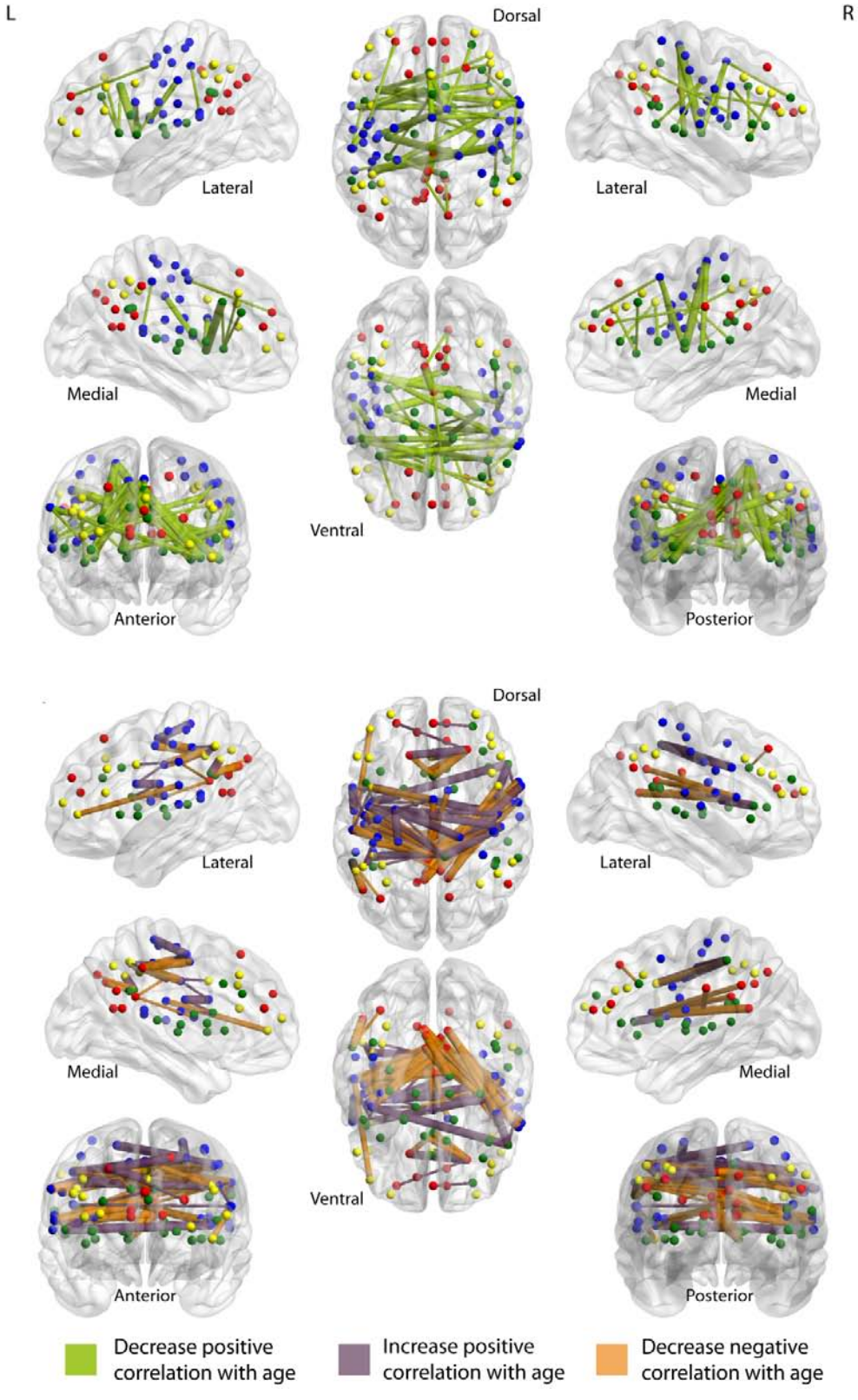
L
R
Dorsal
Lateral
Lateral
Medial
Medial
Ventral
Anterior
Posterior
Dorsal
Lateral
Lateral
Medial
Medial
Ventral
Anterior
Posterior
Decrease positive correlation with age
Increase positive correlation with age
Decrease negative correlation with age

Figure 5.3: Illustration of the consensus features that decreased positive correlation with age (top) and the consensus features that increased positive correlation with age and decreased negative correlation with age (bottom). Connections are scaled by their respective feature weight, with thicker connections representing greater feature weight.

Figure 5.4

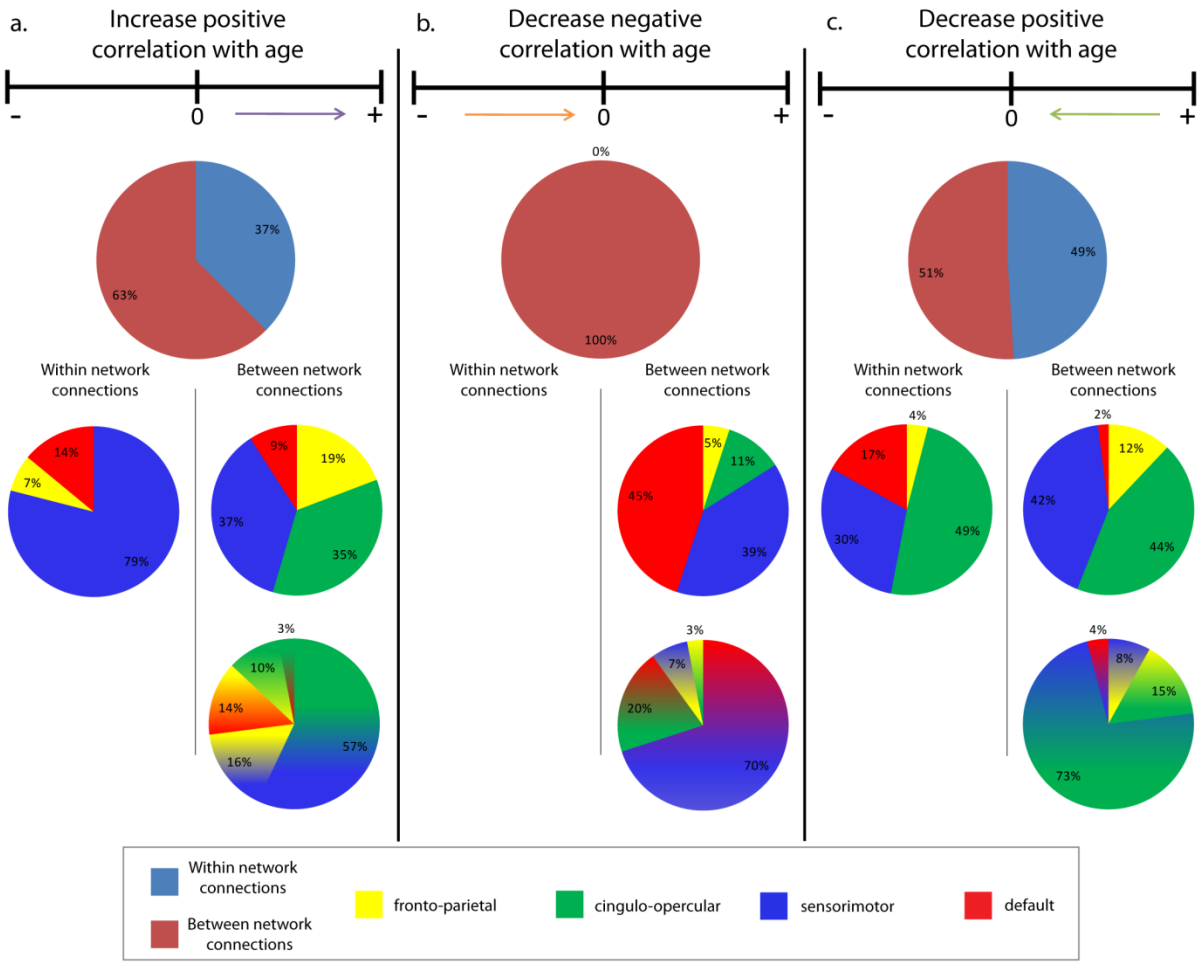
a.
Increase positive correlation with age
-
0
+
37%
63%
Within network connections
Between network connections
14%
7%
79%
9%
19%
37%
35%
3%
10%
14%
16%
57%
b.
Decrease negative correlation with age
-
0
+
0%
100%
Within network connections
Between network connections
5%
11%
45%
39%
3%
7%
20%
70%
c.
Decrease positive correlation with age
-
0
+
49%
51%
Within network connections
Between network connections
4%
17%
30%
49%
2%
12%
42%
44%
4%
8%
15%
73%
Within network connections
Between network connections
fronto-parietal
cingulo-opercular
sensorimotor
default

Figure 5.4: Pie charts illustrating the breakdown of the feature weight coming from (*a*) connections that are more positively correlated with age, (*b*) connections that are less negatively correlated with age, and (*c*) connections that are less positively correlated with age as being between network or within network, and the breakdown of these connection types based on the contributing network or networks.

Figure 5.5

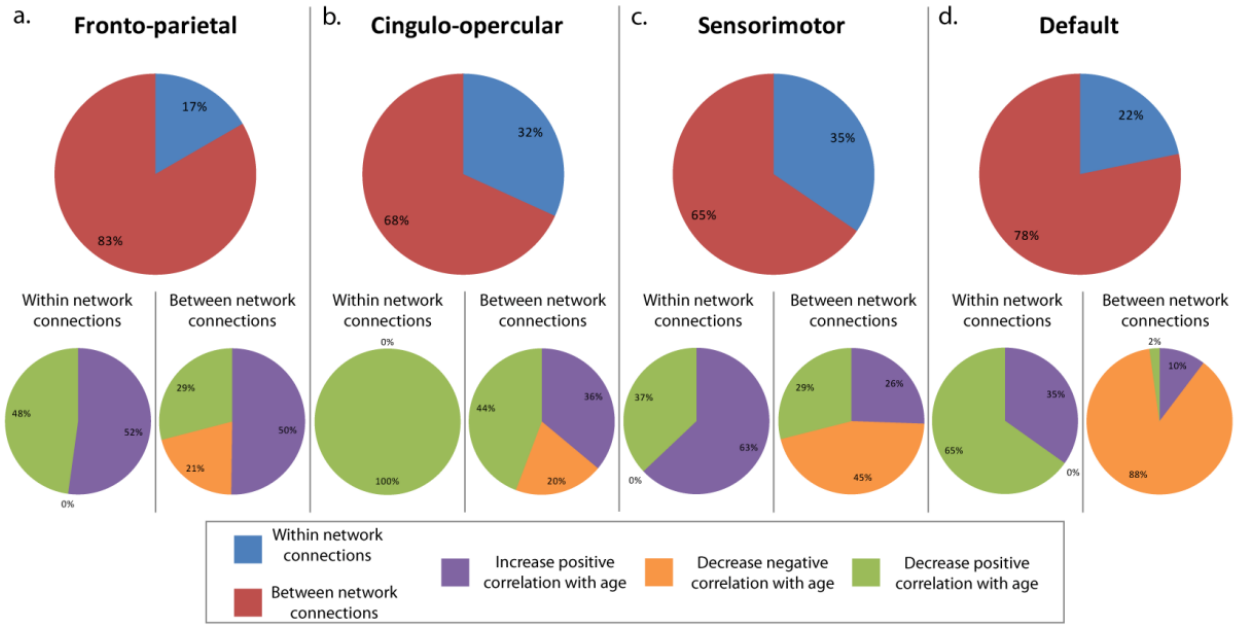
a.
Fronto-parietal
17%
83%
Within network connections
Between network connections
48%
52%
0%
29%
50%
21%
b.
Cingulo-opercular
32%
68%
Within network connections
Between network connections
0%
100%
44%
36%
20%
c.
Sensorimotor
35%
65%
Within network connections
Between network connections
37%
63%
0%
29%
26%
45%
d.
Default
22%
78%
Within network connections
Between network connections
35%
65%
0%
2%
10%
88%
Within network connections
Between network connections
Increase positive correlation with age
Decrease negative correlation with age
Decrease positive correlation with age

Figure 5.5: Pie charts illustrating the percentage of feature weight coming from between network connections and within network connections for the (a) fronto-parietal network, (b) cingulo-opercular network, (c) sensorimotor network, and (d) the default network. Shown is the percentage of the feature weight coming from within and between network connections that either increased positive correlation with age, decreased negative correlation with age, or decreased positive correlation with age is also shown for each network.

Figure 5.6

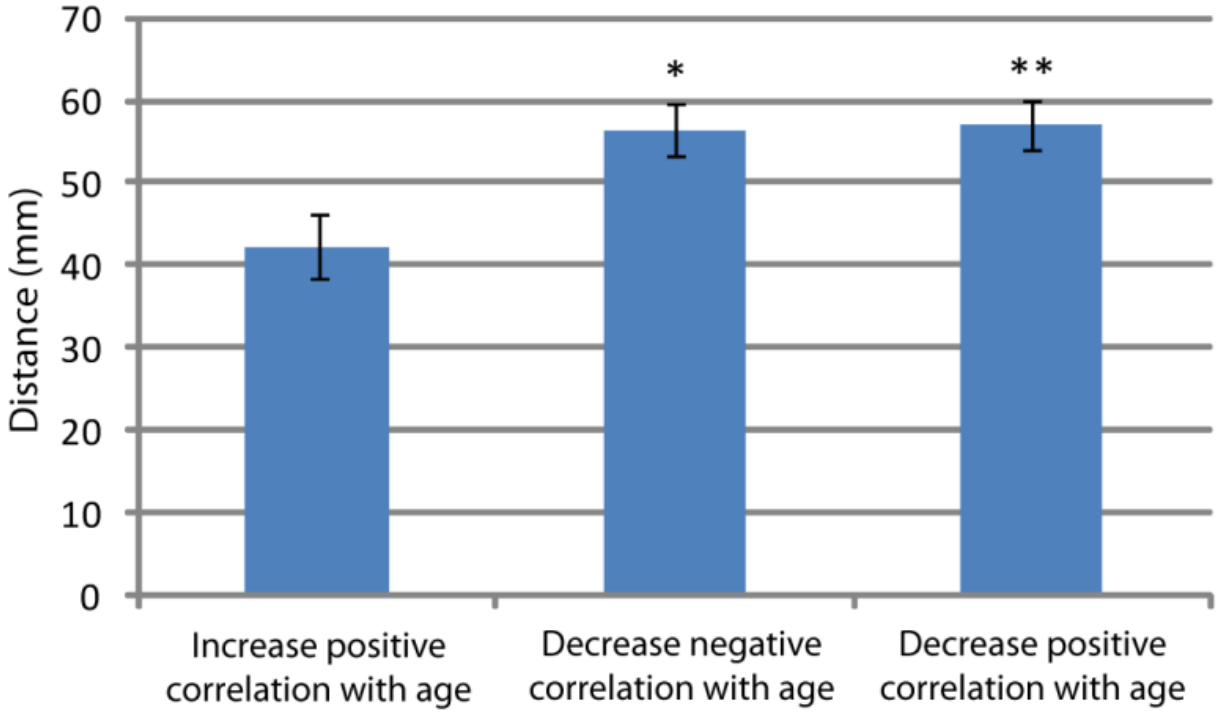
70
60
50
40
30
20
10
0
Distance (mm)
*
**
Increase positive correlation with age
Decrease negative correlation with age
Decrease positive correlation with age

Figure 5.6: Connections that were more positively correlated in older adults than younger adults were significantly shorter than both connections that were less negatively correlated in older adults ($t(76) = -2.826$, * $p < .01$)) and connections that were less positively correlated in older adults ($t(84) = -3.112$, **$p < .005$)). Based on Euclidian distance. Error bars are the standard error of the mean.

References

Andrews-Hanna, J.R., Snyder, A.Z., Vincent, J.L., Lustig, C., Head, D., Raichle, M.E., Buckner, R.L., 2007. Disruption of large-scale brain systems in advanced aging. Neuron 56, 924-935.

Biswal, B., Yetkin, F.Z., Haughton, V.M., Hyde, J.S., 1995. Functional connectivity in the motor cortex of resting human brain using echo-planar MRI. Magn Reson Med 34, 537-541.

Biswal, B.B., Mennes, M., Zuo, X.N., Gohel, S., Kelly, C., Smith, S.M., Beckmann, C.F., Adelstein, J.S., Buckner, R.L., Colcombe, S., Dogonowski, A.M., Ernst, M., Fair, D., Hampson, M., Hoptman, M.J., Hyde, J.S., Kiviniemi, V.J., Kotter, R., Li, S.J., Lin, C.P., Lowe, M.J., Mackay, C., Madden, D.J., Madsen, K.H., Margulies, D.S., Mayberg, H.S., McMahon, K., Monk, C.S., Mostofsky, S.H., Nagel, B.J., Pekar, J.J., Peltier, S.J., Petersen, S.E., Riedl, V., Rombouts, S.A., Rypma, B., Schlaggar, B.L., Schmidt, S., Seidler, R.D., Siegle, G.J., Sorg, C., Teng, G.J., Veijola, J., Villringer, A., Walter, M., Wang, L., Weng, X.C., Whitfield-Gabrieli, S., Williamson, P., Windischberger, C., Zang, Y.F., Zhang, H.Y., Castellanos, F.X., Milham, M.P., 2010. Toward discovery science of human brain function. Proc Natl Acad Sci U S A 107, 4734-4739.

Calautti, C., Serrati, C., Baron, J.C., 2001. Effects of age on brain activation during auditory-cued thumb-to-index opposition: A positron emission tomography study. Stroke; a journal of cerebral circulation 32, 139-146.

Cavanna, A.E., Trimble, M.R., 2006. The precuneus: a review of its functional anatomy and behavioural correlates. Brain : a journal of neurology 129, 564-583.

Chen, N.K., Chou, Y.H., Song, A.W., Madden, D.J., 2009. Measurement of spontaneous signal fluctuations in fMRI: adult age differences in intrinsic functional connectivity. Brain structure & function 213, 571-585.

Cox, R.W., 1996. AFNI: Software for analysis and visualization of functional magnetic resonance neuroimages. Computers and Biomedical Research 29, 162-173.

Craddock, R.C., Holtzheimer, P.E., 3rd, Hu, X.P., Mayberg, H.S., 2009. Disease state prediction from resting state functional connectivity. Magn Reson Med 62, 1619-1628.

Damoiseaux, J.S., Beckmann, C.F., Arigita, E.J., Barkhof, F., Scheltens, P., Stam, C.J., Smith, S.M., Rombouts, S.A., 2008. Reduced resting-state brain activity in the "default network" in normal aging. Cereb Cortex 18, 1856-1864.

Dosenbach, N.U., Fair, D.A., Miezin, F.M., Cohen, A.L., Wenger, K.K., Dosenbach, R.A., Fox, M.D., Snyder, A.Z., Vincent, J.L., Raichle, M.E., Schlaggar, B.L., Petersen, S.E., 2007. Distinct brain networks for adaptive and stable task control in humans. Proc Natl Acad Sci U S A 104, 11073-11078.

Dosenbach, N.U., Nardos, B., Cohen, A.L., Fair, D.A., Power, J.D., Church, J.A., Nelson, S.M., Wig, G.S., Vogel, A.C., Lessov-Schlaggar, C.N., Barnes, K.A., Dubis, J.W., Feczko, E., Coalson, R.S., Pruett, J.R., Jr., Barch, D.M., Petersen, S.E., Schlaggar, B.L., 2010. Prediction of individual brain maturity using fMRI. Science (New York, N.Y.) 329, 1358-1361.

Dosenbach, N.U., Visscher, K.M., Palmer, E.D., Miezin, F.M., Wenger, K.K., Kang, H.C., Burgund, E.D., Grimes, A.L., Schlaggar, B.L., Petersen, S.E., 2006. A core system for the implementation of task sets. Neuron 50, 799-812.

Fox, M.D., Snyder, A.Z., Vincent, J.L., Corbetta, M., Van Essen, D.C., Raichle, M.E., 2005. The human brain is intrinsically organized into dynamic, anticorrelated functional networks. Proc Natl Acad Sci U S A 102, 9673-9678.

Fransson, P., 2005. Spontaneous low-frequency BOLD signal fluctuations: an fMRI investigation of the resting-state default mode of brain function hypothesis. Hum Brain Mapp 26, 15-29.

Grady, C.L., Protzner, A.B., Kovacevic, N., Strother, S.C., Afshin-Pour, B., Wojtowicz, M., Anderson, J.A., Churchill, N., McIntosh, A.R., 2010. A multivariate analysis of age-related differences in default mode and task-positive networks across multiple cognitive domains. Cereb Cortex 20, 1432-1447.

Grady, C.L., Springer, M.V., Hongwanishkul, D., McIntosh, A.R., Winocur, G., 2006. Age-related changes in brain activity across the adult lifespan. Journal of cognitive neuroscience 18, 227-241.

Hagmann, P., Cammoun, L., Gigandet, X., Meuli, R., Honey, C.J., Wedeen, V.J., Sporns, O., 2008. Mapping the structural core of human cerebral cortex. PLoS biology 6, e159.

Hedden, T., Gabrieli, J.D., 2004. Insights into the ageing mind: a view from cognitive neuroscience. Nat Rev Neurosci 5, 87-96.

Heuninckx, S., Wenderoth, N., Debaere, F., Peeters, R., Swinnen, S.P., 2005. Neural basis of aging: the penetration of cognition into action control. J Neurosci 25, 6787-6796.

Heuninckx, S., Wenderoth, N., Swinnen, S.P., 2008. Systems neuroplasticity in the aging brain: recruiting additional neural resources for successful motor performance in elderly persons. J Neurosci 28, 91-99.

Hutchinson, S., Kobayashi, M., Horkan, C.M., Pascual-Leone, A., Alexander, M.P., Schlaug, G., 2002. Age-related differences in movement representation. Neuroimage 17, 1720-1728.

Jones, T.B., Bandettini, P.A., Kenworthy, L., Case, L.K., Milleville, S.C., Martin, A., Birn, R.M., 2010. Sources of group differences in functional connectivity: an investigation applied to autism spectrum disorder. Neuroimage 49, 401-414.

Li, K.Z., Lindenberger, U., 2002. Relations between aging sensory/sensorimotor and cognitive functions. Neurosci Biobehav Rev 26, 777-783.

Lustig, C., Snyder, A.Z., Bhakta, M., O'Brien, K.C., McAvoy, M., Raichle, M.E., Morris, J.C., Buckner, R.L., 2003. Functional deactivations: change with age and dementia of the Alzheimer type. Proceedings of the National Academy of Sciences of the United States of America 100, 14504-14509.

Marchand, W.R., Lee, J.N., Suchy, Y., Garn, C., Johnson, S., Wood, N., Chelune, G., 2011. Age-related changes of the functional architecture of the cortico-basal ganglia circuitry during motor task execution. Neuroimage 55, 194-203.

Mattay, V.S., Fera, F., Tessitore, A., Hariri, A.R., Das, S., Callicott, J.H., Weinberger, D.R., 2002. Neurophysiological correlates of age-related changes in human motor function. Neurology 58, 630-635.

Meunier, D., Achard, S., Morcom, A., Bullmore, E., 2009. Age-related changes in modular organization of human brain functional networks. Neuroimage 44, 715-723.

Naccarato, M., Calautti, C., Jones, P.S., Day, D.J., Carpenter, T.A., Baron, J.C., 2006. Does healthy aging affect the hemispheric activation balance during paced index-to-thumb opposition task? An fMRI study. Neuroimage 32, 1250-1256.

Park, D.C., Polk, T.A., Hebrank, A.C., Jenkins, L.J., 2010. Age differences in default mode activity on easy and difficult spatial judgment tasks. Frontiers in human neuroscience 3, 75.

Pereira, F., Mitchell, T., Botvinick, M., 2009. Machine learning classifiers and fMRI: a tutorial overview. Neuroimage 45, S199-209.

Persson, J., Lustig, C., Nelson, J.K., Reuter-Lorenz, P.A., 2007. Age differences in deactivation: a link to cognitive control? Journal of cognitive neuroscience 19, 1021-1032.

Riecker, A., Groschel, K., Ackermann, H., Steinbrink, C., Witte, O., Kastrup, A., 2006. Functional significance of age-related differences in motor activation patterns. Neuroimage 32, 1345-1354.

Sambataro, F., Murty, V.P., Callicott, J.H., Tan, H.Y., Das, S., Weinberger, D.R., Mattay, V.S., 2010. Age-related alterations in default mode network: impact on working memory performance. Neurobiol Aging 31, 839-852.

Scholkopf, B., Mika, S., Burges, C.C., Knirsch, P., Muller, K.R., Ratsch, G., Smola, A.J., 1999. Input space versus feature space in kernel-based methods. IEEE Trans Neural Netw 10, 1000-1017.

Seidler, R.D., Bernard, J.A., Burutolu, T.B., Fling, B.W., Gordon, M.T., Gwin, J.T., Kwak, Y., Lipps, D.B., 2010. Motor control and aging: links to age-related brain structural, functional, and biochemical effects. Neurosci Biobehav Rev 34, 721-733.

Shen, H., Wang, L., Liu, Y., Hu, D., 2010. Discriminative analysis of resting-state functional connectivity patterns of schizophrenia using low dimensional embedding of fMRI. Neuroimage 49, 3110-3121.

Smith, S.M., Fox, P.T., Miller, K.L., Glahn, D.C., Fox, P.M., Mackay, C.E., Filippini, N., Watkins, K.E., Toro, R., Laird, A.R., Beckmann, C.F., 2009. Correspondence of the brain's functional architecture during activation and rest. Proc Natl Acad Sci U S A 106, 13040-13045.

Smith, S.M., Jenkinson, M., Woolrich, M.W., Beckmann, C.F., Behrens, T.E.J., Johansen-Berg, H., Bannister, P.R., DeLuca, M., Drobnjak, I., Flitney, D.E., Niazy, R., Saunders, J., Vickers, J., Zhang, Y., De Stefano, N., Brady, J.M., Matthews, P.M., 2004. Advances in functional and structural MR image analysis and implementation as FSL. Neuroimage 23, 208-219.

Supekar, K., Musen, M., Menon, V., 2009. Development of large-scale functional brain networks in children. PLoS Biol 7, e1000157.

Van Dijk, K.R., Sabuncu, M.R., Buckner, R.L., 2011. The influence of head motion on intrinsic functional connectivity MRI. Neuroimage.

Wang, L., Li, Y., Metzak, P., He, Y., Woodward, T.S., 2010. Age-related changes in topological patterns of large-scale brain functional networks during memory encoding and recognition. Neuroimage 50, 862-872.

Ward, N.S., Frackowiak, R.S., 2003. Age-related changes in the neural correlates of motor performance. Brain : a journal of neurology 126, 873-888.

Weston, J., Elisseeff, A., Baklr, G., Sinz, F., 2005. The Spider Machine Learning Toolbox.

Woolrich, M.W., Jbabdi, S., Patenaude, B., Chappell, M., Makni, S., Behrens, T., Beckmann, C., Jenkinson, M., Smith, S.M., 2009. Bayesian analysis of neuroimaging data in FSL. Neuroimage 45, 173-186.

Wu, T., Zang, Y., Wang, L., Long, X., Hallett, M., Chen, Y., Li, K., Chan, P., 2007a. Aging influence on functional connectivity of the motor network in the resting state. Neuroscience letters 422, 164-168.

Wu, T., Zang, Y., Wang, L., Long, X., Li, K., Chan, P., 2007b. Normal aging decreases regional homogeneity of the motor areas in the resting state. Neuroscience letters 423, 189-193.

Zuo, X.N., Kelly, C., Di Martino, A., Mennes, M., Margulies, D.S., Bangaru, S., Grzadzinski, R., Evans, A.C., Zang, Y.F., Castellanos, F.X., Milham, M.P., 2010. Growing together and growing apart: regional and sex differences in the lifespan developmental trajectories of functional homotopy. J Neurosci 30, 15034-15043.

Supplementary Information: Support vector machine classification and characterization of age-related reorganization of functional brain networks

Group differences in head motion

SVM classification in sub-set of motion matched subjects

Three separate methods of controlling for motion were considered to alleviate the concern that the results from the primary support vector machine (SVM) were driven by group differences in motion. One possible method would include censoring individual time frames where motion exceeded a certain threshold, as previously done by member of our group in Jones et al (2010). To assess motion, a composite score of total motion for each subject was calculated as the square root of the sum of squares of the derivatives (SSD) for each motion parameter (Jones et al., 2010). An SSD of one is roughly equivalent of 1 mm translation in any one direction, or .577 mm translation in all directions combined. However, this technique was not applicable for this data set, as older adults consistently had more motion in each frame, without large spikes in motion. Lowering the censor threshold resulted in the removal of large amounts of data, preventing the use of this technique. Instead, older subjects with the most motion and younger subjects with the least motion were removed until the groups were matched in their average motion (SSD). This resulted in a sub-set of subjects with 16 younger adults and 16 older adults. There were no group differences in motion parameters between these groups.

For this sub-set of subjects a second soft-margin SVM classification was performed using the Spider Machine Learning Toolbox (Weston et al., 2005) implemented in Matlab (Mathworks) using the same parameters as the primary SVM

presented in the manuscript (C = 0.5; rbf kernel). Leave-one-out cross-validation (LOOCV) was used for tuning the SVM hyper-parameters and estimating the classifier's accuracy. As was done in the original analysis, for each round of LOOCV, a subject's data was removed (all three scans to avoid twinning bias) and the top 200 features (connections) were selected using two-sample t-tests (not assuming equal variance) on the training set and ranked according to their absolute t-statistics in descending order. The classifier was then trained, and feature weights were estimated on the remaining subjects' datasets (serving as the training dataset). The three scans of the subject that were left out of the training set served as the testing dataset, and were each separately classified as being either young or old. This process was repeated for every subject (32 times) and the total accuracy of the classifier was determined by the percent of scans which were correctly categorized.

The second SVM classifier on the motion matched sub-set of subjects successfully discriminated older adults from younger adults at an accuracy of 68%. Given the null hypothesis was 50% accuracy, an accuracy of 68% was highly significant ($p < 0.0005$). For the motion matched SVM, 107 features were found to be consistent for every leave one out cross-validation round. The features with the highest weights were extracted and evaluated in the same manner as was done for the primary analysis. Of the 107 consensus features from the motion matched SVM, 37 overlapped with features from the original SVM (**Suppl. Table 5.1**). However the prediction accuracy of 68%from the motion-matched SVM was also considerably lower than the 84% accuracy of the original SVM.

These results could be interpreted as evidence that group differences in head motion did contribute to the original classifiers ability to successfully discriminate older adults from younger adults based on their resting state functional connectivity. However, it is also plausible that the differences between the two analyses and their prediction accuracies was due in part to the lower power of the second SVM, as this analysis had 20 fewer subjects (with three scans each) than the main SVM. Also, the same motion parameters that were removed from the time series as nuisance regressors were used to classify and remove subjects to match the groups in terms of motion. Therefore, the second SVM analysis may be an overly conservative attempt to account for motion effects.

Head motion SVR classification of subjects by functional connectivity

In a second attempt to investigate the effect head motion had on our results we performed leave one out cross validation (LOOCV) non-linear epsilon-insensitive support vector regression (SVR; radial basis kernel; C = infinity, epsilon = 0.00001) on all 52 subjects to see if the same seed-region connectivity used in the primary analysis could accurately predict the SSD motion parameter for each subject (Drucker et al., 1997). The predicted motion parameter was plotted against the actual motion measurement, and a linear least squares-fit was applied, which accounted for 0.388 of the predicted motion parameter variance. However, more importantly, we performed the motion SVR to see if the consensus features from this analysis overlapped with consensus features from our SVM. There were 76 features (functional connections) that were consistent for every round of LOOCV SVR. These features are functional connections that best predicted the amount of head motion (SSD motion parameters)

for subjects. Twenty-seven of these 'motion' features overlapped with consensus features from our primary age classifier SVM. These are listed in **Supplementary Table 5.2** and marked by an asterisk in **Tables 5.1 and 5.2** in the main manuscript. In addition, from the second age classification using SVM on a subset of 32 subjects matched in motion, only 3 consensus features overlapped with motion consensus features from the SVR. However, for the in depth analysis presented in this study, we focus on the features derived from SVM analysis of all 52 subjects, including those features that overlapped with the motion features derived from the SVR. Although our results show that motion does indeed influence these connections, it is probable that these connections are also reflective of age-related reorganization of neural networks.

Replication of original SVM on age without consensus motion features

In a third attempt to investigate the impact of group differences in head motion on our results, we performed another SVM classification of age identical to the primary SVM reported in the main article (C = 0.5) except without the 76 consensus features found in the head motion classifying SVR (described above). As in the previous SVM, a radial basis function was used as the underlying kernel to map the data in higher-dimension vector space and apply a linear decision function to classify individual scans as being from either the younger or older adult group. Leave-one-out cross-validation (LOOCV) was used for tuning the SVM hyper-parameters and estimating the classifier's accuracy. For each round of LOOCV, a subject's data was removed and the top 200 features were selected. However, for this classification, the 76 consensus features found in the head motion classifying SVR (described above) were removed prior to the analysis as stated. This classifier significantly distinguished older adults from younger

adults based on their resting-state functional connectivity, although at a slightly lower accuracy than the original SVM (82%; $p < 0.0000001$ compared to chance of 50%). Interestingly, this SVM also resulted in 126 consensus features, 99 of which were identical to those found in the original SVM using all possible features. The 27 features that did not match with the original SVM were those features that appear to be sensitive to both age and motion (presented in **Supplementary Table 5.2**). The 27 additional consensus features derived from this that contributed to the successful classification of subjects into age groups are presented in **Supplementary Table 5.3**.

In depth analysis of these two motion-matched SVMs showed that three general findings were robust to the effects of head motion and the reduction of sample size. The first of these is that the majority of the feature weight contributing to the classification came from connections involving the sensorimotor and cingulo-opercular networks, highlighting the age-related reorganization that occurs in these networks. Secondly, there was a large contribution of feature weight from connections between the default network and the sensorimotor network, and connections between the default network and the cingulo-opercular network. Finally, in all analyses, within network connections in the default and cingulo-opercular networks were less positively correlated in older adults than younger adults, and these connections made large contributions to the total feature weight observed in each. Our observation that connections that were more positively correlated in older adults than younger adults were significantly shorter than both connections that were less negatively correlated in older adults and connections that were less positively correlated in older adults was not observed in our more

conservative analyses, and it is uncertain whether this finding is due to group differences in motion or the reduced power of these supplementary analyses.

The effect of motion on functional connectivity presents a critical challenge to investigators. Future research on the effects of motion on measures of functional connectivity will lead to improved methods of controlling for such effects.

Supplementary Table 5.1:

Features common to both age SVM analyses

network 1	seed 1	network 2	seed 2
fronto-parietal	L_IPL_3	cingulo-opercular	L_parietal_8
Default	L_post_cingulate_2	cingulo-opercular	R_basal_ganglia_2
Default	L_post_cingulate_1	cingulo-opercular	R_basal_ganglia_2
Sensorimotor	R_dFC_3	cingulo-opercular	L_ant_insula
cingulo-opercular	M_mFC	cingulo-opercular	L_ant_insula
Sensorimotor	L_parietal_2	Sensorimotor	L_vFC_2
Sensorimotor	L_precentral_gyrus_2	Sensorimotor	L_vFC_2
Default	L_angular_gyrus_2	cingulo-opercular	L_parietal_8
Sensorimotor	L_parietal_5	Sensorimotor	L_mid_insula_1
Sensorimotor	R_parietal_3	cingulo-opercular	R_mid_insula_2
Sensorimotor	M_SMA	Sensorimotor	R_vFC_2
Default	L_IPS_2	cingulo-opercular	L_parietal_8
cingulo-opercular	L_basal_ganglia_1	cingulo-opercular	L_ant_insula
Sensorimotor	R_precentral_gyrus_2	Sensorimotor	L_vFC_2
cingulo-opercular	R_basal_ganglia_1	fronto-parietal	R_dFC_2
Sensorimotor	R_parietal_3	cingulo-opercular	L_mid_insula_3
Sensorimotor	M_SMA	cingulo-opercular	M_ACC_1
cingulo-opercular	R_precuneus_1	cingulo-opercular	L_post_insula
Default	R_precuneus_2	Sensorimotor	L_mid_insula_1
cingulo-opercular	R_basal_ganglia_1	cingulo-opercular	M_mFC
cingulo-opercular	R_precuneus_1	fronto-parietal	R_dFC_2
cingulo-opercular	L_vFC_3	cingulo-opercular	L_basal_ganglia_1
fronto-parietal	L_IPL_1	Default	L_precuneus_1
cingulo-opercular	R_basal_ganglia_1	Sensorimotor	L_vFC_2
Sensorimotor	L_mid_insula_1	cingulo-opercular	R_vFC_1
Sensorimotor	M_SMA	fronto-parietal	L_dFC
Sensorimotor	R_dFC_3	cingulo-opercular	R_vPFC
cingulo-opercular	L_thalamus_1	cingulo-opercular	M_mFC
Default	R_post_cingulate	Sensorimotor	R_vFC_2
Sensorimotor	L_mid_insula_1	cingulo-opercular	L_thalamus_1
cingulo-opercular	L_basal_ganglia_2	Sensorimotor	L_vFC_2
fronto-parietal	L_IPL_2	fronto-parietal	L_IPL_1
cingulo-opercular	R_ant_insula	fronto-parietal	R_dlPFC_1
Default	R_post_cingulate	Sensorimotor	R_frontal_1
Sensorimotor	L_temporal_2	Sensorimotor	L_post_parietal_1
Sensorimotor	R_precentral_gyrus_1	Sensorimotor	R_pre_SMA
Sensorimotor	L_temporal_2	Sensorimotor	R_parietal_1

Supplementary Table 5.1: Displayed are the features (functional connections) that overlapped between the primary SVM and secondary, motion matched SVM. Each seed-region, and its network affiliation, is listed for each feature.

Supplementary Table 5.2

Features sensitive to motion and aging

network 1	seed 1	network 2	seed 2
cingulo-opercular	R_aPFC_2	Default	M_mPFC
cingulo-opercular	M_mFC	Default	R_sup_frontal
Default	L_post_cingulate_1	Sensorimotor	R_frontal_1
Default	R_precuneus_2	Sensorimotor	R_frontal_1
Default	R_precuneus_3	Sensorimotor	R_frontal_1
Default	L_precuneus_2	Sensorimotor	R_frontal_1
Default	L_post_cingulate_3	Sensorimotor	R_frontal_1
Sensorimotor	L_precentral_gyrus_2	cingulo-opercular	L_vFC_1
Default	L_precuneus_1	Sensorimotor	R_dFC_3
cingulo-opercular	R_precuneus_1	Sensorimotor	R_dFC_3
Default	L_precuneus_1	Sensorimotor	R_frontal_2
Default	R_precuneus_2	Sensorimotor	R_precentral_gyrus_1
Sensorimotor	R_parietal_3	Sensorimotor	L_precentral_gyrus_1
Sensorimotor	R_parietal_1	Sensorimotor	L_parietal_1
Sensorimotor	R_parietal_3	Sensorimotor	L_parietal_1
Default	L_precuneus_1	Sensorimotor	R_precentral_gyrus_3
Default	L_precuneus_1	Sensorimotor	L_parietal_2
Default	L_precuneus_1	Sensorimotor	L_parietal_4
Sensorimotor	L_temporal_2	Sensorimotor	R_parietal_1
Sensorimotor	L_temporal_3	Sensorimotor	R_parietal_1
Default	L_precuneus_1	Sensorimotor	R_parietal_1
cingulo-opercular	R_precuneus_1	Sensorimotor	R_parietal_1
Default	L_precuneus_1	Sensorimotor	L_post_parietal_1
fronto-parietal	L_IPL_2	Sensorimotor	L_post_parietal_1
fronto-parietal	L_IPL_1	Default	L_precuneus_1
fronto-parietal	L_post_parietal_2	Default	L_precuneus_1
fronto-parietal	L_IPL_2	fronto-parietal	L_IPL_1

Supplementary Table 5.2: Displayed are the features (functional connections) that overlapped between the primary SVM separating subjects by age group and the SVR classifying subjects based on their head motion. These features can be interpreted as being sensitive to the effects of age and the effects of head motion. Each seed-region, and its network affiliation, is listed for each feature.

Supplementary Table 5.3

Features from SVM using all features minus the motion features				zCC	
Network 1	Seed 1	Network 2	Seed 2	Young	Old
sensorimotor	M_SMA	cingulo-opercular	R_aPFC_2	0.07947	-0.0834
Default	L_precuneus_1	default	L_vmPFC	0.14583	-0.0275
Default	L_precuneus_1	default	R_ACC	0.1571	-0.0166
sensorimotor	R_frontal_1	fronto-parietal	R_dlPFC_1	0.36332	0.16057
cingulo-opercular	M_mFC	cingulo-opercular	M_ACC_1	0.40957	0.23205
fronto-parietal	L_dFC	fronto-parietal	L_vPFC	0.44302	0.27547
cingulo-opercular	L_vFC_3	cingulo-opercular	R_dACC	0.25686	0.09444
fronto-parietal	R_IPL_1	cingulo-opercular	L_ant_insula	0.26697	0.0955
Default	R_post_cingulate	cingulo-opercular	L_ant_insula	-0.2568	-0.0895
cingulo-opercular	L_basal_ganglia_1	fronto-parietal	R_dFC_1	-0.0014	0.14865
sensorimotor	R_precentral_gyrus_1	sensorimotor	R_frontal_1	0.28561	0.46252
sensorimotor	R_mid_insula_1	sensorimotor	R_frontal_1	0.16929	0.31362
sensorimotor	R_temporal_1	cingulo-opercular	L_vFC_1	0.07479	0.22956
sensorimotor	L_precentral_gyrus_3	cingulo-opercular	L_vFC_1	0.18442	0.32186
sensorimotor	R_parietal_3	fronto-parietal	L_dFC	-0.1152	0.01943
cingulo-opercular	R_precuneus_1	sensorimotor	R_pre_SMA	0.15687	0.30734
Default	L_post_cingulate_3	sensorimotor	R_vFC_2	-0.1582	-0.0031
sensorimotor	R_precentral_gyrus_1	sensorimotor	M_SMA	0.25737	0.08842
sensorimotor	R_post_insula	sensorimotor	M_SMA	0.1927	0.04536
Default	L_post_cingulate_3	sensorimotor	R_precentral_gyrus_1	-0.1077	0.04952
sensorimotor	R_parietal_1	sensorimotor	L_mid_insula_1	0.15697	-0.0055
fronto-parietal	L_IPL_1	sensorimotor	L_mid_insula_1	0.11301	-0.0466
cingulo-opercular	R_mid_insula_2	sensorimotor	L_parietal_1	0.05336	-0.0697
cingulo-opercular	R_temporal_3	sensorimotor	L_parietal_2	0.06067	-0.0786
Default	R_precuneus_4	sensorimotor	L_precentral_gyrus_3	-0.082	0.05911
cingulo-opercular	R_precuneus_1	sensorimotor	R_parietal_2	0.14257	0.32749
Default	R_precuneus_2	sensorimotor	R_post_insula	-0.0579	0.10144

Supplementary Table 5.3: Displayed are the additional 27 consensus features (functional connections) from the age-classifier using all possible features except the 76 motion-sensitive features derived from the motion-SVR. That is, these features essentially replaced the 27 motion features that overlapped with overlapped with our original 126 consensus features from the article. Each seed-region, its network affiliation, and the z-transformed correlation coefficient for both the young and old groups are listed for each feature.

References

Drucker, H., Kaufman, B.L., Smola, A., Vapnik, V., 1997. Support Vector Regression Machines. In: Mozer, M.C., Jordan, J.I., Petsche, T. (Eds.), Advances in Neural Information Processing Systems. MIT Press, Cambridge, Massachusetts, pp. 155-161.

Jones, T.B., Bandettini, P.A., Kenworthy, L., Case, L.K., Milleville, S.C., Martin, A., Birn, R.M., 2010. Sources of group differences in functional connectivity: an investigation applied to autism spectrum disorder. Neuroimage 49, 401-414.

Weston, J., Elisseeff, A., Baklr, G., Sinz, F., 2005. The Spider Machine Learning Toolbox.

Chapter 6

Validating age-related functional imaging changes in verbal working memory with acute stroke

Timothy B. Meier, Lin Naing, Lisa E. Thomas, Veena A. Nair, Argye E. Hillis, Vivek Prabhakaran

Published in:

Behavioral Neurology 24(3): 187-199 (2011).

Abstract

Functional imaging studies consistently find that older adults recruit bilateral brain regions in cognitive tasks that are strongly lateralized in younger adults, a characterization known as the Hemispheric Asymmetry Reduction in Older Adults model. While functional imaging displays what brain areas are active during tasks, it cannot demonstrate what brain regions are necessary for task performance. We used behavioral data from acute stroke patients to test the hypothesis that older adults need both hemispheres for a verbal working memory task that is predominantly left-lateralized in younger adults. Right-handed younger (age <51, n = 7) and older adults (age > 50, n = 21) with acute unilateral stroke, as well as younger (n = 6) and older (n = 13) transient ischemic attack (TIA) patients, performed a self-paced verbal item-recognition task. Older patients with stroke to either hemisphere had a higher frequency of deficits in the verbal working memory task compared to older TIA patients. Additionally, the deficits in older stroke patients were mainly in retrieval time while the deficits in younger stroke patients were mainly in accuracy. These data suggest that bihemispheric activity is necessary for older adults to successfully perform a verbal working memory task.

Introduction

Functional imaging is a valuable tool in measuring brain activity during cognitive processes in humans. As such, there is a vast body of literature using techniques such as fMRI to investigate working memory (D'Esposito, 2000; D'Esposito et al., 2000; Smith and Jonides, 1998; Wager and Smith, 2003). While imaging data provides information on what areas of the brain are activated during different cognitive processes, it cannot provide information on what areas of the brain are essential for the process being tested. It is important to validate results obtained from functional imaging studies, and one way to do so in humans is with lesion studies (Muller and Knight, 2006; Rorden and Karnath, 2004). Lesion effects can be studied in stroke patients. Chronic stroke patients have been studied extensively to test the necessity of the affected area for many cognitive tasks, including working memory (for review, see Muller and Knight, 2006). Deficits in cognitive performance can be measured and linked to the stroke-altered areas. While studies of chronic stroke patients can provide valuable information, one drawback is that considerable reorganization is known to occur over time (Prabhakaran et al., 2007; Takahashi et al., 2005). The use of acute stroke patients provides the unique opportunity to test the effect of the lesion on performance before substantial reorganization can occur. Diffusion-weighted imaging (DWI) and perfusion weighted imaging (PWI) can be used to determine structural damage and blood flow abnormalities, respectively, allowing for identification of areas affected by acute stroke thereby directly linking the affected area to any observed deficit in performance (Beaulieu et al., 1999; Hillis et al., 2002). In this study we used acute stroke patients to validate an aging model of cognition.

Normal aging leads to changes in brain anatomy and physiology that are reflected in changes in cognition (Dickstein et al., 2009). These changes have been documented in numerous functional imaging studies (for review, see Daselaar et al., 2006). One example of aging-related changes in the prefrontal cortex, as documented by several functional imaging studies, is a decrease in asymmetry of brain activation in older adults for cognitive tasks that are known to be predominantly unilateral in young adults (Cabeza, 2001; Cabeza et al., 1997; Grady et al., 1994; Reuter-Lorenz et al., 2000). This consistently observed phenomenon has been characterized as the Hemispheric Asymmetry Reduction in Older Adults, or HAROLD model (Cabeza, 2002). The HAROLD model has been supported by studies of several different cognitive facilities including episodic memory, working memory, perception, and inhibitory control (for review, see Cabeza, 2002). Although HAROLD was initially proposed for the prefrontal cortex, there is evidence the model applies to more posterior regions as well. For example, in temporal and parietal regions, age-dependent reductions in activation asymmetries have been observed during a visual facial-affect perception task (Gunning-Dixon et al., 2003), face memory and processing tasks (Grady et al., 2002; Grady et al., 2000), in inhibitory control tasks (Milham et al., 2002; Nielson et al., 2002), in language processing tasks (Bellis et al., 2000), and in a verbal working memory task (Reuter-Lorenz et al., 2001). In addition, age-related reductions in activation asymmetries have also been observed in the occipital lobe during an attention task (Madden et al., 2004) and in the hippocampus during autobiographical memory task (Maguire and Frith, 2003). Furthermore, age-related asymmetry in fronto-parietal connections has also been demonstrated. In a study by Li et al., prefrontal cortex was shown to have strong

functional connectivity to the ipsilateral parietal area during a working memory task, as well as during rest, and that this connectivity was reduced in older participants (Li et al., 2009). Also, Charlton et al. found that most of the age-related variance in working memory is explained by the integrity of the fronto-parietal white matter tracts (Charlton et al., 2009). Together, these studies suggest that the HAROLD model likely extends to more posterior regions in addition to the PFC. Although age-related increased activation has been demonstrated across the cortex for several different tasks, there is little evidence that this increase in activation represents areas essential for task performance.

In this study, we use data collected from acute ischemic stroke patients to validate neuroimaging findings that suggest that older adults need both hemispheres to successfully complete a verbal working memory task. The characterization of activations observed in young and old subjects known as the HAROLD model predicts that older subjects need both hemispheres for tasks that are considered lateralized in young subjects (Cabeza, 2002). In young normal adults, functional imaging studies have shown that the left hemisphere is responsible for verbal working memory (Kapur et al., 1994; Owen et al., 1998; Paulesu et al., 1993; Smith et al., 1996) while the right hemisphere has been shown to be involved in verbal working memory only during high demand tasks (D'Esposito et al., 1998; Rypma et al., 1999). Studies have found that the lateralization of verbal WM extends into posterior regions of the brain as well. In verbal delayed match to sample tasks, Smith et al. observed left lateralization in PFC, supplementary motor area, premotor cortex, and parietal cortex (Smith and Brewer,

1995). In a similar verbal WM task, Salmon et al. observed left lateralized activity in the PFC and parietal cortex (Salmon et al., 1996).

Consistent with the HAROLD model, Reuter-Lorenz et al. (Reuter-Lorenz et al., 2000) found that older adults displayed bilateral PFC activity for verbal working memory while young adults showed more lateralized activity. In a subsequent study, Reuter-Lorenz observed bilateral activation in older adults in the parietal cortex during a verbal working WM task while younger adults had activation in the left parietal cortex (Reuter-Lorenz et al., 2001). The bilateral activation observed in older adults suggests that both hemispheres are necessary for successful performance during verbal working memory tasks. To our knowledge, the HAROLD model has not been validated with lesion data, although it has been investigated in regards to episodic memory using transcranial magnetic imaging (Manenti et al., 2011; Rossi et al., 2004). Here we test the hypothesis that older individuals need this bilateral activation to perform successfully in a cognitive task that is known to be lateralized in normal young adults by comparing the effect of left or right hemisphere stroke on old patients. If both hemispheres are needed in old adults for successful verbal working memory task performance, stroke localized to either side should negatively affect task performance.

Methods

Participants for this study were recruited in order to investigate the lateralization of working memory processes in young and old adults. An extension of the analyses were carried out from the original published data and results which were on findings regarding the lateralization of spatial and verbal working memory regardless of age,

reported previously by Philipose and colleagues (Philipose et al., 2007). Consenting right-handed adults with acute ischemic stroke were studied within three days of symptom-onset and within 24 hours of hospitalization. Only acute stroke patients were included in order to limit post-stroke reorganization. In addition, consenting right-handed adults with transient ischemic attack (TIA; defined as resolution of symptoms within 24 hours and exclusion of stroke by MRI) were enrolled. These patients provided a unique control population for acute stroke patients, as they shared similar hospitalization stressors, age, and vascular risk factors with the stroke patients. Any differences in performance between stroke patients and TIA patients can be attributed to the actual lesion. Patients with the following conditions were excluded: (1) premorbid dementia, neurological, or psychiatric disease; (2) contraindication for MRI; (3) diminished level of consciousness; (4) lack of premorbid proficiency in English; (5) visual field deficits as determined by medical records and bedside examination; (6) motor deficits precluding performance of computer tasks; (7) language deficits that interfered with task comprehension; or (8) left neglect, defined by >10% errors on the left half of the page in line cancellation. The following MRI sequence were used on all patients as part of the Johns Hopkins Acute Stroke Protocol: diffusion weighted imaging (DWI) and perfusion weighted imaging (PWI), axial T2, fluid attenuated inversion recovery (FLAIR), gradient echo (GE), and apparent diffusion coefficient (ADC) maps. The reported analyses used DWI (after confirming the acuity of the lesion on ADC maps) and PWI (co-registered to T2 to provide anatomical boundaries that are less visible on PWI). Whole brain coverage was obtained by DWI and PWI scans of 5 mm thick slices. Volumes of tissue dysfunction on DWI and/or PWI were calculated using the Image J program. If a patient

had imaging abnormalities on both DWI and PWI, the larger calculated volume was used. Volume of PWI abnormality was measured on time to peak maps, defining hypoperfused tissue as voxels where there was >4 seconds delay in time to peak arrival of contrast, relative to the homologous region in the normal hemisphere.

Stroke was defined as acute infarct on DWI and/or hypoperfusion on PWI with corresponding neurological deficits, while TIA was defined as normal DWI/PWI and resolution of neurological deficits within 24 hours. In the current study, stroke and TIA patients were classified by age as either young or old. The old group included all patients of age > 50 years, while the young group included all individuals ≤ 50 years of age. The age cut-off of 50 years was chosen here based on the finding that white matter volume is known to start declining during the fifth decade of life (Ge et al., 2002; Giorgio et al., 2010). Older stroke patients were further separated as either left hemisphere or right hemisphere depending on the location of the stroke.

Behavioral tasks performed were described in detail elsewhere (Philipose et al., 2007). Briefly, patients performed a self-paced computerized verbal working memory task (Sternberg, 1966). Subjects were asked to remember 3, 4, 5, or 6 upper-case letters and presented with a lower-case probe letter after the 5 second delay (**Figure 1**). Responses were made with their dominant hand, unless they preferred to use the opposite hand due to right hand or arm weakness. Responses that were two standard deviations from the mean of a participant's total trials were excluded from the analysis. This removed trials that were interrupted by other factors related to the bed-side testing.

To contrast performance in the WM tasks, preplanned comparisons of deficits in encoding time, response time, and accuracy (percent correct) were carried out between groups across all loads (that is, the 3, 4, 5, and 6 letter conditions combined). Given the known effect of WM load on performance (Rypma et al., 1999), preplanned comparisons were also done at the low (3 letters) and high (6 letters) loads alone. A composite WM score was calculated by summing the deviations from the mean, as measured by z-scores, for encoding time, response time, and accuracy. Deficits were defined as having a score more than two standard deviations from the mean scores taken from 20 healthy normal volunteers recruited for a different study that were given the same behavioral protocol as patients. Chi-squared tests were performed as different groups (e.g. left stroke, tia) were compared with respect to presence or absence of behavioral deficits in which frequencies of deficits were compared across groups using contingency tables. Contingency tables were used due to the nonparametric nature of the data in order to reduce the effect of the large amount of between subject variability in the performance measures. Due to the low n for some comparisons, Fisher's Exact Tests (FET) were used when chi-square tests were not appropriate (i.e. when the expected values were <5).

Results

Data for this study were reported in a previous study by Philipose et al. (Philipose et al., 2007). The purpose of the previous study was to investigate lateralization of working memory processes regardless of age. From those data, 28 stroke patients and 19 TIA patients were used for the retrospective analyses reported here. Age ranged

from 38-79 years (57.17 ± 2.1; mean and SEM) for stroke patients and 21-84 years (56.89 ± 3.5) for TIA patients. Information regarding gender, lesion volume, lesion location, and education level is included in **Table 6.1**. A two-sample t-test comparing the mean lesion volume between older and younger stroke patients was not significant, nor was the test between older left stroke patients and older right stroke patients ($t(18) = -0.15$, $p = 0.84$, $t(13) = 1.24$, $p = 0.25$). Thus, infarct volume was roughly equivalent between groups. A two-sample t-test comparing education levels between groups revealed that older stroke patients had a trend of having more years of education compared to older TIA patients ($t(13) = 2.0$, $p = 0.066$). Education levels were not statistically different between young stroke patients and young TIA patients.

Age Effects

To examine effects of age on performance, stroke and TIA patients were split into young (up to 50 years old) and old (51 years and older) groups. Demographics are presented in **Table 6.1**.

Across All Loads: To determine whether there was an age-dependent effect of stroke on verbal WM collapsed across all loads, relative performance of both the young and old stroke groups was compared to age-matched TIA patients (**Figure 6.2**). While both the old stroke group and the young stroke group displayed a trend of having a higher frequency of deficits than age-matched TIA patients on the composite WM measure ($p = 0.051$and $p = 0.061$, FET, respectively), the deficits seemed to be driven by different aspects of the task. For younger stroke patients, there was a significantly higher frequency of deficits in accuracy compared to young TIA patients ($p < 0.05$,

FET). In contrast, older stroke patients displayed more deficits in response time than old TIA patients ($\chi^2 = 6.482$, *df* = 1, $p < 0.05$).

Low and High Verbal Loads: In order to investigate the specific contribution of load on these effects, performance on the WM task was also compared at the high load and low load conditions. At the low verbal load (3 letters; **Figure 6.3a**), older stroke patients had significantly more performance deficits than older TIA patients in encoding time and response time ($\chi^2 = 5.134$, *df* = 1, $p < 0.05$; $\chi^2 = 8.016$, *df* =1, $p < 0.005$, respectively). In contrast, young stroke patients did not differ in terms of performance compared to young TIA patients at the low load. As would be expected, deficits were observed for each group at the high verbal load (**Figure 6.3b**). Old stroke patients had significantly more deficits than old TIA patients in the composite score and in response time ($p < 0.05$, FET and $\chi^2 = 8.016$, df = 1, $p < 0.005$, respectively). While the deficits in older stroke patients were driven heavily by deficits in response time, younger stroke patients displayed a trend of having more deficits than young TIA patients in both accuracy and response time ($p = 0.061$ and $p = 0.08$, FET, respectively.

Age and Hemisphere Effects

In order to test the hypothesis that older subjects need both hemispheres in order to perform a WM task that younger subjects use predominantly one hemisphere for, the performance of old left and old right stroke patients was compared to the performance of old TIA patients. For this analysis all strokes were classified as either left or right hemisphere. Demographics are presented in **Table 6.1**.

Across All Loads: The performance of each group on the verbal WM task across all loads is shown in **Figure 6.4**. Old patients in the right stroke group displayed a trend of having a higher frequency deficits in the composite score compared to old TIA patients ($p = 0.074$, FET). Both old left and right stroke patients had a higher frequency of deficits in response time than old TIA patients, with the old right comparison being significant ($p < 0.05$, FET) and the old left comparison trending towards significance ($p = 0.055$).

Low and High Verbal Loads: In order to compare performance between the old stroke groups and control group performance on the verbal WM task was compared at the low and high WM loads alone. A similar pattern emerged at the low and high verbal load compared to that observed across all loads. At the low verbal load (**Figure 6.5a**) old right stroke patients displayed a trend towards having a higher frequency of deficits in the composite score than old TIA patients ($p = 0.089$, FET). In addition, old right stroke patients had significantly more deficits than old TIA patients in encoding time ($p < 0.05$, FET) and response time ($p < 0.05$, FET). Although no effects on the composite score were observed for old left stroke patients, they did display a trend towards significance for having more deficits than old TIA patients in response time ($p = 0.056$, FET).

At the high verbal load, older right stroke patients had significantly more deficits in response time than older TIA patients ($p < 0.005$, FET) and also displayed a trend towards more deficits as measured by the composite score ($p = 0.089$, FET, **Figure**

6.5b). Old left stroke patients did not display any statistical difference in the frequency of deficits in any measure compared to old TIA patients.

Discussion

In the present study, we used acute unilateral ischemic stroke patients to validate a characterization of fMRI activation patterns observed in older adults. In healthy young adults, verbal working memory is associated predominantly with the left hemisphere, with the right hemisphere only being involved at higher loads (D'Esposito et al., 1998; Owen et al., 1998; Prabhakaran et al., 2000; Rypma and D'Esposito, 1999). The HAROLD model posits that PFC activity for known lateralized cognitive tasks, such as working memory, becomes more bilateral in older adults compared to younger adults (Cabeza, 2002). Additional evidence suggests that increased bilateral activity in older adults is seen in posterior regions as well (Grady et al., 2002; Grady et al., 2000; Nielson et al., 2002). In two separate studies, Reuter-Lorenz found that PFC and parietal activity became more bilateral in older adults compared to younger adults for both spatial and verbal working memory tasks (Reuter-Lorenz et al., 2001; Reuter-Lorenz et al., 2000). To our knowledge the HAROLD model has not been tested directly with lesion data. We hypothesized that acute unilateral stroke to either hemisphere would disrupt the performance of old patients in a verbal working memory task.

Age and Hemispheric Effects

We measured performance in four different components of our working memory task: accuracy, encoding time, response time, and a composite score. In addition, we compared these measurements across all verbal loads, and at the low and high verbal

loads alone. If stroke patients displayed deficits in any one of these components we considered the stroke-affected area to be necessary for comparable performance to the TIA patients. Several results from the verbal item-recognition tasks appear to be consistent with the HAROLD model. We compared the effect of stroke to either hemisphere on task performance to test whether older adults need both hemispheres to perform a verbal working memory task. If the bilateral activation observed in functional neuroimaging studies of working memory represents the recruitment of essential brain areas for performance, then we hypothesized stroke to either hemisphere should result in performance impairment in a verbal working memory task. Our results are consistent with this hypothesis (**Figure 6.2 and 6.3**). Overall, there appears to be bihemispheric deficits on multiple measures in older stroke patients.

Our hypothesis that older stroke patients with damage to either the right or left hemisphere would have deficits in performance was also supported when considered separately (**Figure 6.4 and 6.5**). Across all verbal loads both old right and old left stroke patients had deficits in some measure of performance. This supports the HAROLD model as it suggests that older patients need both hemispheres intact in order to successfully perform the verbal WM task. Interestingly, old left stroke patients did not have deficits in the composite score, but old right patients did. Also, only the old right stroke patients had deficits at the high verbal load. This suggests that older individuals may rely on the right hemisphere more so than on the left hemisphere for verbal working memory, although both hemispheres are needed to perform successfully. Previous studies have shown right PFC recruitment at high WM loads (Prabhakaran et al., 2000; Rypma and D'Esposito, 1999). It has been posited that the bilateral activity

observed in older adults is due to the recruitment of areas used by younger adults only at high loads and that older adults need to recruit these additional areas at much lower loads than younger adults (Cappell et al., 2010; Park and Reuter-Lorenz, 2009b). Overall, these data suggest that older subjects do indeed need both hemispheres, with a high reliance on the right hemisphere, to perform a verbal working memory task

The increase in bilateral brain activity observed in older adults is thought to represent necessary involvement of additionally recruited areas, a process known as compensation. The idea that the observed bilateral activity is compensatory has been supported by the finding that older subjects that had more bilateral PFC activity performed better than older subjects that displayed less bilateral PFC activity (Cabeza et al., 2002). The hypothesis that bilateral activity represents compensation has further been refined as one of the tenets of the Scaffolding Theory of Aging and Cognition, or STAC model (Park and Reuter-Lorenz, 2009b). This model proposes that the observed bilateral activity in older adults represents “the recruitment of additional circuitry that shores up declining structures whose functioning has become noisy, inefficient, or both (p. 183).” The inability to recruit these additional areas, due to neural insults such as stroke, would impair performance in older individuals compared to older individuals that retain the ability to recruit these areas. This could explain the results present here. In addition, he data presented here support the idea that the increase in bilateral activation in older adults is compensatory. In fact, the data presented here suggests that the verbal working memory network may in fact be more localized to the right hemisphere in older adults, as suggested by the fact that older adults with stroke to the right

hemisphere in our study were consistently more impaired than older adults with left unilateral stroke.

Speed-Accuracy Tradeoff

An additional interesting finding was that young stroke patients had deficits in accuracy, while old stroke patients had deficits in response time. This pattern emerged when comparing all young stroke patients and all old stroke patients to age-matched controls, as well as in many of our unilateral stroke and age comparisons. One explanation for the different deficits observed in young and old stroke patients is the speed-accuracy trade-off (for review, see Wickelgren, 1977). Older subjects have been shown to perform slower, but more accurately than younger subjects in many different tasks (Brebion, 2003; Smith and Brewer, 1995). This phenomenon could explain the results seen in the present study even though in this study performance was compared to age-matched controls. In order for older patients to perform accurately it is possible that a further slowing of response time was needed due to the stroke. This would be consistent with the hypothesis put forth by Grady and colleagues that the over-activations observed in older adults could represent the older adults' compensatory attempt to enhance accuracy at the expense of response time (Grady et al., 1994). Similarly, if young subjects sacrifice accuracy for response time, those with stroke require additional decrements in accuracy in order to respond quickly. Age-related reduction in processing speed has been proposed to be the main cause of age-related cognitive deficits (Salthouse, 1996) and most of the age-related variance observed in working memory tasks is associated with the integrity of white matter tracts (Charlton et

al., 2009). If older healthy adults are impaired in response time compared to young adults, then stroke could further impair response time in old stroke patients. For young stroke patients, white matter tracts unaffected by age are reflected by normal response time, therefore the effect of stroke manifests itself in accuracy deficits, although younger stroke patients did have impairments in response time at the high verbal load. Rypma and D'Esposito propose that the neural efficiency hypothesis explains the slower processing speed observed in older subjects (2000). This theory posits that young subjects respond faster than old subjects because they need to recruit fewer areas to accurately complete the task. Aging degrades the integrity of the connections between areas, resulting in older subjects recruiting additional areas to complete the task which slows processing time. Older subjects that do not recruit additional areas perform even slower. Our finding that old stroke patients had more deficits in response time than old TIA patients supports the neural efficiency hypothesis. For old patients, stroke potentially prevents the recruitment of additional brain areas that are available to TIA patients. This leads to further slowing of processing time. For young stroke patients, the neural efficiency model hypothesizes that the recruitment of additional areas slows processing speed. In our study, unilateral stroke to either hemisphere could prevent such recruitment. This could explain why no response time deficits were observed in young stroke patients except at the high verbal load. This suggests that stroke preferentially impairs accuracy at lower levels of cognitive demand compared to response time.

Methodological Issues and Limitations

Lesion studies provide the means to test the necessity of brain areas that are shown to be active during specific tasks. While fMRI and other functional imaging techniques allow the correlation of brain activity to task performance, lesion studies allow us to determine what areas of the brain are essential in the performance of a task. Although there have been studies on the effects of PFC and parietal lesions on WM function in humans, no lesion studies have directly tested the hypothesis that older adults need more bilateral involvement than younger adults in tasks primarily associated with one hemisphere (Baldo and Dronkers, 2006; D'Esposito et al., 2006; Koenigs et al., 2009; Tsuchida and Fellows, 2009; Volle et al., 2008). In addition, this study is unique from many lesion studies in two important ways. First, acute stroke patients were used as opposed to chronic stroke patients. One concern with lesion studies is the reorganization of normal brain functions that occurs over time in response to brain damage (Muller and Knight, 2006). The use of acute stroke patients circumvents this problem and allows for the evaluation of the effects of the lesion before substantial reorganization can occur. However, the use of acute stroke patients presents different issues. Among these are the stressors that accompany hospitalization and the vascular risk factors associated with stroke. To control for this we enrolled transient ischemic attack patients (TIA) as our control group. The inclusion of TIA patients is the second important distinction of this study. In addition to controlling for hospitalization stressors, the use of TIA patients as controls also takes into account the vascular risk factors and medication histories that are shared between acute stroke and TIA patients. To measure relative performance, we compared performance of old and young acute stoke patients to performance of age-matched TIA patients. Any differences in performances

between these groups should be due to the lesion resulting from the stroke, as all other factors were controlled for with the TIA patients.

This study has inherent limitations. First, the use of extreme age groups might improve the ability to detect differences. However, we chose a cut-off of 50 in order to increase participation in the study based on the finding that white matter volume begins declining at this time (Giorgio et al., 2010). Secondly, by characterizing stroke patients by affected-hemisphere we have necessarily grouped heterogeneous stroke sites together. The particular aim of this study was to test the necessity of a hemisphere as a whole, and assumed that strokes to any location in a hemisphere would equally affect working memory performance. Due to limited recruitment of young stroke patients, we were unable to compare performance of patients with stroke to the left or right hemisphere alone. An additional confound is the use of patients with dominant hand weakness. Unfortunately, information regarding how many subjects chose to use their dominant hand is not available. These patients were included to increase participation in this study. Issues such as dominant hand weakness are unavoidable in acute stroke patients. The subject-paced nature of the experiment was due to these issues. It's interesting to note that older stroke patients showed reaction time deficits while younger stroke patients showed deficits in accuracy in comparison to their respective age-matched controls. Accuracy effects should not be a consequence of non-dominant hand use. Likewise, due to the subject paced design of the study, non-dominant hand use should affect both encoding time and response time, irrespective of load. Encoding deficits were only observed at the low loads whereas response time deficits were more prevalent, suggesting the lesions had different effects on the different sub-processes of

the task. Given the number of patients in our study, testing for specific stroke location's effect on reaction time is difficult due to power. Future studies should explore the effect of unilateral stroke to more restricted areas (e.g. frontal and/or parietal cortices), and in younger stroke patients in a more controlled manner.

Conclusion

This study provides evidence for strong bilateral involvement in older patients for verbal WM, a process that is left-lateralized in younger adults (Kapur et al., 1994; Paulesu et al., 1993; Smith et al., 1996). This validates the Harold model of increased bilateral activity in older adults as being essential and also helps to extend this to areas posterior to the PFC for verbal WM. The results from our verbal WM task support this model and advance the idea that the increased bilateral activity measured in older adults represents essential recruitment of bilateral areas. Although we employed a task that is known to involve fronto-parietal brain regions, we do not predict that these results are specific to this task, as the HAROLD model applies to several cognitive functions (Cabeza, 2002). We also present evidence that stroke impairs processing speed in old adults and accuracy in young adults, suggesting that stroke impairs different aspects of performance in old and young adults. In addition to the HAROLD model, these results are consistent with other models of cognitive aging, including the STAC model and the Neural Efficiency model (Park and Reuter-Lorenz, 2009b; Rypma et al., 2005; Rypma and D'Esposito, 2000). Future studies are needed to further validate and potentially consolidate these models of cognitive aging in order for us to better understand age-related reorganization of essential cognitive functions.

Table 6.1

Patient Group	Older Stroke	Younger Stroke	Old Left Stroke	Old Right Stroke	Older TIA	Younger TIA
Number	18	6	*8*	*10*	13	6
% Male	78%	50%	87.5%	70%	46%	33%
Age range	53-79	38-50	53-64	53-79	52-84	21-50
Age mean and SEM	61.9 ± 1.6	43 ± 1.67	59.8 ± 1.5	63.6 ± 2.6	64.0 ± 3.1	41.5 ± 4.3
Years of education	19.9 ± 1.1	21 ± 0	21 ± 0	18.8 ± 2.3	15.3 ± 2.1	15 ± 3
Posterior stroke(n)	9	0	5	4	--	--
Frontal stroke (n)	3	0	1	2	--	--
Frontal and posterior stroke (n)	3	3	1	2	--	--
Sub-cortical stroke(n)	3	3	1	2	--	--
Stroke Volume mm^3 (mean, SEM)	22502 ± 10724	25519 ± 10610	9365 ± 3632	33997 ± 19518	--	--

Table 6.1- Group Demographics: Listed are the ages and numbers of patients included in the analysis. Educational information was only available for eight stroke patients (four old left and four old right), two young stroke patients, seven old TIA patients, and three young stroke patients. Posterior refers to temporal, parietal, and/or occipital cortex. Information regarding stroke volume was not available for one old left stroke patient, two old right stroke patients, and one young stroke patient. The old right stroke group has a larger average lesion volume than the old left stroke group however this was neither significant nor trending towards significance. The discrepancy was due in large part to one old right stroke patient with lesion volume of 155,796.2 mm^3. The remaining old right stroke patients had a average lesion volume of 16,597.3 mm^3.

Figure 6.1

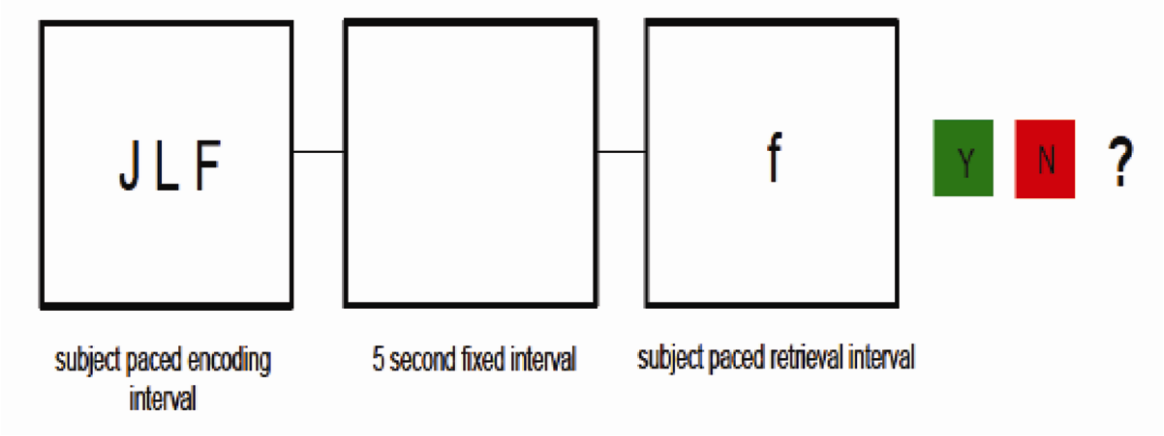
JLF
f
Y
N
?
subject paced encoding interval
5 second fixed interval
subject paced retrieval interval

Figure 6.1: Participants performed a self-paced verbal working memory tasks**.** Subjects were asked to encode a set of three (low load), four, five, or six (high load) letters upper-case letters. After a 5 second delay, subjects were asked to decide whether a single lower-case letter was included in the encoding period.

Figure 6.2

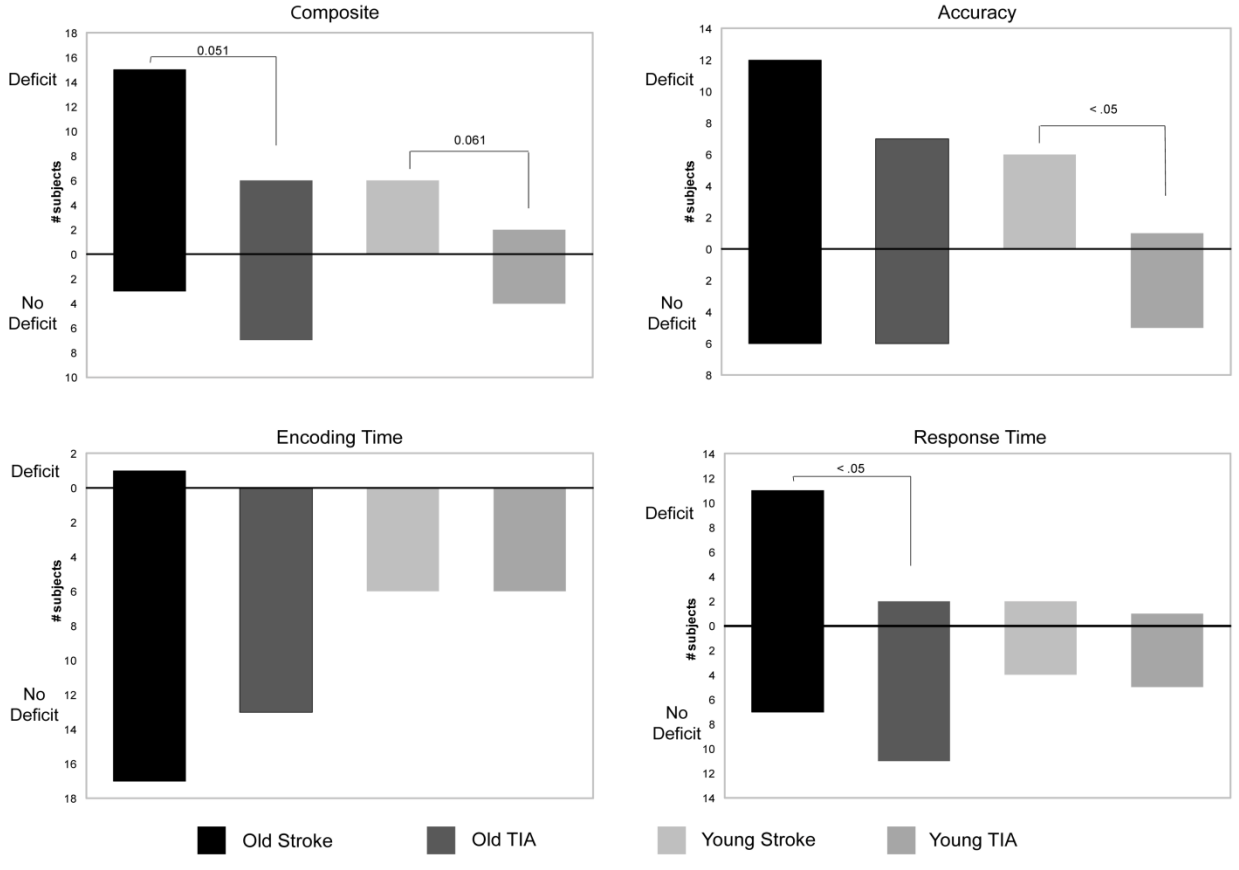
Composite
0.051
0.061
Deficit
No Deficit
#subjects
Accuracy
< .05
Deficit
No Deficit
#subjects
Encoding Time
Deficit
No Deficit
#subjects
Response Time
< .05
Deficit
No Deficit
#subjects
Old Stroke
Old TIA
Young Stroke
Young TIA

Figure 6.2: Number of old and young patients with stroke to either hemisphere with and without deficits in the composite score, accuracy, encoding time, and response time. Old and young strokes involving the left or right hemisphere displayed a trend of having more deficits in composite score than age-matched TIA patients. The overall impairment in old stroke patients was driven by deficits in response time with respect to old TIA patients. In contrast, overall impairment in young stroke patients was driven by deficits in accuracy with respect to young TIA patients.

Figure 6.3

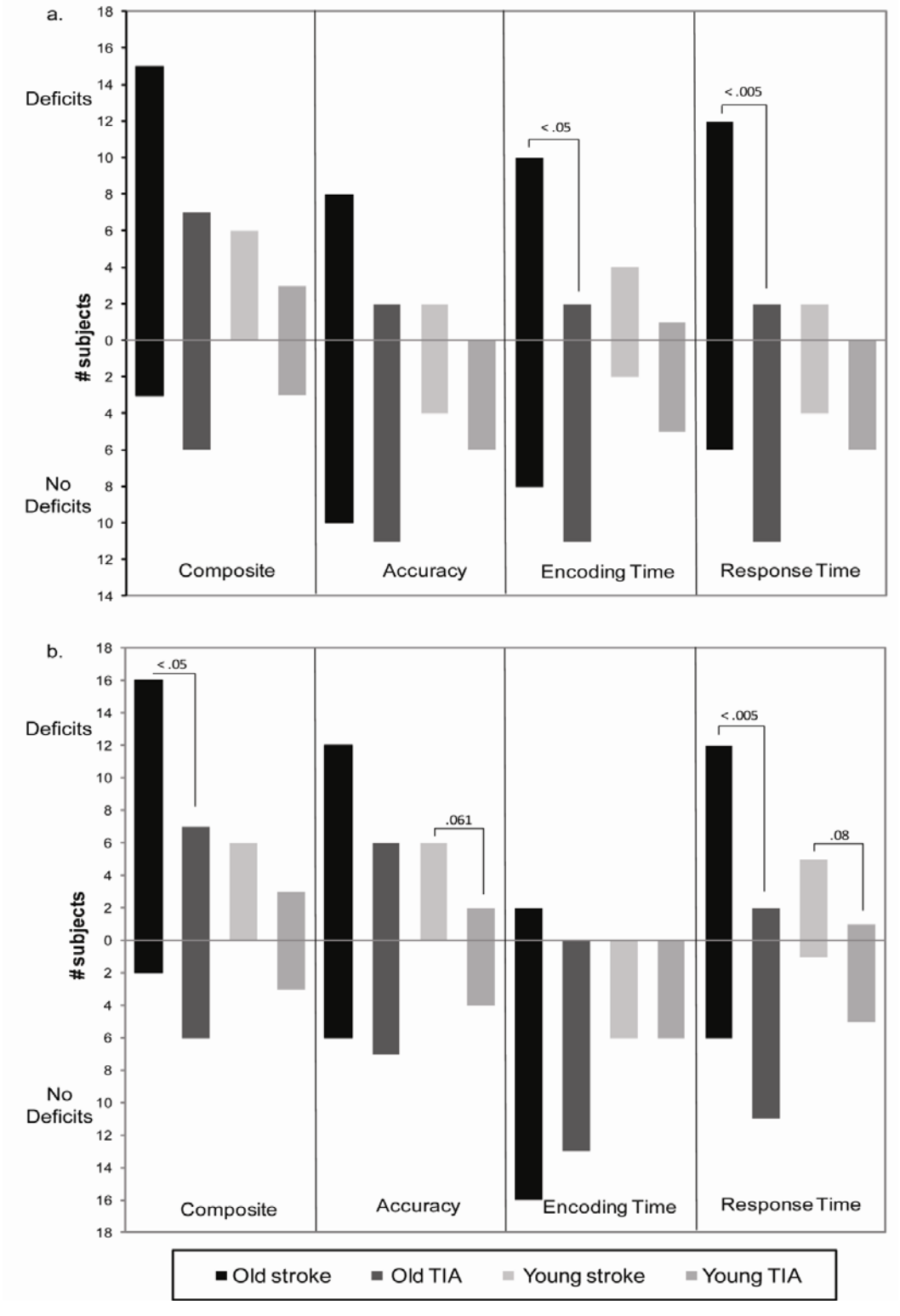
a.
Deficits
No Deficits
#subjects
< .05
< .005
Composite
Accuracy
Encoding Time
Response Time
b.
Deficits
No Deficits
#subjects
< .05
.061
< .005
.08
Composite
Accuracy
Encoding Time
Response Time
Old stroke
Old TIA
Young stroke
Young TIA

Figure 6.3: Number of old and young patients with stroke to either hemisphere with and without deficits at the low verbal load and the high verbal load. At the low load (*a*), old stroke patients were significantly more impaired in encoding time and response time than old TIA patients, while young stroke patients did not differ from young TIA patients in terms of performance. At the high load (*b*), old stroke patients were significantly more impaired in the composite score and in response time with respect to old TIA patients. Young stroke patients displayed a trend of more deficits in both accuracy and in response time than young TIA patients.

Figure 6.4

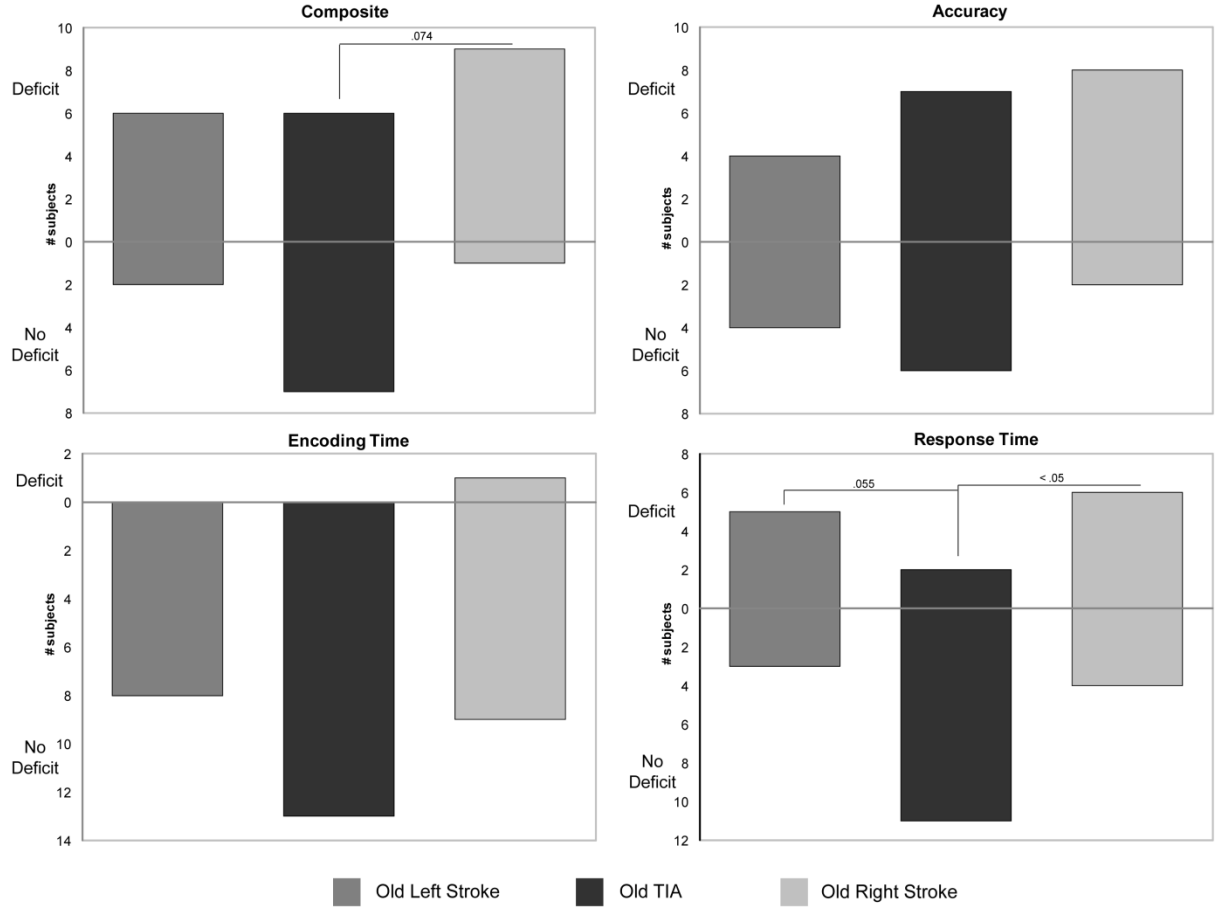
Composite
.074
Deficit
No Deficit
subjects
Accuracy
Encoding Time
Response Time
.055
< .05
Old Left Stroke
Old TIA
Old Right Stroke

Figure 6.4: Number of old patients with left and right unilateral stroke with and without deficits across all verbal loads. Old right stroke patients had a trend of more deficits in the composite score and significantly more deficits in response time than old TIA patients. Old left stroke patients had a trend of more deficits in response time than old TIA patients.

Figure 6.5

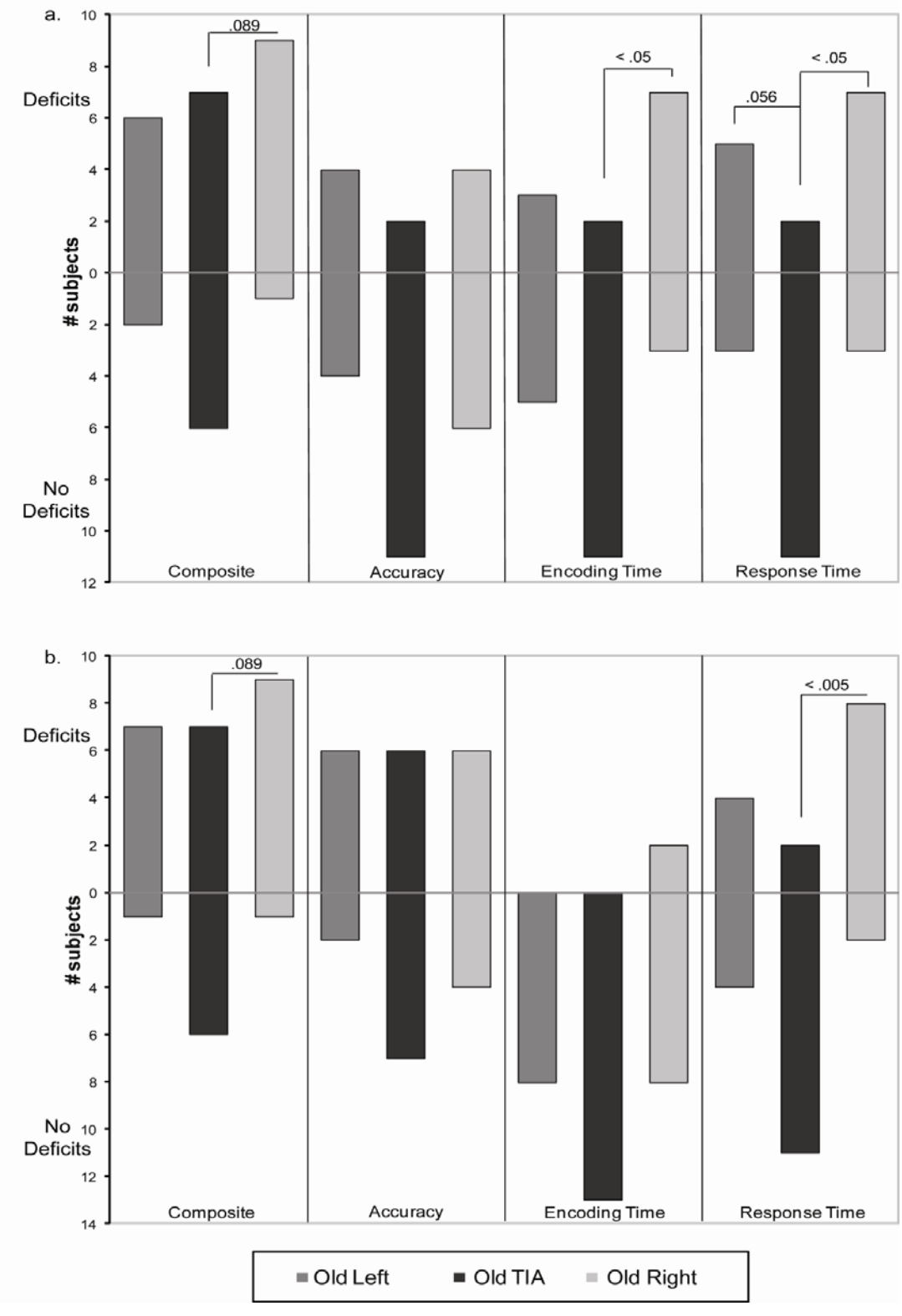
a.
.089
< .05
.056
< .05
Deficits
No Deficits
#subjects
Composite
Accuracy
Encoding Time
Response Time
b.
.089
< .005
Deficits
No Deficits
#subjects
Composite
Accuracy
Encoding Time
Response Time
Old Left
Old TIA
Old Right

Figure 6.5: Number of old patients with left and right unilateral stroke with and without deficits at the low and high verbal load. At the low load (*a*), old right stroke patients displayed a trend towards more deficits in the composite score, and had significantly more deficits in encoding time and response time than old TIA patients. Old left stroke patients had a trend towards more deficits than old TIA patients in response time. At the high load (*b*), old right stroke patients displayed a trend towards more deficits in composite score and had significantly more deficits in response time compared to old TIA patients.

References

Baldo, J.V., Dronkers, N.F., 2006. The role of inferior parietal and inferior frontal cortex in working memory. Neuropsychology 20, 529-538.

Beaulieu, C., de Crespigny, A., Tong, D.C., Moseley, M.E., Albers, G.W., Marks, M.P., 1999. Longitudinal magnetic resonance imaging study of perfusion and diffusion in stroke: evolution of lesion volume and correlation with clinical outcome. Ann Neurol 46, 568-578.

Bellis, T.J., Nicol, T., Kraus, N., 2000. Aging affects hemispheric asymmetry in the neural representation of speech sounds. J Neurosci 20, 791-797.

Brebion, G., 2003. Working memory, language comprehension, and aging: four experiments to understand the deficit. Exp Aging Res 29, 269-301.

Cabeza, R., 2001. Cognitive neuroscience of aging: contributions of functional neuroimaging. Scand J Psychol 42, 277-286.

Cabeza, R., 2002. Hemispheric asymmetry reduction in older adults: the HAROLD model. Psychol Aging 17, 85-100.

Cabeza, R., Anderson, N.D., Locantore, J.K., McIntosh, A.R., 2002. Aging gracefully: compensatory brain activity in high-performing older adults. Neuroimage 17, 1394-1402.

Cabeza, R., Grady, C.L., Nyberg, L., McIntosh, A.R., Tulving, E., Kapur, S., Jennings, J.M., Houle, S., Craik, F.I., 1997. Age-related differences in neural activity during memory encoding and retrieval: a positron emission tomography study. J Neurosci 17, 391-400.

Cappell, K.A., Gmeindl, L., Reuter-Lorenz, P.A., 2010. Age differences in prefontal recruitment during verbal working memory maintenance depend on memory load. Cortex 46, 462-473.

Charlton, R.A., Barrick, T.R., Lawes, I.N., Markus, H.S., Morris, R.G., 2009. White matter pathways associated with working memory in normal aging. Cortex.

D'Esposito, M., 2000. Functional neuroimaging of cognition. Semin Neurol 20, 487-498.

D'Esposito, M., Aguirre, G.K., Zarahn, E., Ballard, D., Shin, R.K., Lease, J., 1998. Functional MRI studies of spatial and nonspatial working memory. Brain Res Cogn Brain Res 7, 1-13.

D'Esposito, M., Cooney, J.W., Gazzaley, A., Gibbs, S.E., Postle, B.R., 2006. Is the prefrontal cortex necessary for delay task performance? Evidence from lesion and FMRI data. J Int Neuropsychol Soc 12, 248-260.

D'Esposito, M., Postle, B.R., Rypma, B., 2000. Prefrontal cortical contributions to working memory: evidence from event-related fMRI studies. Exp Brain Res 133, 3-11.

Daselaar, S.M., Browndyke, J., Cabeza, R., 2006. Functional neuroimaging of cognitive aging. In: Cabeza, R., Kingstone, A. (Eds.), Handbook of functional neuroimaging and cognition. MIT Press, Cambridge, MA.

Dickstein, D.L., Morrison, J.H., Hof, P.R., 2009. Neuropathology of Aging. In: Jagust, W., D'Esposito, M. (Eds.), Imaging the Aging Brain. Oxford University Press, New York, New York.

Ge, Y., Grossman, R.I., Babb, J.S., Rabin, M.L., Mannon, L.J., Kolson, D.L., 2002. Age-related total gray matter and white matter changes in normal adult brain. Part I: volumetric MR imaging analysis. AJNR Am J Neuroradiol 23, 1327-1333.

Giorgio, A., Santelli, L., Tomassini, V., Bosnell, R., Smith, S., De Stefano, N., Johansen-Berg, H., 2010. Age-related changes in grey and white matter structure throughout adulthood. Neuroimage 51, 943-951.

Grady, C.L., Bernstein, L.J., Beig, S., Siegenthaler, A.L., 2002. The effects of encoding task on age-related differences in the functional neuroanatomy of face memory. Psychol Aging 17, 7-23.

Grady, C.L., Maisog, J.M., Horwitz, B., Ungerleider, L.G., Mentis, M.J., Salerno, J.A., Pietrini, P., Wagner, E., Haxby, J.V., 1994. Age-related changes in cortical blood flow activation during visual processing of faces and location. J Neurosci 14, 1450-1462.

Grady, C.L., McIntosh, A.R., Horwitz, B., Rapoport, S.I., 2000. Age-related changes in the neural correlates of degraded and nondegraded face processing. Cognitive Neuropsychology 217, 165-186.

Gunning-Dixon, F.M., Gur, R.C., Perkins, A.C., Schroeder, L., Turner, T., Turetsky, B.I., Chan, R.M., Loughead, J.W., Alsop, D.C., Maldjian, J., Gur, R.E., 2003. Age-related differences in brain activation during emotional face processing. Neurobiol Aging 24, 285-295.

Hillis, A.E., Wityk, R.J., Barker, P.B., Beauchamp, N.J., Gailloud, P., Murphy, K., Cooper, O., Metter, E.J., 2002. Subcortical aphasia and neglect in acute stroke: the role of cortical hypoperfusion. Brain 125, 1094-1104.

Kapur, S., Rose, R., Liddle, P.F., Zipursky, R.B., Brown, G.M., Stuss, D., Houle, S., Tulving, E., 1994. The role of the left prefrontal cortex in verbal processing: semantic processing or willed action? Neuroreport 5, 2193-2196.

Koenigs, M., Barbey, A.K., Postle, B.R., Grafman, J., 2009. Superior parietal cortex is critical for the manipulation of information in working memory. J Neurosci 29, 14980-14986.

Li, Z., Moore, A.B., Tyner, C., Hu, X., 2009. Asymmetric connectivity reduction and its relationship to "HAROLD" in aging brain. Brain Res 1295, 149-158.

Madden, D.J., Whiting, W.L., Provenzale, J.M., Huettel, S.A., 2004. Age-related changes in neural activity during visual target detection measured by fMRI. Cereb Cortex 14, 143-155.

Maguire, E.A., Frith, C.D., 2003. Aging affects the engagement of the hippocampus during autobiographical memory retrieval. Brain 126, 1511-1523.

Manenti, R., Cotelli, M., Miniussi, C., 2011. Successful physiological aging and episodic memory: a brain stimulation study. Behavioural brain research 216, 153-158.

Milham, M.P., Erickson, K.I., Banich, M.T., Kramer, A.F., Webb, A., Wszalek, T., Cohen, N.J., 2002. Attentional control in the aging brain: insights from an fMRI study of the stroop task. Brain Cogn 49, 277-296.

Muller, N.G., Knight, R.T., 2006. The functional neuroanatomy of working memory: contributions of human brain lesion studies. Neuroscience 139, 51-58.

Nielson, K.A., Langenecker, S.A., Garavan, H., 2002. Differences in the functional neuroanatomy of inhibitory control across the adult life span. Psychol Aging 17, 56-71.

Owen, A.M., Stern, C.E., Look, R.B., Tracey, I., Rosen, B.R., Petrides, M., 1998. Functional organization of spatial and nonspatial working memory processing within the human lateral frontal cortex. Proc Natl Acad Sci U S A 95, 7721-7726.

Park, D.C., Reuter-Lorenz, P.A., 2009. The adaptive brain: aging and neurocognitive scaffolding. Annu Rev Psychol 60, 173-196.

Paulesu, E., Frith, C.D., Frackowiak, R.S., 1993. The neural correlates of the verbal component of working memory. Nature 362, 342-345.

Philipose, L.E., Alphs, H., Prabhakaran, V., Hillis, A.E., 2007. Testing conclusions from functional imaging of working memory with data from acute stroke. Behav Neurol 18, 37-43.

Prabhakaran, V., Narayanan, K., Zhao, Z., Gabrieli, J.D., 2000. Integration of diverse information in working memory within the frontal lobe. Nat Neurosci 3, 85-90.

Prabhakaran, V., Raman, S.P., Grunwald, M.R., Mahadevia, A., Hussain, N., Lu, H., Van Zijl, P.C., Hillis, A.E., 2007. Neural substrates of word generation during stroke recovery: the influence of cortical hypoperfusion. Behav Neurol 18, 45-52.

Reuter-Lorenz, P.A., Marshuetz, C., Jonides, J., Smith, S.E., Hartley, A., Koeppe, R.A., 2001. Neurocognitive ageing of storage and executive processes. European Journal of Cognitive Psychology 13, 257-278.

Reuter-Lorenz, P.A., Jonides, J., Smith, E.E., Hartley, A., Miller, A., Marshuetz, C., Koeppe, R.A., 2000. Age differences in the frontal lateralization of verbal and spatial working memory revealed by PET. J Cogn Neurosci 12, 174-187.

Rorden, C., Karnath, H.O., 2004. Using human brain lesions to infer function: a relic from a past era in the fMRI age? Nat Rev Neurosci 5, 813-819.

Rossi, S., Miniussi, C., Pasqualetti, P., Babiloni, C., Rossini, P.M., Cappa, S.F., 2004. Age-related functional changes of prefrontal cortex in long-term memory: a repetitive transcranial magnetic stimulation study. J Neurosci 24, 7939-7944.

Rypma, B., Berger, J.S., Genova, H.M., Rebbechi, D., D'Esposito, M., 2005. Dissociating age-related changes in cognitive strategy and neural efficiency using event-related fMRI. Cortex 41, 582-594.

Rypma, B., D'Esposito, M., 1999. The roles of prefrontal brain regions in components of working memory: effects of memory load and individual differences. Proc Natl Acad Sci U S A 96, 6558-6563.

Rypma, B., D'Esposito, M., 2000. Isolating the neural mechanisms of age-related changes in human working memory. Nat Neurosci 3, 509-515.

Rypma, B., Prabhakaran, V., Desmond, J.E., Glover, G.H., Gabrieli, J.D., 1999. Load-dependent roles of frontal brain regions in the maintenance of working memory. Neuroimage 9, 216-226.

Salmon, E., Van der Linden, M., Collette, F., Delfiore, G., Maquet, P., Degueldre, C., Luxen, A., Franck, G., 1996. Regional brain activity during working memory tasks. Brain 119 (Pt 5), 1617-1625.

Salthouse, T.A., 1996. The processing-speed theory of adult age differences in cognition. Psychol Rev 103, 403-428.

Smith, E.E., Jonides, J., 1998. Neuroimaging analyses of human working memory. Proc Natl Acad Sci U S A 95, 12061-12068.

Smith, E.E., Jonides, J., Koeppe, R.A., 1996. Dissociating verbal and spatial working memory using PET. Cereb Cortex 6, 11-20.

Smith, G.A., Brewer, N., 1995. Slowness and age: speed-accuracy mechanisms. Psychol Aging 10, 238-247.

Sternberg, S., 1966. High-speed scanning in human memory. Science 153, 652-654.

Takahashi, C.D., Der Yeghiaian, L., Cramer, S.C., 2005. Stroke recovery and its imaging. Neuroimaging Clin N Am 15, 681-695, xii.

Tsuchida, A., Fellows, L.K., 2009. Lesion evidence that two distinct regions within prefrontal cortex are critical for n-back performance in humans. J Cogn Neurosci 21, 2263-2275.

Volle, E., Kinkingnehun, S., Pochon, J.B., Mondon, K., Thiebaut de Schotten, M., Seassau, M., Duffau, H., Samson, Y., Dubois, B., Levy, R., 2008. The functional architecture of the left posterior and lateral prefrontal cortex in humans. Cereb Cortex 18, 2460-2469.

Wager, T.D., Smith, E.E., 2003. Neuroimaging studies of working memory: a meta-analysis. Cogn Affect Behav Neurosci 3, 255-274.

Wickelgren, W.A., 1977. Speed-Accuracy Tradeoff and Information Processing Dynamics. Acta Psychologica 41, 67-85.

Chapter 7

Overall conclusions and general discussion

In this collection of work, I have used three different, but complementary, methods in an attempt to advance understanding of age-related decline in working memory. To date, theories of neurocognitive aging have been based primarily on neuroimaging and behavioral data collected during performance of a variety of cognitive tasks (Park and Reuter-Lorenz, 2009a; Reuter-Lorenz and Cappell, 2008; Stern, 2009). One hypothesis that has been put forth is that age-related deficits in cognition are due to the reduced ability of older adults to successfully form, maintain, and retrieve associations between different types of information (Naveh-Benjamin, 2000). This process, often referred to as binding, occurs at multiple levels of memory, including working memory (Wheeler and Treisman, 2002; Zimmer, 2008). In Chapter 2, I first characterized brain activity associated with binding in younger adults using an event-related working memory task. This allowed investigation of the effect of age on working memory binding in Chapter 3.

The primary conclusion drawn from the task-fMRI data is that the neural correlates of binding in working memory are not as efficient in older adults as they are in younger adults. This is possibly due to the greater connectivity between regions that were active during the bound task and regions that were deactive during the bound task that was observed in older adults. The relative inability of older adults to suppress activity in a common set of regions, referred to as the default mode network, during cognitive tasks has been previously established (Grady et al., 2006; Persson et al., 2007; Sambataro et al., 2010). However, I identified a relationship between task-induced deactivations and activations that were specific to the binding task. In younger adults, the performance of a letter-location binding working memory task resulted in

greater deactivations, and less connectivity between task-negative regions and task-positive regions, than the performance of a working memory task where letters and locations were presented separately. However, older adults did not have these differences in brain activity and connectivity between the bound and unbound tasks. Older adults not only had more binding-specific connectivity between task-positive regions and task-negative regions, but they also displayed more binding-specific activity in canonical working memory regions. Thus, there appears to be a binding-specific deficit that occurs with advancing age, likely due to a decreased efficiency in brain activity and connectivity.

The use of task-fMRI has inherent limitations which could explain discrepancies between different theories of neurocognitive aging. The use of resting state fMRI allows investigation of intrinsic organization of the brain without confounds that are associated with tasks (Biswal et al., 1995; Smith et al., 2009). Importantly, brain networks measure at rest can be linked to behavioral differences. As more and more data are being collected in individual subjects, it is becoming increasingly important to develop new methods that can find real relationships between data modalities. In Chapter 4, I demonstrate the utility of resting state fMRI data in cognitive studies by applying a novel multi-modal, multivariate method that identified sub-components of common resting state networks that covaried with specific behavioral measures. In Chapter 5, I applied another multivariate method, machine learning classifiers, to identify changes in resting state functional connectivity that occur with age. I found that a machine learning classifier was able to successfully discriminate older adults and younger adults based only on their resting state connectivity from four networks. More importantly, the

classifier identified changes in connectivity that were the distinguishing characteristics of age-related reorganization of the brain.

The findings of age-related changes in resting state functional connectivity again suggest that neural networks in older adults are less efficient than younger adults. I found that the intrinsic connectivity between the sensorimotor network and cingulo-opercular network (a cognitive control network) undergoes the greatest age-related change. In addition, echoing the results from the task data, I found that there was a robust decrease in negative correlations between the default network (regions that usually deactivate during cognitive tasks) and the cingulo-opercular and sensorimotor networks in older adults compared to younger adults. Finally, I found that connections within the cingulo-opercular network and default network were less connected in older adults than in younger adults.

Unlike traditional fMRI or resting state-fMRI, lesion studies allow questions regarding necessity of brain regions for different cognitive tasks. In Chapter 6, I use verbal working memory data collected from acute unilateral stroke patients to test a common finding in the neuroimaging aging literature. In task fMRI studies, older adults consistently have bilateral brain activity during verbal working memory tasks while younger adults have highly left lateralized brain activity (Cabeza, 2002). I show that acute stroke to either the left or right hemisphere negatively affects performance on a verbal working memory task in older adults, indicating that older adults do indeed need both hemispheres to perform the task. The contralateral recruitment observed in older adults is often viewed as compensatory recruitment (Cabeza, 2002; Park and Reuter-

Lorenz, 2009a). In line with this, the results from the work presented in this thesis leads me to suggest that additional activity observed in older adults is a result of the general decline in the efficiency in interactions between and within brain networks that accompanies normal aging. With advancing age, there is a decline in the integrity of specialized cognitive networks that we observe in younger adults, for example the default network and the task positive network, and in the specialized interaction between these networks. I present evidence for this in both the task-fMRI study and in the resting fMRI study. At rest, the negative correlation between the default and cognitive control networks becomes less negative with age, while during task performance older adults had more binding-specific connectivity between regions of the default network and regions activated during the binding task. Therefore, the natural consequence of this degradation in specialization is that more brain regions are recruited for task performance. As demonstrated in the lesion work, these additional brain regions are necessary for successful task performance.

The ultimate goal of research on age-related differences in the neural underpinnings of cognitive decline is to identify ways to attenuate this decline. With a more thorough knowledge of the exact changes in cognitive networks that occur with age, suppressing or restoring particular brain regions and connections may eventually lead to new and improved methods of promoting successful cognitive aging.

References

Biswal, B., Yetkin, F.Z., Haughton, V.M., Hyde, J.S., 1995. Functional connectivity in the motor cortex of resting human brain using echo-planar MRI. Magn Reson Med 34, 537-541.

Cabeza, R., 2002. Hemispheric asymmetry reduction in older adults: the HAROLD model. Psychol Aging 17, 85-100.

Grady, C.L., Springer, M.V., Hongwanishkul, D., McIntosh, A.R., Winocur, G., 2006. Age-related changes in brain activity across the adult lifespan. Journal of cognitive neuroscience 18, 227-241.

Naveh-Benjamin, M., 2000. Adult age differences in memory performance: tests of an associative deficit hypothesis. J Exp Psychol Learn Mem Cogn 26, 1170-1187.

Park, D.C., Reuter-Lorenz, P., 2009. The adaptive brain: aging and neurocognitive scaffolding. Annu Rev Psychol 60, 173-196.

Persson, J., Lustig, C., Nelson, J.K., Reuter-Lorenz, P.A., 2007. Age differences in deactivation: a link to cognitive control? Journal of cognitive neuroscience 19, 1021-1032.

Reuter-Lorenz, P., Cappell, K.A., 2008. Neurocognitive Aging and the Compensation Hypothesis. Curr Dir in Psych Sci 17, 177-182.

Sambataro, F., Murty, V.P., Callicott, J.H., Tan, H.Y., Das, S., Weinberger, D.R., Mattay, V.S., 2010. Age-related alterations in default mode network: impact on working memory performance. Neurobiol Aging 31, 839-852.

Smith, S.M., Fox, P.T., Miller, K.L., Glahn, D.C., Fox, P.M., Mackay, C.E., Filippini, N., Watkins, K.E., Toro, R., Laird, A.R., Beckmann, C.F., 2009. Correspondence of the brain's functional architecture during activation and rest. Proc Natl Acad Sci U S A 106, 13040-13045.

Stern, Y., 2009. Cognitive reserve. Neuropsychologia 47, 2015-2028.
Wheeler, M.E., Treisman, A.M., 2002. Binding in short-term visual memory. J Exp Psychol Gen 131, 48-64.

Zimmer, H.D., 2008. Visual and spatial working memory: from boxes to networks. Neurosci Biobehav Rev 32, 1373-1395.